IMAGE RESOLUTION ENHANCEMENT USING HYBRID WAVELETS AND BICUBIC INTERPOLATION

Thesis Submitted towards the partial fulfillment of requirement for the award of degree of

Master of Engineering

in

Electronics and Communication Engineering

Submitted by:

Gaurav Kumar

Roll No: 821086001

Under the guidance of:

Dr. Kulbir Singh

Associate Professor

ELECTRONICS AND COMMUNICATION ENGINEERING DEPARTMENT

THAPAR UNIVERSITY

(Established under the section 3 of UGC Act, 1956)

PATIALA – 147004 (PUNJAB)

May 2013

CERTIFICATE

I hereby certify that the work which is being presented in the thesis entitled, "**Image resolution enhancement using hybrid wavelets and bicubic interpolation**", in partial fulfillment of the requirement for the award of degree of Master of Engineering in Electronics and Communication Engineering from Thapar University, Patiala, is an authentic record of my own work carried out under the supervision of Dr. Kulbir Singh and refers other researcher's work which are duly listed in the reference section.

The matter presented in this thesis has not been submitted in any other University /Institute for the award of any other degree.

Date: 15/5/13

Gaurav Kumar

821086001

It is certified that the above statement made by the student is correct to the best of my knowledge and belief.

Date: 15/05/2013

(Dr. Kulbir Singh)

Associate Professor, ECED

Thapar University, Patiala

Countersigned by:

(Dr. Rajesh Khanna)

Professor and Head, ECED

Thapar University, Patiala

(Dr. S. K. Mohapatra)

Dean of Academic Affairs

Thapar University, Patiala

ACKNOWLEDGMENT

I would like to take this opportunity to first and foremost thank God for giving the strength, knowledge to complete the thesis work. Without Him I would not have had the wisdom or the physical ability to do so.

I am extremely grateful to my supervisor **Dr. Kulbir Singh**, Associate Professor, ECED for his guidance and all the useful discussion and brainstorming sessions, especially during the difficult conceptual development stage. I consider myself fortunate to have had the opportunity to work with such as caring academician.

I also wish to extend my sincere thanks to **Mr. Ankush Kansal**, Assistant Professor**,** ECED for his stimulating guidance and continuous encouragement throughout this work.

My thanks are due to **Dr. Rajesh Khanna,** Professor and Head, ECED for providing facilities for the completion of this thesis and his moral support at every step. I am also thankful to the entire faculty and staff members of ECED for their unyielding encouragement.

I take pride of myself in being the son of ideal great parents whose everlasting desire, sacrifice, affectionate blessings and help without which it would have not been possible for me to complete my thesis work.

Gaurav Kumar

821086001

ABSTRACT

Digital Image Processing is a rapidly evolving field with growing applications in Science and Engineering. The need of digital image processing is motivated due to the improvement of pictorial information for human interpretations, for autonomous machine applications, for efficient storage and transmission. Broadly, image processing may be classified into following categories: restoration, segmentation, and enhancement. Image enhancement techniques are used to emphasize and sharpen image features for display and analysis. A lot of techniques are available for the improving the quality of an image such as contrast stretch, density slicing, spatial filtering, Edge enhancement, and image interpolation which has been discussed by the authors [4], [30], [46]. In the last few years, Wavelet transforms have been found as most important tool for image processing, especially for the applications such as time-frequency analysis, segmentation, enhancement and data compression.

The thesis presents the theory of fundamental mathematical tools (Discrete wavelet transform, and Stationary wavelet transform) for image resolution enhancement. First method describes a super resolution technique based on interpolation of the high-frequency subband images obtained by DWT and the input image. DWT is used to decompose an image into different subband images. Then the high-frequency subband images and the low-resolution input image have been interpolated, followed by combining all these images to generate a new super resolved image by using IDWT. Second method is based on interpolation of the high frequency subband images obtained by DWT and the input image. The edges are enhanced by introducing an intermediate stage by using SWT. DWT is applied in order to decompose an input image into different subbands. Then the high frequency subbands as well as the input image are interpolated. The estimated high frequency subbands are being modified by using high frequency subband obtained through SWT. Then all these subbands are combined to generate more enhanced image by using IDWT. These two approaches also turned out to be extremely efficient for preservation of edge. The performance of these image resolution enhancement techniques are quantitatively accessed using different criteria namely the MSE, PSNR and the visual appearance. It has been observed that these techniques give better PSNR results. Hybrid wavelet and bicubic interpolation provide significant improvement in texture based images.

An image zooming result shows that hybrid wavelets and bicubic interpolation gives less aliasing effects as compared to DWT and bicubic interpolation, but gives less PSNR in images having pixels at same intensity level as compared to DWT and bicubic interpolation.

CONTENTS

LIST OF ABBREVIATIONS

CCD	Charge Coupled Device
CWT	Complex Wavelet Transform
CWT-SR	Complex Wavelet Transform -Super Resolution
DCT	Discrete Cosine Transform
DICOM	Digital Imaging and Communication in Medicine
DT-CWT	Dual Tree Complex Wavelet Transform
DWT	Discrete Wavelet Transform
DWT-SR	Discrete Wavelet Transform- Super Resolution
FT	Fourier Transform
HE	Histogram Equalization
HH	high high
HL	high low
HMT	Hidden Markov Tree
HSV	Hue Saturation Value
IDWT	Inverse Discrete Wavelet Transform
IHS	Intensity Hue Saturation
ISWT	Inverse Stationary Wavelet Transform
LH	low high
LL	low low
LoG	Laplacian of Gaussian

MAP	Maximum a posteriori
MRA	Multi Resolution Analysis
MSE	Mean Square Error
NEDI	New Edge Directed Interpolation
PSNR	Peak Signal-To-Noise Ratio
QMF	Quadrature Mirror Filter
SR	Super Resolution
SRHE	Sub Regions Histogram Equalization
STFT	Short Time Fourier Transform
SVD	Singular Value Decomposition
SWT	Stationary Wavelet Transform
WT	Wavelet Transform
WZP-CS	Wavelet Zero Padding Cycle Spinning
WZP-CS-ER	Wavelet Zero Padding Cycle Spinning with Extended precision

LIST OF FIGURES

LIST OF TABLES

CHAPTER 1

INTRODUCTION

1.1 PREAMBLE

We depend heavily on our vision to make sense of the world around us. We can identify a face in an instant; we can differentiate colors; we can process a large amount of visual information very quickly. For our purposes, images are one of the most convenient ways to convey the information. An image may be defined as two dimensional function $f(x, y)$, where x, y are spatial coordinates and the amplitude of f at any pair of coordinates (x, y) is called the intensity or gray level of an image at that point. When x, y and the intensity value of f are all finite, discrete quantities, we call the image, a digital image.

Fields which traditionally used analog imaging are now switching to digital system, for their flexibility and affordability. Personal computers, in addition to a plethora of hand-held electronic devices, have become the preferred mode of communication for increasingly large portions of the population. Digital cameras and camera phones have made acquiring, processing, and sharing photos almost instantaneous, making digital images a common component of hi-tech communications. Resolution refers to the sharpness of image detail, smoothness of curved lines, and the faithful reproduction of an image. Super resolution is the process of combining multiple low resolution images to form high resolution image. An image resolution can be increased by reducing the pixel size, by increasing the chip-size, and by super resolution. Reduced pixel size increase the spatial resolution, but amount of light decreases. Increased chip-size also enhance the spatial resolution, but cost of high precision optics increases. [7].

1.2 DIGITAL IMAGE PROCESSING

The word digital relates to calculation by numerical methods or by discrete units. If we now define a digital image to be a numerical representation of an object, the pixels are the discrete units, and the quantized gray scale gives the numerical component.

Processing is a series of actions or operations leading to a desired result. Thus a series of actions is performed upon an object to alter its form in a desired manner. Now we can define digital image processing as subjecting a numerical representation of an object to a series of

operations in order to obtain a desired result [24]. The need of digital image processing is motivated due to the improvement of pictorial information for human interpretation, analysis and making the image more suitable for autonomous machine perception.

Improvement of pictorial information includes **"enhancing the edges"** of an image to make it appear sharper, **"removing noise"** from an image and **"removing motion blur"** from an image. While the autonomous machine perception includes **"obtaining the edges"** of an image, and **"removing detail"** from an image.

Digital image processing has many advantages over analog image processing; it allows a much wider range of algorithms to be applied to the input data, and can avoid problems such as the build-up of noise and signal distortion during processing [8]. Digital image processing involves following operations:

- Geometric transformations such as enlargement, reduction, and rotation.
- Color corrections such as brightness and contrast adjustments, quantization, or conversion to a different color space.
- Registration (or alignment) of two or more images.
- Interpolation and recovery of a full image from a RAW image format.
- Segmentation of the image into regions.
- Image editing and digital retouching.
- Extending dynamic range by combining differently exposed images.

1.3 ASPECTS OF DIGITAL IMAGE PROCESSING

Digital image processing starts with an image and produces a modified version of that image. It is therefore a process that takes an image into an image. Digital image analysis is taken to mean a process that takes a digital image into something other than a digital image, such as a set of measurement data or a decision [2]. Image processing techniques can be classified into three broad categories:

1.3.1 Image Restoration

Image restoration is based on the attempt to improve the quality of an image through knowledge of the physical processes which led to its formation. Consider image formation as a process which transforms an input distribution into an output distribution. The input distribution

represents the ideal, i.e. it is the 'perfect' image to which we do not have direct access but which we wish to recover or at least approximate by appropriate treatment of the imperfect or corrupted output distribution. Image Restoration includes:

- Removal of blur caused by linear motion,
- Removal of optical distortions,
- Removing periodic interference.

1.3.2 Image Segmentation

Image Segmentation is an important technology for image processing. Image segmentation divides an image into its constituent regions or objects. The segmentation of an image is application dependent. The level to which the subdivision is carried depends on the problem being solved i.e. Segmentation should stop when object of interest in an application have been isolated. Image Segmentation includes:

- finding lines, circles, or particular shapes in an image,
- Identify cars, trees, buildings, or roads in an aerial photograph.

1.3.3 Image Enhancement

Image enhancement techniques improve the quality of an image as perceived by a human. These techniques are most useful because many digital images will give inadequate information for image interpretation. Image enhancement is attempted after the image is corrected for geometric and radiometric distortions. Image enhancement methods are applied separately to each band of a multi spectral image. Digital techniques have been found to be most satisfactory than the photographic technique for image enhancement, because of the precision and wide variety of digital processes. Image enhancement includes:

- Sharpening or de-blurring an out of focus image,
- Highlighting edges,
- Improving image contrast, or brightening an image,
- Removing noise.

The primary condition for image enhancement is that the information that we want to extract, emphasize or restore must exist in the image. Fundamentally, 'we cannot make something out of

nothing' and the desired information must not be totally swamped by noise within the image. There exists a wide variety of techniques for improving image quality. The contrast stretch, density slicing, edge enhancement, and spatial filtering are the more commonly used techniques.

1.4 EDGE DETECTION

Edges are significant local changes of intensity in an image and typically occur on the boundary between two different regions in an image. Edge detection significantly reduces the amount of data and filters out useless information, while preserving the important structural properties in an image. The effectiveness of image processing tasks depends on the perfection of detecting meaningful edges. There are basically four steps of edge detection:

- Suppressing the noise as much as possible, without destroying the true edges.
- Apply a filter to enhance the quality of the edges in the image (sharpening).
- Determine which edge pixels should be discarded as noise and which should be retained (usually, thresholding provides the criterion used for detection).
- Determine the exact location of an edge (sub-pixel resolution might be required for some applications, that is, estimate the location of an edge to better than the spacing between pixels) [6].

1.5 IMAGE TRANSFORMS

Many image processing algorithms have been applied in the frequency domain rather than the spatial domain and transformation between the two domains can often permit more useful visualization of the image content. Transform theory plays a key role in image processing and will be applied during image enhancement [4]. A 'transform' represents the pixel values in some other, but equivalent form. In the Fourier theory, a signal (an image is considered as a finite 2-D signal) is expressed as a sum, theoretically infinite, of sines and cosines, making the FT suitable for infinite and periodic signal analysis. The output of the transformation represents the image in the frequency domain, while the input image is the spatial domain equivalent.

Due to non stationary nature of an image, traditional Fourier analysis is not adequate to analyze the image completely. We need to resolve the property of the image both in time and frequency domain. The STFT is modified version of FT. During STFT analysis, an image is divided into overlapping windows and it is assumed that the image is stationary within the small

region. The Fourier analysis of this small region is analyzed and estimation of time and frequency information is obtained. The problem associated with STFT is that the time and frequency resolutions are determined by the width of analysis window, which is selected once for the entire analysis, i.e., both time and frequency resolutions are constant.

1.5.1 Wavelet Transform

A wave is an oscillating function of time or space and is periodic. In contrast, wavelets are localized waves [49]. They have their energy concentrated in time or space and are suited for analysis of transient signals. The WT provides a time-frequency representation of the signal. The WT uses multi-resolution analysis technique by which different frequencies are analyzed at different resolutions.

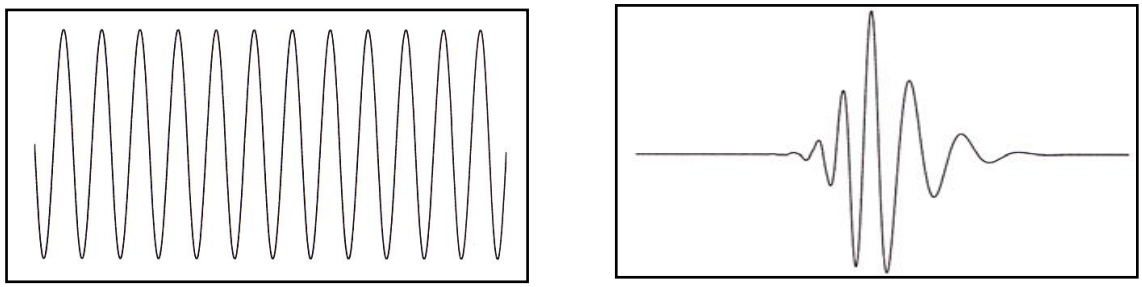

(a) **(b)**

Figure 1.1 Representation of (a) wave and (b) wavelet [49].

The Wavelet Transforms have advantages over traditional Fourier transforms and cosine transform for representing functions that have discontinuities and sharp peaks, and for accurately deconstructing and reconstructing finite, non-periodic and/ or non-stationary signals. In WT, as frequency increases, the time resolution increases; likewise, as frequency decreases, the frequency resolution increases. Thus, a certain high frequency component can be located more accurately in time than a low frequency component and a low frequency component can be located more accurately in frequency compared to a high frequency component. Figure 1.1(a) shows the time-frequency tiling in the time-domain plane and figure 1.1(b) shows the tiling in frequency-domain plane. It is seen that figure 1.1(a) does not give any frequency information and figure 1.1(b) does not give any time information.

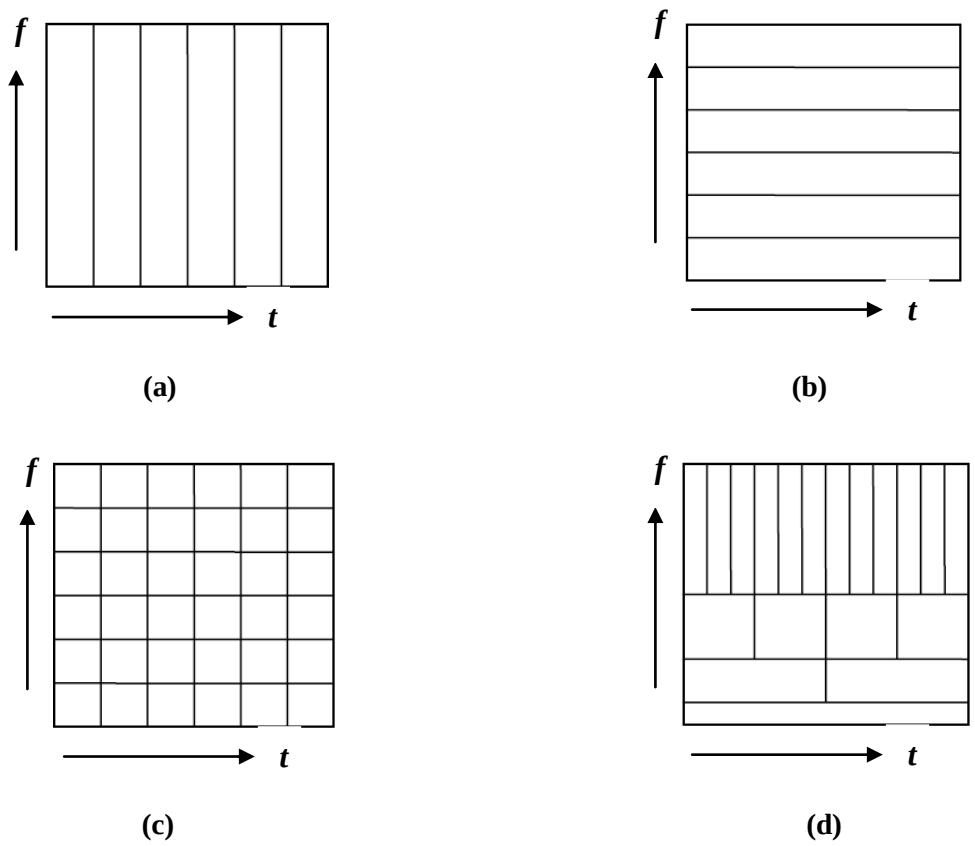

Figure 1.2 Time-Frequency Representation [3]

Similarly figure 1.1(c) shows the tiling in STFT and figure 1.1(d) shows the tiling in WT. It is seen that STFT gives a fixed resolution at all times, whereas WT gives a multi resolution analysis.

1.5.2 Discrete Wavelet Transform

DWT is based on sub-band coding, is found to yield a fast computation of WT. It is easy to implement and reduces the computation time and resources required. In Wavelet analysis, a signal can be divided into two parts namely approximation and details. The resolution of the signal is a measure of the amount of detail information in the signal and is determined by the filtering operations, and the scale is determined by upsampling and downsampling operations.

The two-dimensional wavelet transforms are slightly different from one-dimensional and can be easily extended by simply multiply the one-dimensional scaling and wavelet functions. DWT decomposes an image into different subband namely LL, LH, HL, and HH, where LL represent the approximation coefficients, and LH, HL, HH represents the detailed coefficients

[5]. The detailed coefficients measure the variation for the intensity for an image in horizontal, vertical, and diagonal direction respectively.

1.5.3 Stationary Wavelet Transform

SWT is similar to the DWT in that the high-pass and low-pass filters are applied to the input signal at each level. However, in the SWT, the output signal is never sub-sampled (not decimated). Instead, the filters are up sampled at each level [40].The general idea of SWT denoising is to zero out small wavelet coefficients whose absolute values are below a certain threshold¸ in the detail coefficients, and then reconstruct the signal using the threshold detail coefficients and the intact approximation coefficient. Compare with the DWT, the SWT has such advantage as follows. First each subband has the same size, so it is easier to gain the relationship among the subbands. Second the resolution can be kept since the original data is not decimated, at the same time the wavelet coefficients has more redundant information which helps to distinguish the noise from feature [42].

1.6 IMAGE INTERPOLATION

Interpolation is the process of determining the values of a function at positions lying between its samples. It achieves this process by fitting a continuous function through the discrete input samples. This permits input values to be evaluated at arbitrary positions in the input, not just those defined at the sample points. While sampling generates an infinite bandwidth signal from one that is band limited, interpolation plays an opposite role: it reduces the bandwidth of a signal by applying a low-pass filter to the discrete signal. That is, interpolation reconstructs the signal lost in the sampling process by smoothing the data samples with an interpolation function [16].

Interpolation is used extensively in digital image processing to magnify or reduce images and to correct spatial distortions. The goal of image interpolation is to produce acceptable images at different resolutions from a single low-resolution image [30]. The actual resolution of an image is defined as the number of pixels, but the effective resolution is a much harder quantity to define as it depends on subjective human judgment and perception. Image interpolation is used for several different purposes such as image resolution enhancement, multi-resolution pyramidal compressing, and position computing for rotated image pixels etc.

1.7 GAPS IN STUDIES

Conventional image enhancement techniques usually introduce over-shoots and under-shoots in the areas of sharp edges. The main requirement for image resolution enhancement is that the algorithm should only enhance the image details; the filter is not sensitive to noise and does not smooth sharp edges. In image resolution enhancement by using interpolation, the main loss is on its high frequency components i.e. edges which are due to the smoothing caused by interpolation. One level DWT is used to decompose an input image into different subband images. Three high frequency subbands (LH, HL, HH) contains the high frequency components of the input image. Downsampling in each of the DWT subband cause loss of information in the respective subbands. SWT is used to fill the gap caused by DWT during decimation. But this will lead to over determined and redundant representation of data.

1.8 OBJECTIVE

The objectives of thesis are:

(i) To achieve image super resolution by using DWT and interpolation.

(ii) To achieve image resolution enhancement by using Hybrid Wavelets and interpolation.

(iii) To compare the performance of these techniques in terms of MSE, PSNR, and visual quality with existing ones.

1.9 METHODOLOGY

The basic research method used in this thesis is a combination of approaches with the beneficiaries of the study prior to the design of the output product with the experimental results to follow. First method uses DWT to decompose an image into different subbands, and then high frequency subband images have been interpolated. The interpolated high frequency subband coefficients are combined with low resolution image (low frequency sub band), and super resolved image is obtained by applying IDWT. In the second method, interpolated high frequency subband coefficients are combined with high frequency subbands obtained by applying SWT to an input image. An original input image is interpolated with half of the interpolation factor used for the interpolation of high frequency subbands. After words all these images all these images have been combined using IDWT to generate an enhanced image.

Simulations have been developed in MATLAB on an Intel Core 2 Duo desktop computer with specifications: 2.80 GHz processor, 2GB RAM, and Windows XP operating System.

1.10 ORGANISATION OF THESIS

This thesis is organized in six chapters as follows.

Chapter 1 is an introduction with the comprehensive description of the central theme of this research. It consists of brief introduction and aspects to digital image processing, Image transforms, interpolation, methodology and objectives of the thesis. Chapter 2 is the review of the previous works and introduces some of the definitions and concepts which are required later on.

Chapter 3 presents a thorough study of the interpolation. The evolution and recent advances in the field of image interpolation are comprehensively analyzed. Recent developments and newer extensions of image interpolation with their theories, structures and properties are critically explored. Advantages and limitations are analyzed through individual implementations and simulations.

Chapter 4 begins with brief introduction and fundaments of wavelet transforms are presented. This is followed by the description of various types of wavelet transforms, like CWT, DWT, and SWT.

Chapter 5 is about the various image resolution enhancement techniques. Bi orthogonal wavelet filter banks are implemented as a case study and their results are analyzed on different test images. Chapter 6 describes the conclusion and prospects of future scope.

CHAPTER 2

LITERATURE REVIEW

2.1 IMAGE ENHANCEMENT TECHNIQUES

Sub regions Histogram equalization (SRHE) is presented by [19]. Histogram equalization improves the contrast of an image by changing the intensity level of the pixels based on the intensity distribution of the input image. In SRHE, the method partitions the image based on the smoothed intensity values, which are obtained by convolving the input image with Gaussian filter. By doing this, the transformation function used by Histogram equalization is not based on the intensity of the pixels only, but the intensity values of the neighboring pixels are also taken into consideration. This paper also presents a more robust histogram equalization transformation function. Experimental result shows that the proposed method is not only can enhance the contrast, but this method also successfully sharpens the image.

In [20], the author proposed a new image regularization that measures the complexity of the dyadic tree representation of its sublevel sets. By penalizing unbalanced trees less, the regularization preserves the sharp edges. The main contribution of this paper is the connection of concept from structured dyadic tree complexity measures, wavelet shrinkage, morphological wavelets, and smoothness regularization in besov space into a single coherent image regularization framework. An important challenge is to preserve sharp edges and other meaning full high frequency features in the image. This new image regularization measure the complexity of dyadic decision trees and then for real-valued function. Experimental result shows that adaptive dyadic structures yield the better signal representation. In terms of PSNR, the proposed algorithm gives best performance compared with other methods and visual results shows clear edge preservation.

Y. Niu *et al.* [21] proposed a novel psycho visually motivated edge-based low-bit-rate image codec. This algorithm offers a compact description of scale-invariant second order statistics of natural images, the preservation of which is crucial to the perceptual quality of coded images. The edge regions are refined by a residual coding technique based on edge dilation and sequential scanning in the edge direction. The proposed algorithm works with the arbitrary edge

trajectories in spatial domain, and it is, in this regard, more flexible and effective than other conventional techniques.

In [22], the authors present a computationally efficient technique for maximum a posteriori (MAP) estimation of images in the presence of both blur and noise. An image is divided into statistically independent regions. Each region is modeled with separate Gaussian prior. By utilizing the shift-invariant nature of prior with in each region, Wiener filter is used at all points in the image. This algorithm is suitable for a range of image processing problems, and it provides a computationally efficient approach.

An adaptive IHS Pan Sharpening method is presented by [23]. In this paper, the author introduced two modifications to improve the spectral quality of the image. Firstly, they proposed image adaptive coefficients for IHS to obtain more accurate spectral resolution. Second, an edge adaptive IHS method was proposed to enforce spectral fidelity away from the edges. In order to minimize spectral distortion, the intensity band should approximate the panchromatic image as closely as possible. In edge adaptive method, they transfer edges from panchromatic image to the fused image. This approach extracts the edges from the panchromatic image. The adaptive HIS method produces an image with higher spectral resolution while maintaining the high quality spatial resolution of the original IHS. Experimental result shows that these two modifications improve spectral resolution compared to original IHS.

An effective method for contrast enhancement in an image which was controlled by the trial-and-error tuning of one parameter [24]. The same parameter was used for the entire image resulting in over blurring or sharpening of features in the image. H. S. Kam *et al.* [25] applied Russo's algorithm on impulse noise and propose an efficient method for to automatically obtaining the parameter value. Each pixel is adaptively assigned a different parameter value by evaluating the local features. Results of the proposed method are compared with those of Russo's algorithm and of other methods for sharpening of image features. Experimental values indicate that the proposed method effectively tunes the operator yielding superior performance.

High dynamic range image rendering with retinex based adaptive filter is presented by [26].The proposed method is based on centre surround retinex model. First, they use an adaptive filter

whose shape follows image high contrast edges. Second, the luminance channel is processed. Retinex is simplified model of HVS and working on the principle to assign new value to each pixel in the image based on spatial comparison of light intensity. The proposed method is tested on various HDR image and compared with other methods to show that it efficiently increases the local contrast and provide good rendition of colors.

In [27], the author presents a generalized Unsharp masking algorithm, which is designed to address three issues: First, simultaneously enhancing contrast and sharpness by means of individual treatment of the model component and the residual. Second, reducing the halo effect by means of an edge preserving filters and third, solving the out-of-range problem by means of log-ratio and tangent operations. The proposed algorithm converts a color image from the RGB color space to HSI color space. The chrominance components such as H and S components are not processed, the inverse conversion is performed. An enhanced color image in its RGB color space is obtained. The log-ratio approach in the algorithm eliminates the need of rescaling process and systematically tackles the out of range problem in image restoration. The proposed algorithm uses an iterative median filter and adaptive gain controller for the enhancement of the detail signal. Experimental results show that proposed algorithm is able to significantly improve the contrast and the sharpness of an image.

A cubic unsharp masking technique for contrast enhancement is presented by [28]. The proposed technique is based on fundamental unsharp masking. The input signal is added to the processed version of signal in which high frequency components are enhanced .An effect of high pass filter is also the amplification of noise. In the proposed technique, they are modulating the sharpen signal using function dependant on local gradient of the data. Experimental results shows the proposed technique sharpen the image better than conventional method.

2.2 INTERPOLATION TECHNIQUES

An edge-directed interpolation algorithm for natural images is presented by [29]. The basic idea is to first estimate local covariance coefficients from a low-resolution image and then use these covariance estimates to adapt the interpolation at a higher resolution based on the geometric duality between the low-resolution covariance and the high-resolution covariance. The edge-directed property of covariance-based adaptation attributes to its capability of tuning the interpolation coefficients to match an arbitrarily oriented step edge. The proposed algorithm can

be used for resolution enhancement of grayscale images and reconstruction of color images from CCD samples. Simulation results demonstrate that new edge-directed interpolation better preserves the geometric regularity around the edges and thus generates interpolated images with higher visual quality.

H. Aftab *et al*. [30] proposed a new single image interpolation technique for super resolution which uses fast hybrid method of switching between covariance based interpolation technique and curvature based interpolation technique. An image is expanded on both horizontal and vertical axis. The edges and smooth areas in the image are determined first; consequently the interpolation of the edges is carried out using the covariance based method, whereas the smooth areas are handled by the iterative curvature based approach. The new approach depicts reduced processing time and better visual perceptibility. The performance of the proposed approach was compared with another hybrid approach iNEDI algorithm. The proposed method showed significantly improved performance in terms of processing time, PSNR and visual quality.

In [31], the authors propose a method to improve piecewise-linear interpolation by shifting the interpolation kernel. They describe a theoretical method to estimate the quality of an interpolator using mathematical tools such as a Fourier approximation kernel and an asymptotic interpolation constant, which maximizes the quality of shifted linear interpolation. They have also tested these interpolation methods in a zoom experiment. Experimental results show that the standard piecewise-linear method blurs the zoomed image very much. The proposed method gives sharper results than key's cubic kernel.

An image enlargement method using bi-directional shifted linear interpolation is presented by [32].Shifted linear interpolation excels in edge reconstruction, but it sometimes causes oscillations that deteriorating the precision of image interpolation. The proposed method utilizes two shifted-linear interpolation functions in two opposing directions as the basis to increase the precision of interpolation. At the same time, two parameters are used to suppress the oscillation effect that may occur in the image enlargement process by the conventional shifted-linear interpolation. Subjective and objective evaluations are carried out to verify the basic performance and relative superiority of proposed methods.

2.3 WAVELET TRANSFORMS

In [33], the authors proposed method for image enhancement using wavelet transform and Haar transform followed by using the Sobel the Laplacian operator to obtain the sharper image. Firstly, they decompose the image with wavelet transform. Secondly, all high frequency sub images were decomposed with Haar transform. Thirdly, noise in the frequency fields was reduced by soft-threshold method. Fourthly, high frequency coefficients were enhanced by different weight values in different sub-images. Then, the enhanced image was obtained through inverse wavelet transform and inverse Haar transform. At last, the filters are applied to sharpen the image; the resulting image is then subtracted from the original image. Edges can be found when the difference between the luminance intensity from one point to another appears. Practically, the more difference of light luminance, the edges are easier to define. In contrast, the lesser the difference of light luminance, the harder the edges to define. Specifying the threshold level may perform loss of edges in certain parts of image which the level is lower than threshold. Images enhanced with the proposed method are better than with histogram equalization. The result of the experiment shows that the algorithm not only can enhance an image's contrast, but also can preserve the original image's edge property effectively.

A Wavelet Based Image Sharpening Algorithm is presented by [34]. The fundamental idea of image sharpening is to add to the input signal a high-pass filtered version of the signal itself. Wavelet coefficients provide multi resolution high frequency components of an image. Making use of this property, a sharpening algorithm is proposed in this paper. First, an image containing the edge information of the original image is obtained from a selected set of wavelet coefficients. This image is then combined with the original image to generate a new image with enhanced visual quality. In addition, an effective approach to remove those coefficients related with noise rather than the real image to further enhance the image quality is designed. Experimental results demonstrate the effectiveness of the proposed algorithm for image sharpening purpose.

H. Demirel and G. Anbarjafari [35] proposed a Discrete Wavelet based image resolution enhancement algorithm. Interpolation in image processing is a method to increase the number of pixels in a digital image. Three well known interpolation techniques, namely nearest neighbor,

bilinear, and bicubic. Bicubic interpolation is more sophisticated than the other two techniques and produces smoother edges. Edges identified by an edge detection algorithm in lower frequency subbands were used to prepare a model for estimating the edges in higher frequency subbands and only the coefficients with significant values were estimated as the evaluation of the wavelet coefficients. Experimental result shows that higher frequency components have been preserved in the proposed techniques. By comparing with conventional techniques such as bicubic interpolation, WZP-CS based image resolution enhancement techniques, the proposed technique provide more sharp image.

In [36], the authors proposed a DWT-based Image sharpening technique in which high frequency details are extracted using wavelet transform and then added with blurred image to enhance the edge details and visual quality. Wavelet provides frequency information and space localization as well as high frequency detail of an image. MRA in wavelet provides the information about the high frequency detail at different levels of decomposition. In proposed algorithm, they perform some spatial domain processing on the high pass images, based on hysteresis, to suppress the pixels which may not belong to the edges but retained in the high pass image.

Y. Piao *et al.* [37] proposed an image resolution enhancement method using inter-subband correlation in which the sampling phase in DWT is considered. Interpolation filters are designed by analyzing correlations between subbands having different sampling phases in the lower level, and applied to the correlated subbands in the higher level. The proposed algorithm is based on the point that the estimating the same phase high frequency subband is more reasonable than estimating different frequency subband. The filters are estimated under the assumption that correlations between two subbands in the higher level are similar to that in the lower level in DWT. The experimental result shows that the proposed method outperforms the conventional interpolation methods with respect to PSNR as well as the visual quality.

The algorithm proposed in this paper [38] creates new wavelet subbands by extrapolating the local coefficient decay. These new fine-scale subbands are used together with the original wavelet subbands to synthesize an image of twice the original size. Extrapolation of the coefficient decay preserves the local regularity of the original image, thus avoiding the over smoothing problems associated with traditional interpolation methods. The wavelet transform,

however, provides a means by which the local smoothness of a signal may be quantified. The regularity-preserving interpolation algorithm maintains sharp edges without smoothing, unlike bilinear and bicubic interpolation. The algorithm provides the most improvement over traditional methods on images with strong, well defined edges that separate smooth, high-regularity regions.

F. C. Fernandes *et al.* [39] proposed two-stage mapping-based CWT that consists of a mapping on to a complex function space followed by a DWT of the complex mapping. First, the controllable redundancies of the mapping stage offer a balance between degrees of shift sensitivity and transform redundancy. This allows us to create a directional, non-redundant CWT with potential benefits for image coding systems. In the proposed algorithm, forward CWT consists of an arbitrary DWT filter bank preceded by a mapping stage, then invert the CWT by appending an inverse-mapping stage after an inverse-DWT filter bank. The proposed mapping-based framework for CWTs mitigates DWT shortcomings and provides important advantages that engender new complex wavelet transforms with unprecedented properties.

An appropriate low pass and high pass filters applied to the data at each level to produce two sequences at the next level. In this method no decimation is required, and two new sequences each have the same length as the original sequence. Instead they modify at each level, by padding them with zeros [40]. The main applied interest of this paper will be use of the SWT for exploratory purposes and for local spectral estimation. Experimental results shows that at a given frequency band, the DWT has a sampling rate is too low to give any clear picture of data. It is better to sacrifice the orthogonality of the successive filter in order to attain the higher sampling rate of SWT.

H. Demirel and G. Anbarjafari [41] proposed an image resolution enhancement technique in which DT-CWT is used to decompose an input high frequency subband image into different subband images. The high frequency subband images and the input images are interpolated, followed by combining all these images to generate a new high resolution image by inverse DT-CWT. The resolution enhancement is achieved by using directional selectivity provided by CWT, where the high frequency subbands in six different directions contribute to the sharpness of the high frequency details such as edges. Experimental results show that the proposed technique gives quantitatively PSNR and better visual results as compared to conventional image enhancement techniques.

An image resolution enhancement technique proposed by [45], which uses DWT to decompose a low resolution image into different subbands. Then three high frequency subband images interpolated using bicubic interpolation. The high frequency subbands obtained by SWT of an input image are being incremented into the interpolated high frequency subband in order to correct the estimated coefficient. The input image is interpolated separately. Finally, corrected interpolated high frequency subbands and interpolated input images are combined by using IDWT. In order to show the effectiveness of proposed technique, the author compares the PSNR of proposed technique with WZP, DWT-SR, CWT-SR, WZP-CS, WZP-CS-ER techniques.

In [42], the authors proposed a method to enhance the quality of the given image. The enhancement is done both with respect to resolution and contrast. The proposed technique uses DWT and SVD to increase the resolution and DWT and SWT to increase contrast. The proposed enhancement process is based on the interpolation of HF subband images obtained by DWT and input image. The edge detail is enhanced by using intermediate stage using SWT. DWT can be used to decompose the input image into different subbands, and then the HF subbands are interpolated. HF subbands obtained by SWT of input are incremented into interpolated HF subbands in order to correct the estimated co-efficient. In parallel input image is also interpolated separately and corrected HF subbands and interpolated input image are combined through IDWT, to achieve high resolution output. The experimental results show that proposed technique gives good results over conventional methods.

The low resolution image is the approximation sub band of a higher resolution image and attempts to estimate the unknown detail coefficients to reconstruct a high resolution image [43]. The author proposed an algorithm of Image resolution enhancement using Wavelet domain HMT and coefficient sign estimation. HMT based methods using Gaussian mixture models have been shown to produce promising results. HMT models are used to find out the most probable state for the coefficient to be estimated. The posterior state is found using state-transition information from lower resolution scales and the coefficient estimates are generated using this distribution. The visual quality improvement over HMT method is mostly perceptible in the neighborhood of the edges where correct sign information has the most visible effect.

J. Yang *et.al.* [44] proposed a new algorithm of image denoising based on multi-scale and adaptive thresholding. Firstly, use stationary wavelet to transform an image. Then determine adaptive threshold of every decomposition progression according to characteristic of ratio of noise variance and wavelet coefficient variance and adaptively optimization wavelet coefficient processing window. Secondly, process the wavelet coefficient matrices with threshold neighborhood sliding window and adaptively optimization wavelet coefficient processing window. Lastly, obtain reconstructed image through ISWT. Compared to traditional discrete orthogonal wavelet transform, SWT is the over expression of original signal. Its characteristic is containing redundancy and translation invariance. The number of wavelet coefficients of sub-bands on every layer is equal to the number of pixels of original image. So it can make sure that subbands on every layer have enough coefficients to compute asymptotic optimal value, which remedies shortcoming of losing image details when reduce noise. The experimental results show that, the algorithm can not only obtain clearer image edges, but also de noise effectively compared to existing methods.

CHAPTER 3

INTERPOLATIONS

3.1 INTRODUCTION

Interpolation is the process of determining the values of a function at points lying between its samples. It achieves this process by fitting a continuous function through the discrete input samples. Interpolation process allows input values to be evaluated at arbitrary positions in the input, not just those defined at the sample points [18]. An interpolation function is a special type of approximating function. A fundamental property of interpolation functions is that they must coincide with the sampled data at the interpolation nodes, or sample points, In other words, if f is a sampled function, and if g is the corresponding interpolation function, then $g(x_k) = f(x_k)$, where x_k is the interpolation node. For equally spaced data, interpolation function can be written as:

$$g(x) = \sum_k c_k u\left(\frac{x - x_k}{h}\right) \tag{3.1}$$

where, h represents the sampling increment, the $x_k's$ are the interpolation nodes, u is the interpolation kernel, and g is the interpolation function. The $c_k's$ are parameters which depend upon the sampled data. They are selected so that the interpolation condition, $g\ (x_k) = f\ (x_k)$ for each x_k is satisfied [9].

Interpolation arises from the concept of resampling, which is the process of transforming a discrete image that is defined at one set of coordinate locations to a new set of coordinate points [12]. Conceptually resampling is divided into two processes: interpolation of the discrete image to a continuous image and then sampling the interpolated image. Figure 3.1 illustrates the two processes of resampling. In the interpolation process, a discrete function, x[n], is convolved with an interpolating function h[t], to produce a continuous function y[t]. In the sampling process, the continuous function is multiplied by a sampling function to produce a discrete function resampled at a new set of points y [n'].

Step 1 Interpolation

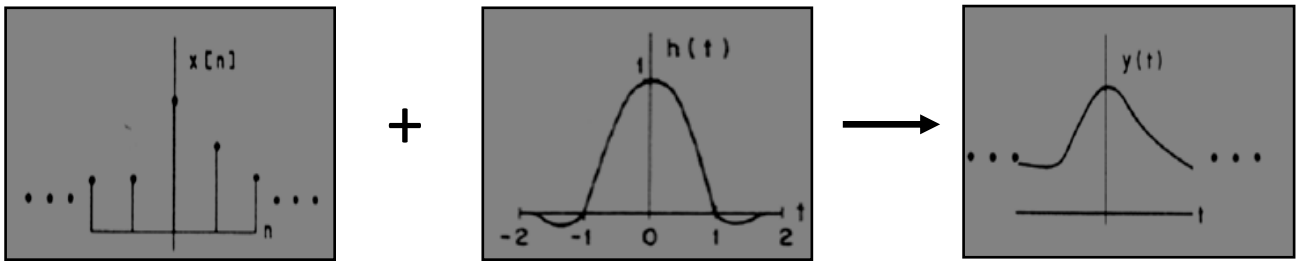

Signal Interpolating function Interpolated Signal

(a)

Step 2 Sampling

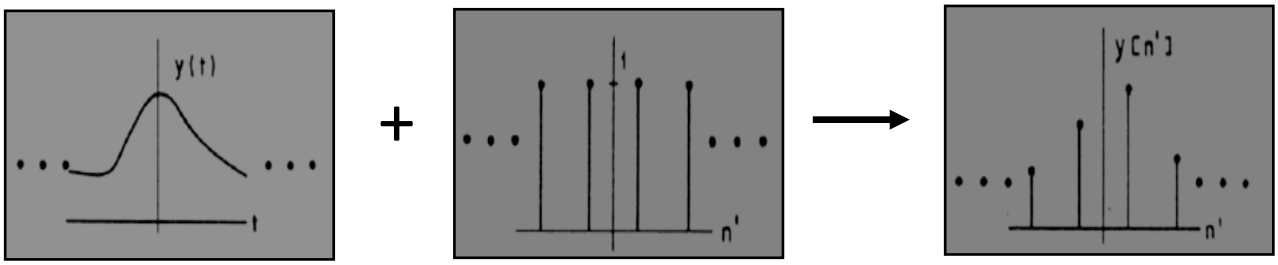

Interpolated Signal Sampling function Resampled Signal

(b)

Figure 3.1 Resampling Processes: (a) Interpolation, (b) Sampling [12]

3.2 IMAGE INTERPOLATION

Image interpolation is the process to find the information for undefined pixels or missed pixels in an image based on the information provided by given pixels, so that the interpolated image is as close to the actual one as possible. Image interpolation is involved in almost all applications where digital images are involved. Applications include image transformation (rotation, scaling), image enhancement, de-blurring, and SR [10]. To rotate an image, interpolation has to be used to fill in the output grid points between the input grid points. The image sensor in a digital camera has a fixed resolution. If we want to capture image at a different resolution, interpolation is used to save the data at the specified resolution. Similarly, all scanners or printers have a fixed native resolution, if we scan or print an image that is different from their native resolution, the scanner or printer will use interpolation to change the image's resolution to match the requirements [11].

The following properties are the most important criteria for the selection of good interpolation method:

- **Geometric Invariance:** The interpolation method should preserve the geometry and relative size of objects in an image. That is subject matter should not change under interpolation.
- **Contrast invariance:** The method should preserve the luminance values of objects in an image and overall contrast of an image.
- **Noise:** The method should not add noise or other artifacts to the image, such as ringing artifacts near the boundaries.
- **Edge Preservation:** The method should preserve the edges and boundaries, should sharpen them where possible.
- **Aliasing:** The method should not produce jagged or "staircase" edges.
- **Texture Preservation:** The method should not blur or smooth textured regions.
- **Over-smoothing:** The method should not produce undesirable piecewise constant or blocky regions.

Image interpolation generates a larger image from a smaller image. Two different types of interpolation can be classified as **enlargement** and **zooming.** In the image enlargement, an image is decomposes into a collection of basis function. For example, projecting an image onto a large screen. In this category, some well known methods are pixel replication (the basis function are assumed to be the standard piecewise constant functions), zero padding in the frequency domain (the basis functions are the sine and/or cosine functions), and zero padding in the wavelet domain (the basis functions are wavelets). The enlargement method works well when the image resembles the basis functions. The second type of interpolation is image zooming. In this method, one would like to add extra detail as the image is enlarged. It requires an image model to predict the lost details. The number of pixels in an image is increased using interpolation which results into SR [30]. Referring to Figure 3.2, a 6 X 6 image has been constructed by inserting new pixels through interpolation into a LR image of size 3 X 3.

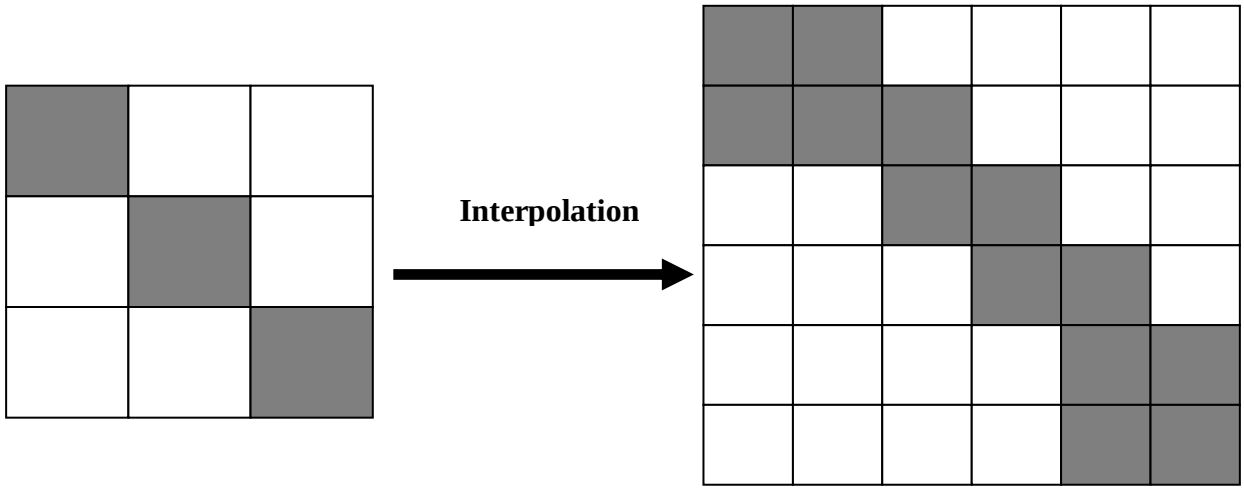

Figure 3.2 Resolution improvement using interpolation (a) 3 X 3 image, and (b) 6 X 6 image [5]

3.3 INTERPOLATION METHODS

Interpolation in two dimensions for the general case is sometimes is difficult to describe. For gridded data, the *n*-dimensional interpolation function can be described as the product of *n* one-dimensional interpolation functions. Therefore it is permitted to look at one dimensional interpolation functions to discuss the behavior of the *n*-dimensional interpolation functions. Several interpolation methods have been developed in the last few decades [52]. The most commonly used interpolation methods are:

3.3.1 Nearest Neighbor interpolation

The simplest interpolation from a computational point of view is the nearest neighbor, where each interpolated output pixel is assigned the value of the nearest sample point in the input image. This technique is also known as point shift algorithm and pixel replication. Figure 3.3 shows the working of nearest neighbor interpolation. Nearest neighbor interpolation determines the grey scale value from the closest pixel to the specified input coordinates, and assigns that value to the output coordinates or we can say that the nearest neighbor interpolation uses the digital value from the pixel in the original image which is nearest to the new pixel location in the corrected image.

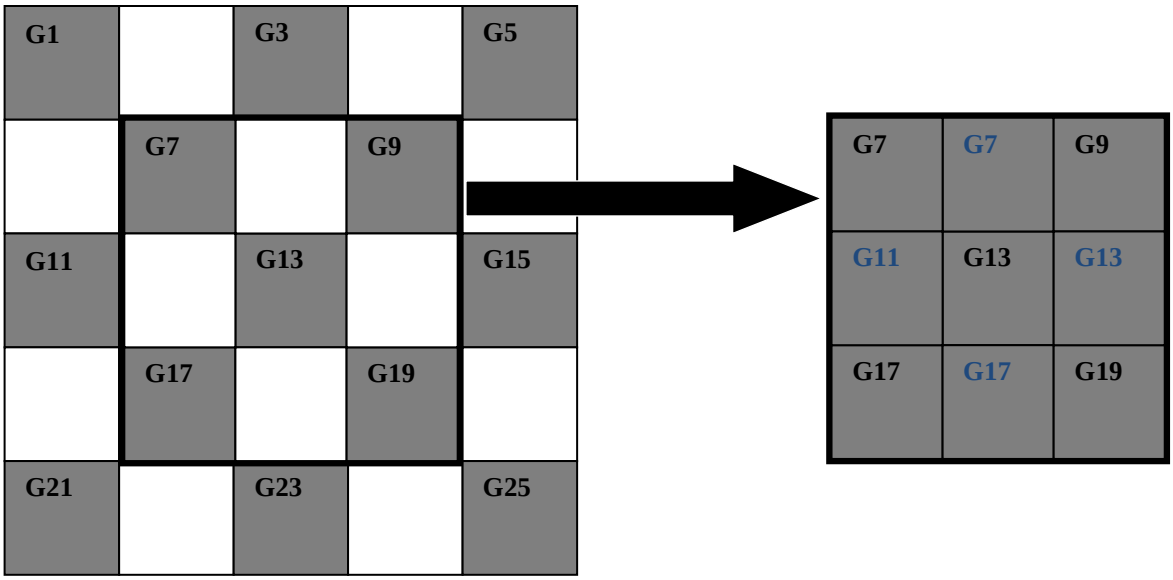

(a) **(b)**

Figure 3.3 Nearest neighbor interpolation (a) Before interpolation, and (b) After interpolation

Figure 3.4 shows an example of nearest neighbor interpolation method. Because it does not alter the grey scale value, a nearest neighbor interpolation is preferred if subtle variations in the grey levels need to be retained [18]. This type of interpolation basically assigns to any point $P(x, y)$ in the plane, the value of the closest data point to *P*. Formally, given a series of data points (x_i, y_i, z_i) , for *i*= 1,2,…..,N, the corresponding nearest-neighbor interpolation function is given by

$$f(x, y) = f(x^*, y^*) \tag{3.2}$$

where $(x^*, y^*)$is the closest data point to (x, y) in the sense of Euclidean distance. In other words, (x^*, y^*)minimizes the following objective function

$$\delta(x_i, y_i) = \sqrt{(x - x_i)^2 + (y - y_i)^2} \tag{3.3}$$

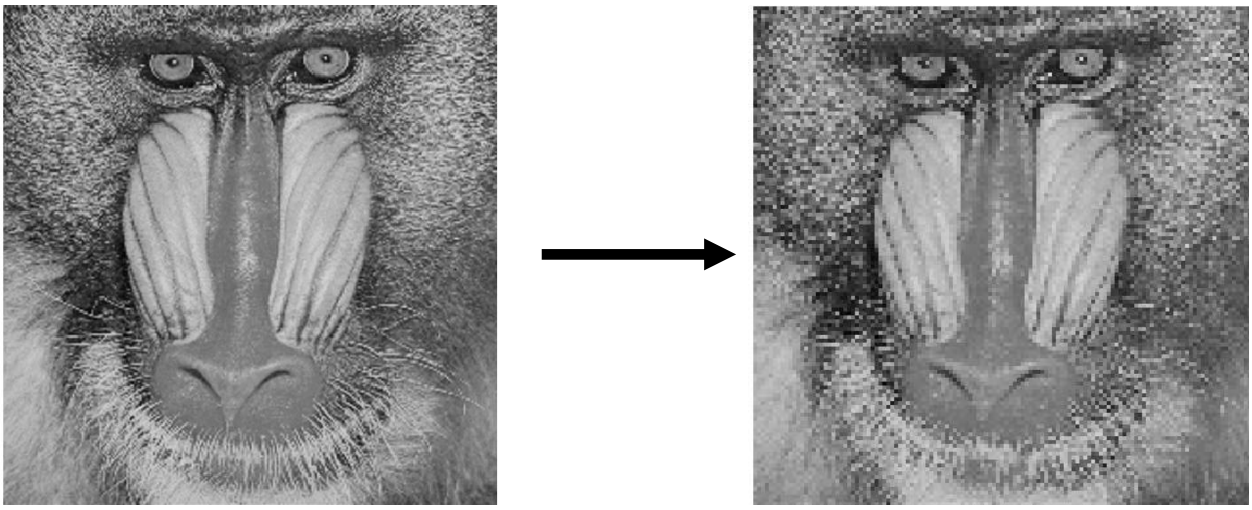

(a) **(b)**

Figure 3.4 (a) Original image, and (b) Nearest neighbor interpolated image

3.3.2 Bilinear interpolation

Bilinear interpolation determines the grey level from the weighted average of the four closest pixels to the specified input coordinates, and assigns that value to the output coordinates, or bilinear interpolation takes a weighted average of 4 pixels in the original image nearest to the new pixel location. Figure 3.5 shows the working of bilinear interpolation.

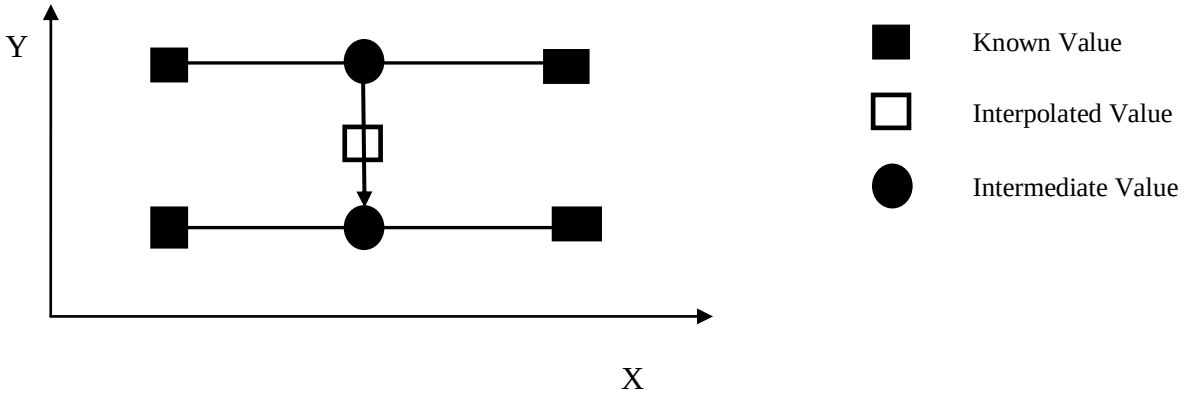

Figure 3.5 Bilinear Interpolation

This method is used to find the value of the unknown function f at the point $P = (x, y)$. It is assumed that the value of f at the four points $Q_{11} = (x_1, y_1)$, $Q_{12} = (x_1, y_2)$, $Q_{21} = (x_2, y_1)$, and $Q_{22} = (x_2, y_2)$.

Apply linear interpolation in the *x*-direction. This yield

$$f(R_1) \approx \frac{x_2 - x}{x_2 - x_1} f(Q_{11}) + \frac{x - x_1}{x_2 - x_1} f(Q_{21}) \tag{3.4}$$

where $R_1=(x,y_1)$

$$f(R_2) \approx \frac{x_2 - x}{x_2 - x_1} f(Q_{12}) + \frac{x - x_1}{x_2 - x_1} f(Q_{22}) \tag{3.5}$$

where $R_1=(x,y_2)$

Apply linear interpolation in the y-direction

$$f(P) \approx \frac{y_2 - y}{y_2 - y_1} f(R_1) + \frac{y - y_1}{y_2 - y_1} f(R_2) \tag{3.6}$$

This gives us the desired estimate of *f (x, y)*

$$f(x,y) \approx \frac{f(Q_{11})}{(x_2 - x_1)(y_2 - y_1)}(x_2 - x)(y_2 - y) + \frac{f(Q_{21})}{(x_2 - x_1)(y_2 - y_1)}(x - x_1)(y_2 - y)$$
$$+ \frac{f(Q_{12})}{(x_2 - x_1)(y_2 - y_1)}(x_2 - x)(y - y_1) + \frac{f(Q_{22})}{(x_2 - x_1)(y_2 - y_1)}(x - x_1)(y - y_1)$$

$$f(x,y) = \frac{1}{(x_2 - x_1)(y_2 - y_1)}[f(Q_{11})(x_2 - x)(y_2 - y) + f(Q_{21})(x - x_1)(y_2 - y)$$
$$+ f(Q_{12})(x_2 - x)(y - y_1) + f(Q_{22})(x - x_1))(y - y_1)] \tag{3.7}$$

This method generates an image of smoother appearance than nearest neighbor, but the grey level values are altered in the process, resulting in blurring or loss of image resolution (equivalent to a low pass filtering). The image is less “blocky” but linear features still remain sharp. Because of these changes in the grey level values, any image classification processes

should be performed before the interpolation [52]. Bilinear interpolation requires 3 to 4 times the computation time of the nearest neighbor method.

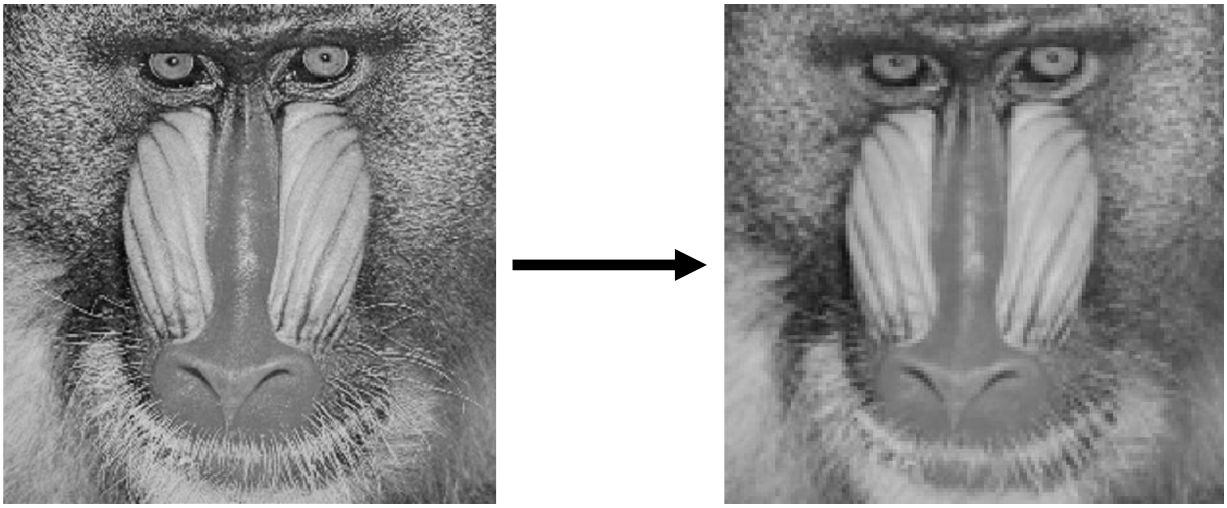

(a) **(b)**

Figure 3.6 (a) Original image, and (b) Bilinear interpolated image

3.3.3 Bicubic Interpolation

Bicubic interpolation uses the closest 4 X 4 area of known pixels surrounding an unknown pixel. It takes an average of the four pixels to create the unknown pixel. The weighted average of the closest 16 pixels is calculated on the basis of distance. Figure 3.7 shows the working of bicubic interpolation.

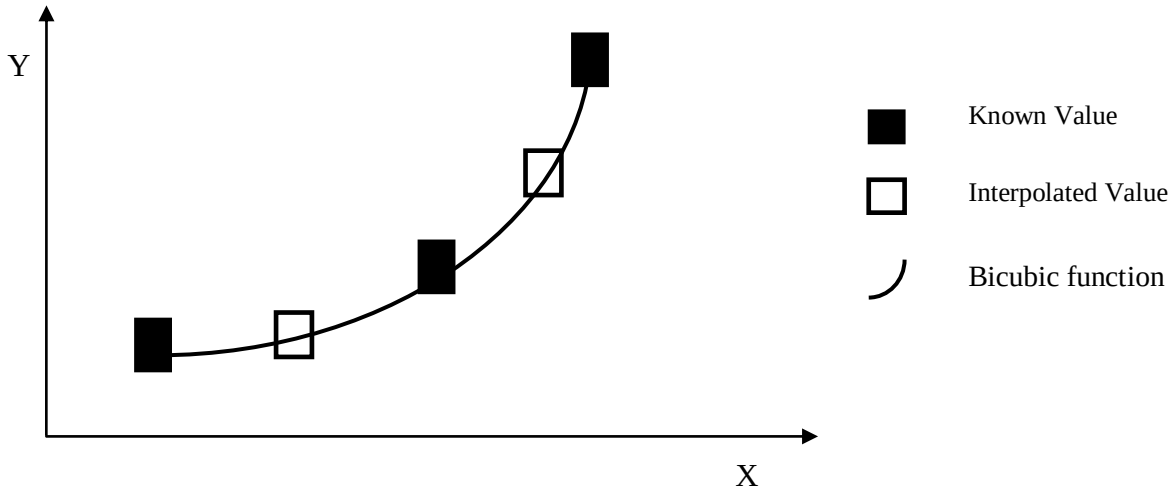

Figure 3.7: Bicubic Interpolation

Suppose the function values f and the derivatives f_x, f_y, f_{xy} are known at four corners (0,0), (0,1), (1,0), (1,1) of the unit square. The interpolated surface can be written as

$$p(x,y) = \sum_{i=0}^{3}\sum_{j=0}^{3} a_{ij}\, x^i y^j \tag{3.8}$$

The bicubic interpolation problem consists of determining the 16 coefficients a_{ij} . Matching $p(x,y)$ with the function values yields the four equations,

$$f(0,0) = p(0,0) = a_{00} \tag{3.9.1}$$

$$f(0,1) = p(0,1) = a_{00} + a_{01} + a_{02} + a_{03} \tag{3.9.2}$$

$$f(1,0) = p(1,0) = a_{00} + a_{10} + a_{20} + a_{30} \tag{3.9.3}$$

$$f(1,1) = p(1,1) = \textstyle\sum_{i=0}^{3}\sum_{j=0}^{3} a_{ij} \tag{3.9.4}$$

Apply bicubic interpolation in x-direction

$$f_x(0,0) = p_x(0,0) = a_{10} \tag{3.10.1}$$

$$f_x(0,1) = p_x(0,1) = a_{10} + a_{11} + a_{12} + a_{13} \tag{3.10.2}$$

$$f_x(1,0) = p_x(1,0) = a_{10} + 2a_{20} + 3a_{30} \tag{3.10.3}$$

$$f_x(1,1) = p_x(1,1) \textstyle\sum_{i=0}^{3}\sum_{j=0}^{3} a_{ij}{}^{i} \tag{3.10.4}$$

Apply bicubic interpolation in y-direction

$$f_y(0,0) = p_y(0,0) = a_{01} \tag{3.11.1}$$

$$f_y(0,1) = p_y(0,1) = a_{01} + 2a_{02} + 3a_{03} \tag{3.11.2}$$

$$f_y(1,0) = p_y(1,0) = a_{01} + a_{11} + a_{21} + a_{31} \tag{3.11.3}$$

$$f_x(1,1) = p_x(1,1) = \textstyle\sum_{i=0}^{3}\sum_{j=0}^{3} a_{ij}{}^{j} \tag{3.11.4}$$

Apply bicubic interpolation in x y-direction (cross derivative)

$$f_{xy}(0,0) = p_{xy}(0,0) = a_{11} \tag{3.12.1}$$

$$f_{xy}(0,1) = p_{xy}(0,1) = a_{11} + 2a_{12} + 3a_{13} \tag{3.12.2}$$

$$f_{xy}(1,0) = p_{xy}(1,0) = a_{11} + 2a_{21} + 3a_{31} \tag{3.12.3}$$

$$f_{xy}(1,1) = p_{xy}(1,1) = \sum_{i=0}^{3} \sum_{j=0}^{3} a_{ij}{}^{ij} \tag{3.12.4}$$

These equations help to find the coefficients a_{ij} and bicubic interpolation function $p(x, y)$. The image produced by bicubic interpolation is slightly sharper than that produced by bilinear interpolation and it does not have the disjointed appearance produced by nearest neighbor interpolation.

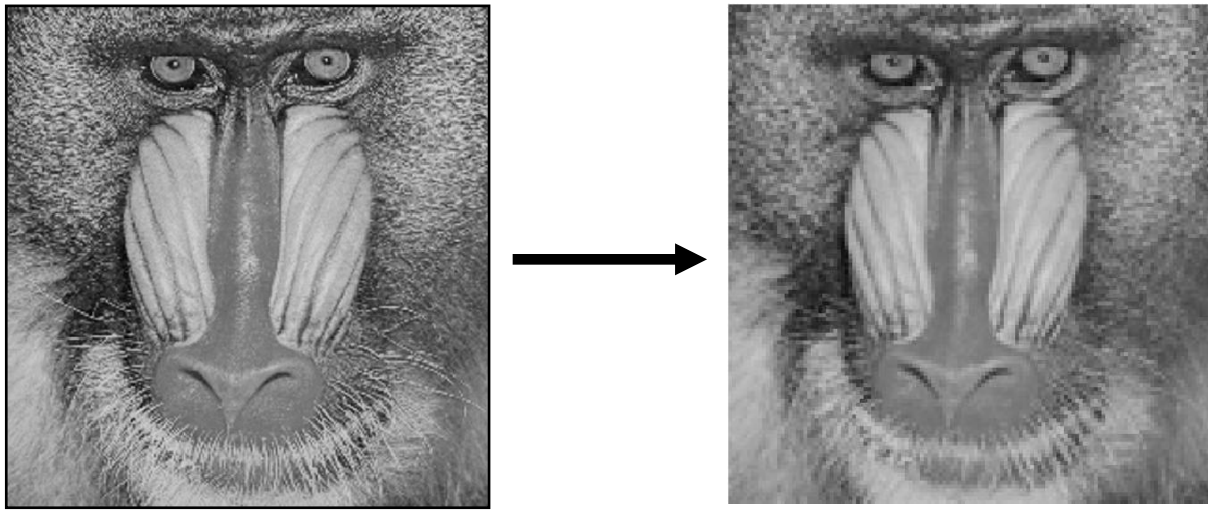

(a) **(b)**

Figure 3.8 (a) Original image, and (b) Bicubic interpolated image

3.4 IMAGE INTERPOLATION EXAMPLE

The goal of image interpolation is to produce acceptable images at different resolutions from a single LR image. The actual resolution of an image is defined as the number of pixels, but the effective resolution is a much harder quantity to define as it depends on subjective human judgment and perception. Some image interpolation examples [10] are chosen to demonstrate the

effects of three interpolation method in Figure 3.9. The main problem of the nearest-neighbor interpolation is jaggedness while the main problem associated with bilinear interpolation is image blurring. Bicubic interpolation adds proper high frequency information to the image and reduces blurring effects at the same time.

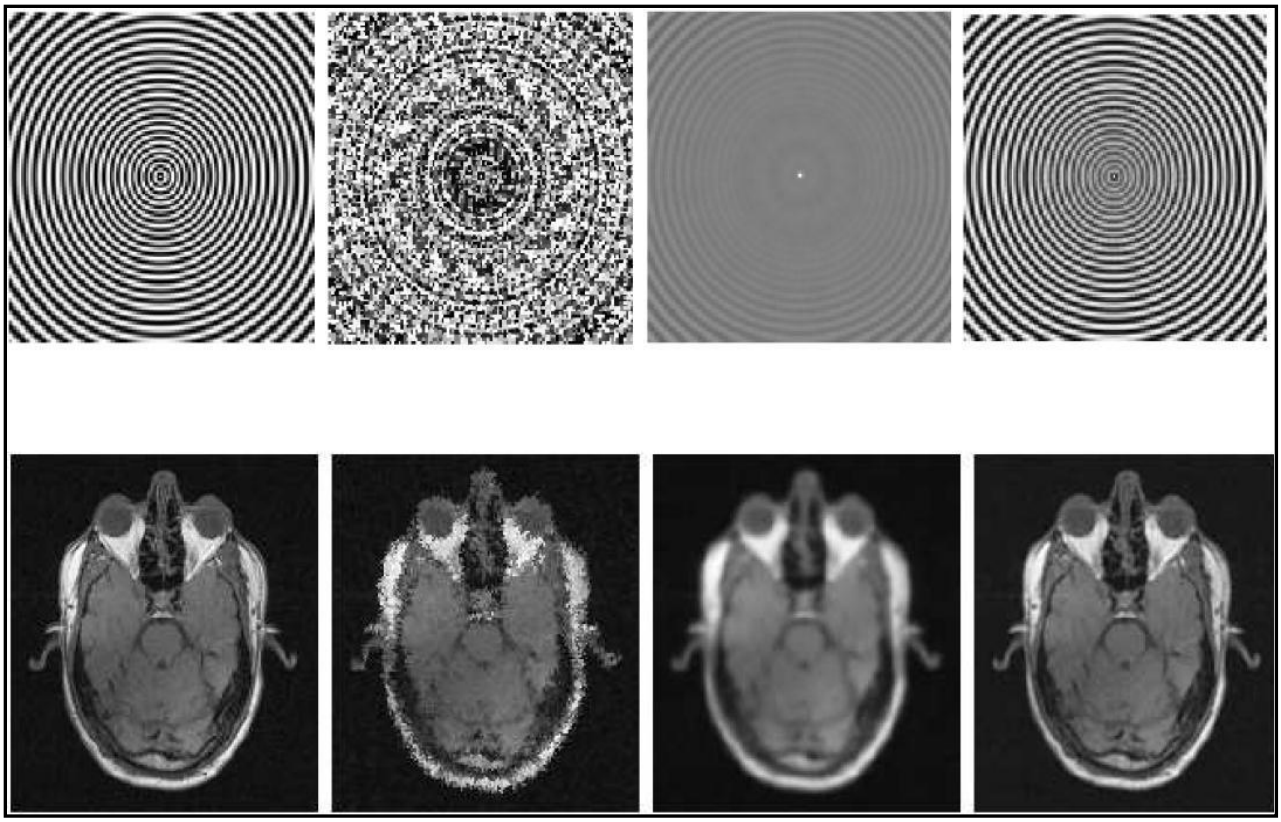

(a) **(b)** **(c)** **(d)**

Figure 3.9 Effects of image interpolation (a) Original image, (b) Nearest neighbor interpolated image, (c) Bilinear interpolated image, and (d) Bicubic interpolated image [10]

CHAPTER 4

WAVELET TRANSFORMS

4.1 INTRODUCTION

Wavelet and its theory is one of the most exciting developments in the last decade. In fact, WT has been developed independently for various fields such as signal processing, image processing, speech processing, communication and applied mathematics. Due to the wavelet representation has characteristics of the efficient time-frequency localization and MRA, the WT are suitable for processing image resolution enhancement. The first literature that relates to the WT is Haar wavelet. It was proposed by the mathematician Alfrd Haar in 1909. However, the concept of the wavelet did not exist at that time. Until 1981, the concept was proposed by the Jean Morlet. Afterward, Morlet and Alex Grossman invented the term wavelet in 1984. Before 1985, Haar wavelet was the only orthogonal wavelet people know. A lot of researchers even thought that there was no orthogonal wavelet except Haar wavelet. Fortunately, the mathematician Yves Meyer constructed the second orthogonal wavelet called Meyer wavelet in 1985. In 1988, Stephane Mallat and Meyer proposed the concept of multi resolution. In the same year, Ingrid Daubechies found a systematical method to construct the compact support orthogonal wavelet. In 1989, Mallat proposed the fast wavelet transform. With the appearance of this fast algorithm, the wavelet transform had numerous applications in the field of image processing [13].

4.2 CLASSIFICATION OF WAVELETS

We can classify wavelets into two classes: (a) orthogonal and (b) bi-orthogonal. Based on the application, either of them can be used [14].

(a) Features of orthogonal wavelet filter banks

The coefficients of orthogonal filters are real numbers. The filters are of the same length and are not symmetric. The low pass filter and the high pass filter are alternated flip of each other. The alternating flip automatically gives double-shift orthogonality between the low pass and high pass filters. For Perfect reconstruction, the synthesis filters should be identical to the analysis filters except for a time reversal. Orthogonal filters offer a high number of vanishing moments.

This property is useful in many signal and image processing applications. They have regular structure which leads to easy implementation and scalable architecture. Figure 4.1 shows a Four-coefficient Daubechies Wavelet.

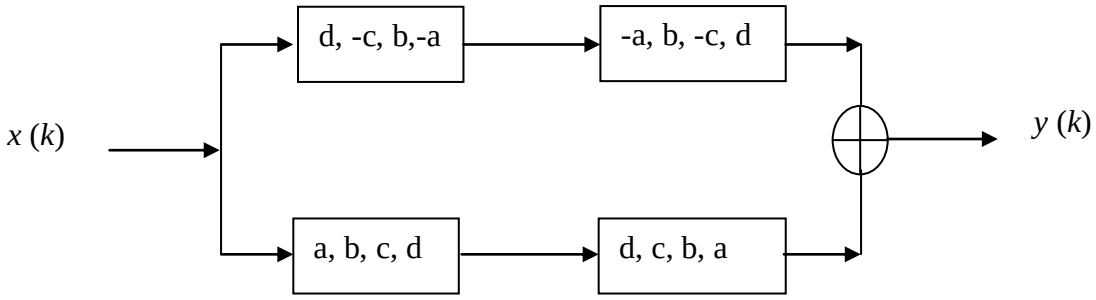

Figure 4.1 Four coefficient Daubechies Wavelet Filter Bank [17]

(b) Features of bi- orthogonal wavelet filter banks

In the case of the bi-orthogonal wavelet filters, the low pass and the high pass filters do not have the same length. The low pass filter is always symmetric, while the high pass filter could be either symmetric or anti-symmetric. The coefficients of the filters are either real numbers or integers. Figure 4.2 shows bi-orthogonal wavelet filter bank. For perfect reconstruction, bi-orthogonal filter bank has all odd length or all even length filters. The two analysis filters can be symmetric with odd length or one symmetric and the other anti symmetric with even length.

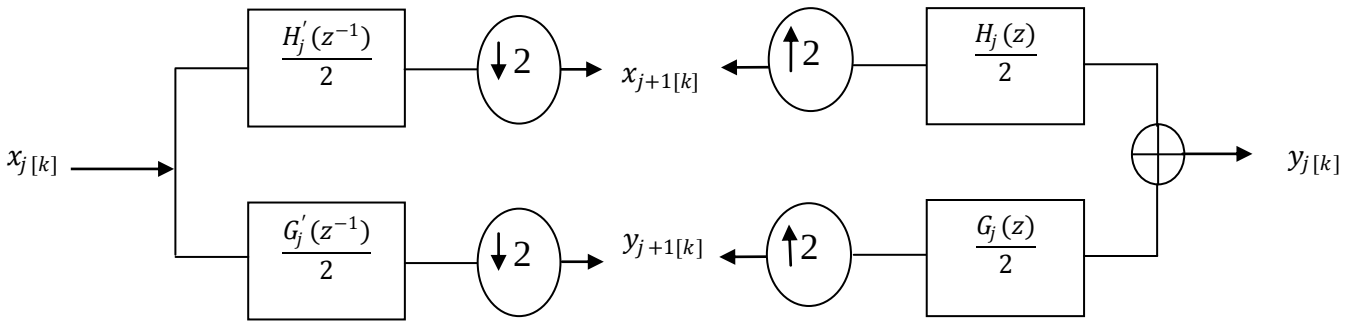

Figure 4.2 Bi-orthogonal Wavelet Filter Bank [17]

4.3 WAVELET FAMILIES

There are a number of basis functions that can be used as the mother wavelet for wavelet transformation. Since the mother wavelet produces all wavelet functions used in the transformation through translation and scaling, it determines the characteristics of the resulting WT. Therefore, the details of the particular application should be taken into account and the appropriate mother wavelet should be chosen in order to use the WT effectively. Figure 4.3 illustrates some of the commonly used wavelet functions [53]. Haar wavelet is one of the oldest and simplest wavelet. Daubechies wavelets are the most popular wavelets. They represent the foundations of wavelet signal processing and are used in numerous applications. These are also called Maxflat wavelets as their frequency responses have maximum flatness at frequencies 0 and π. This is a very desirable property in some applications. The Haar, Daubechies, Symlets and Coiflets are compactly supported orthogonal wavelets. These wavelets along with Meyer wavelets are capable of perfect reconstruction. The Meyer, Morlet and Mexican Hat wavelets are symmetric in shape. The wavelets are chosen based on their shape and their ability to analyze the signal in a particular application. WTcan be represented in continuous as well as discrete domain as follows:

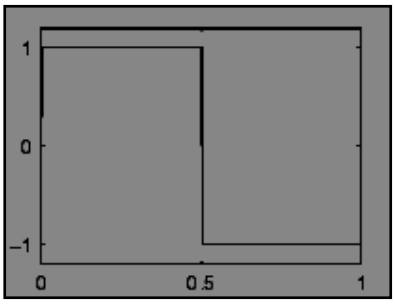

(a)

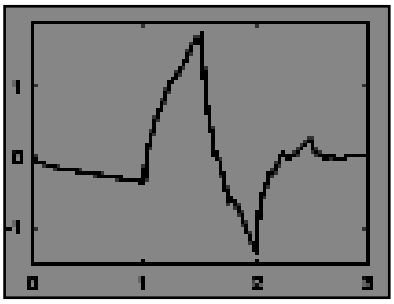

(b)

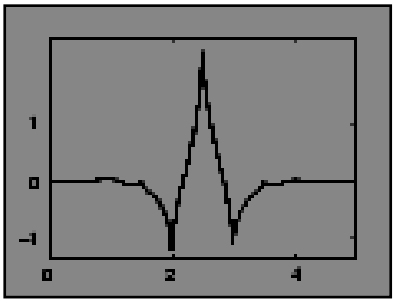

(c)

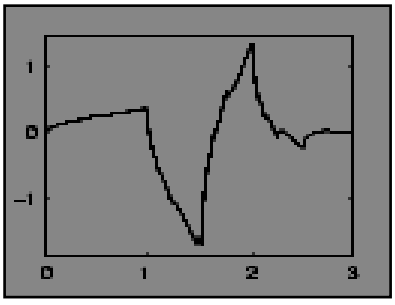

(d)

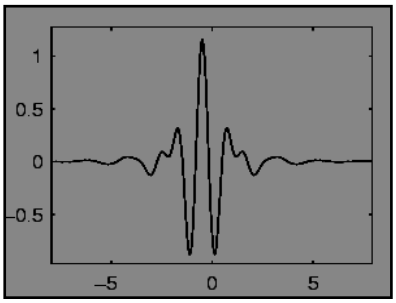

(e)

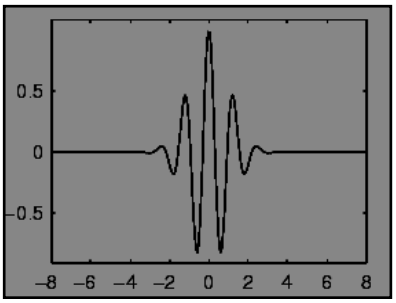

(f)

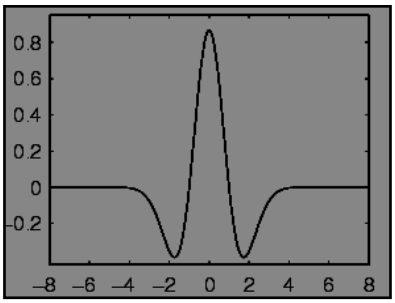

(g)

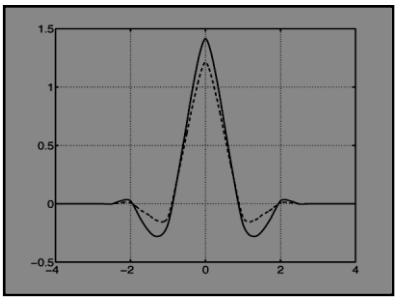

(h)

Figure 4.3 Wavelet families (a) Haar, (b) Daubechies 4, (c) Coiflet, (d) Symlet2, (e) Meyer, (f) Morlet, (g) Mexican Hat, and (h) Bi-orthogonal wavelet [53]

4.4 CONTINUOUS WAVELET TRANSFORM

Continous wavelet transform is provided by equation (4.1). All the wavelet functions used in the transformation are derived from the mother wavelet through translation (shifting) and scaling (dilation or compression). The formal definition of Continous wavelet transform follows:

Given a continuous time signal $f(t), -\infty\ to + \infty$, its CWT $W(s,\tau)$ is defined as

$$W(s,\tau) = \left[f(t), \varphi_{s,\tau}\right] = \int_{-\infty}^{+\infty} f(u)\varphi_{s,\tau}(u)du \qquad (4.1)$$

The translation parameter $\boldsymbol{\tau}$ relates to the location of the wavelet function as it is shifted through the signal. Thus, it corresponds to the time information in the Wavelet Transform. The scale parameter $\boldsymbol{s}$ is defined as |1/frequency| and corresponds to frequency information. Scaling either dilates (expands) or compresses a signal. Large scales (low frequencies) dilate the signal and provide detailed information hidden in the signal, while small scales (high frequencies) compress

the signal and provide global information about the signal [54]. The mother wavelet used to generate all the basis functions and is based on some desired characteristics associated with that function and is given by

$$\varphi_{s,\tau}(t) = \frac{1}{\sqrt{s}}\left(\frac{t}{\tau - s}\right) \tag{4.2}$$

WT merely performs the convolution operation of the signal and the basis function. The above analysis becomes very useful as in most practical applications, high frequencies (low scales) do not last for a long duration, but instead, appear as short bursts, while low frequencies (high scales) usually last for entire duration of the signal.

4.5 WAVELET SERIES

If the scale and shift parameters in equation (4.1) are discrete rather than continuous, then it is possible to expand $f(t)$ in a wavelet series, that is, summation rather than integral. More specifically, if the scale parameter is allowed to take on values that are integer power of two (called binary scaling) and the shift parameter is allowed to take on integer values (known as dyadic translation), then the wavelet series of $f(t)$ is expanded in terms of infinite sum of scaling functions and infinite sum of wavelets. Thus, the wavelet series of $f(t)$ is written as

$$f(t) = \sum_{k} a(j_0, k)\emptyset_{j_0,k}(t) + \sum_{j=j_0}^{\infty}\sum_{k=-\infty}^{+\infty} d(j,k)\varphi_{j,k}(t) \tag{4.3}$$

We can see here that $f(t)$ need not be periodic in order for us to expand it in a wavelet series. Corresponding to the scaling and wavelet functions, the coefficients $a(j_0, k)$ are called the scaling coefficients and the $d(j,k)$ coefficients are called the detail coefficients [55].

4.6 DISCRETE WAVELET TRANSFORM

The Wavelet Series is just a sampled version of Continuous wavelet transform and its computation may consume significant amount of time and resources, depending on the resolution required. DWT, which is based on sub-band coding, is found to yield a fast computation of

Wavelet Transform. It is easy to implement and reduces the computation time and resources required. In Continuous wavelet transform, the signals are analyzed using a set of basis functions which relate to each other by simple scaling and translation. In the case of DWT, a time-scale representation of the digital signal is obtained using digital filtering techniques. The signal to be analyzed is passed through filters with different cut-off frequencies at different scales.

One drawback of the Continuous wavelet transform is that the representation of the signal is often redundant. Due to the orthonormal properties, there is no information redundancy in the discrete wavelet transform [55]. Mathematically, DWT for an *N*-point sequence $x(n), 0 \leq n \leq N-1$ can be written as

$$DWT = \{f(t)\} = W_{\emptyset}(j_0, k) + W_{\varphi}(j, k) \tag{4.4}$$

where,

$$W_{\emptyset}(j_0, k) = \frac{1}{\sqrt{N}} \sum_{n=0}^{N-1} x(n)\, \emptyset_{j_0,k}(n) \tag{4.5}$$

$$W_{\varphi}(j, k) = \frac{1}{\sqrt{N}} \sum_{n=0}^{N-1} x(n)\, \varphi_{j,k}(n) \qquad j \geq j_0 \tag{4.6}$$

The sequence $x(n), 0 \leq n \leq N-1$ can be recovered from DWT coefficients, $W_{\emptyset}\ and\ W_{\varphi}$ as given by

$$x(n) = \frac{1}{\sqrt{N}} W_{\emptyset}(j_0, k) \emptyset_{j_0,k}(n) + \frac{1}{\sqrt{N}} \sum_{j=j_0}^{\infty} \sum_{k} W_{\varphi}(j, k) \varphi_{j_0,k}(n) \tag{4.7}$$

In Wavelet analysis, a signal can be divided into two parts namely approximation and details. The resolution of the signal is a measure of the amount of detail information in the signal and is determined by the filtering operations, and the scale is determined by up sampling and down sampling operations. The DWT is computed by successive low pass and high pass filtering of the discrete time-domain signal as shown in Figure 4.4.

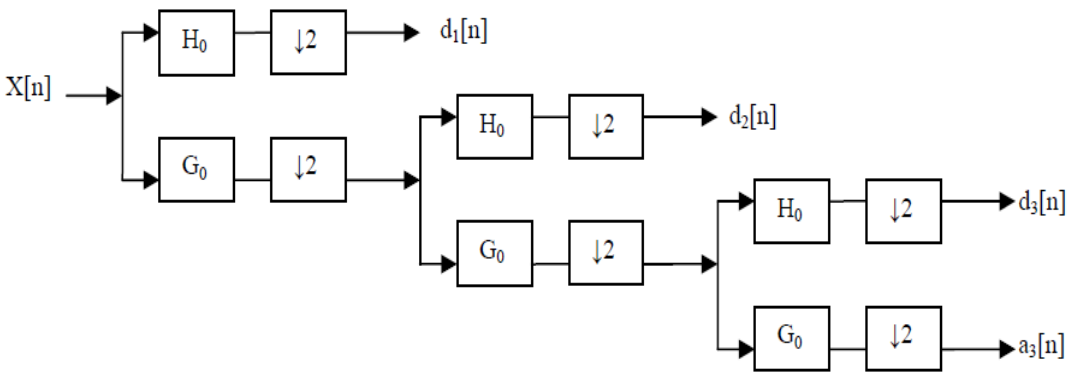

Figure 4.4 Block Diagram of three level wavelet decompositions [6]

This is called the Mallat algorithm or Mallat-tree decomposition. The signal is denoted by the sequence x[n], where n is an integer [49]. The low pass filter is denoted by G_0 while the high pass filter is denoted by H_0. At each level, the high pass filter produces detail information d[n], while the low pass filter associated with scaling function produces coarse approximations a[n].

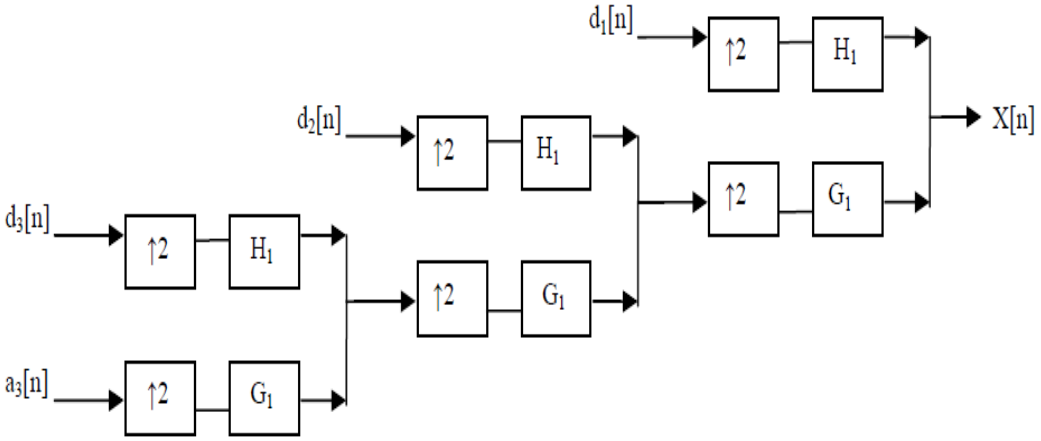

Figure 4.5 Block Diagram of three level wavelet reconstructions [49]

At each decomposition level, the half band filters produce signals spanning only half the frequency band. This doubles the frequency resolution as the uncertainty in frequency is reduced by half. In accordance with Nyquist's rule if the original signal has a highest frequency of ω, which requires a sampling frequency of 2ω radians, then it now has a highest frequency of ω/2 radians. It can now be sampled at a frequency of ω radians thus discarding half the samples with no loss of information. This decimation by 2 halves the time resolution as the entire signal is now represented by only half the number of samples. Thus, while the half band low pass filtering removes half of the frequencies and thus halves the resolution, the decimation by 2 doubles the scale. So, we can say that DWT is designed to give good time resolution and poor frequency resolution at high frequencies and good frequency resolution and poor time resolutions at low frequencies. This approach makes sense when signal has high frequency components for short durations and low frequency components for long durations. The filtering and decimation process is continued until the desired level is reached. The maximum number of levels depends on the length of the signal. The DWT of the original signal is then obtained by concatenating all the coefficients, a[n] and d[n], starting from the last level of decomposition.

Figure 4.5 shows the reconstruction of the original signal from the wavelet coefficients. Basically, the reconstruction is the reverse process of decomposition. The approximation and detail coefficients at every level are upsampled by two, passed through the low pass and high pass synthesis filters and then added. This process is continued through the same number of levels as in the decomposition process to obtain the original signal. The Mallat algorithm works equally well if the analysis filters, G_0 and H_0, are exchanged with the synthesis filters, G_1 and H_1. Due to filtering and sub sampling by 2, the filtered signals suffer from aliasing distortion. Similarly, up sampling followed by filtering introduces image frequency. Therefore, use of low pass and high pass filters with arbitrary frequency responses will result in a synthesized signal that suffers from aliasing and image distortions even without any signal quantization. This problem is negated when the analysis and synthesis filters satisfy certain properties. This results in what is known as the QMF bank. Because of certain symmetries that exist between the analysis and synthesis filters, the filtering becomes very efficient.

4.6.1 Two Dimensional Discrete Wavelet Transform

The DWT is extensively used in its non-redundant form known as standard DWT. Images are 2-D and are analyzed using a separable 2-D wavelet transform. As we know that in 2-D Fourier Transform, the basis are modified into

$$\exp\big(j(\omega t1 + \omega t2)\big) \tag{4.8}$$

instead of $\exp(j\omega t)$. The transformed coefficients become two variable functions so as the 2D wavelet transform. The scaling and wavelet function are two variable functions can be denoted as $\emptyset(x, y)$ and $\varphi(x, y)$. The scaled and translated basis functions are defined as

$$\emptyset_{j0,m,n}(x, y) = 2^{j/2}\emptyset\big(2^j x - m, 2^j y - n\big),$$

$$\varphi_{j,m,n}(x, y) = 2^{j/2}\varphi^i\big(2^j x - m, 2^j y - n\big) \tag{4.9}$$

$$i = \{H, V, D\}$$

There are three different wavelet functions, $\varphi^H(x, y), \varphi^V(x, y), \varphi^D(x, y)$. conceptually; the scaling function is the low frequency component of the previous scaling function in two dimensions. Therefore, there is one 2-D scaling function. However, the wavelet function is related to the order to apply the filters [51]. If the wavelets function is separable, i.e. $f(x, y) = f_1(x)f_2(y)$. These wavelet functions can be rewritten as

$$\emptyset(x, y) = \emptyset(x)\emptyset(y) \tag{4.10.1}$$

$$\varphi^H(x, y) = \varphi(x)\emptyset(y) \tag{4.10.2}$$

$$\varphi^V(x, y) = \emptyset(x)\varphi(y) \tag{4.10.3}$$

$$\varphi^D(x, y) = \varphi(x)\varphi(y) \tag{4.10.4}$$

With the help of scaled and translated basis function, we can define the discrete wavelet transform for the image which can be found from equation 4.11.1 to equation 4.11.4, where M

and N represent the number of columns and number of rows respectively. *H, V, D,* $W_{\emptyset}(j_0, m, n)$, $W_{\varphi}^{H}(j, m, n)$, $W_{\varphi}^{V}(j, m, n)$, $W_{\varphi}^{D}(j, m, n)$ represents horizontal, vertical, diagonal, approximate coefficients at scale j_0 which is usually equal to 0, horizontal, vertical, and diagonal detail coefficients at scale j where $j \geq j_0$ respectively [51].

$$W_{\emptyset}(j_0, m, n) = \frac{1}{\sqrt{MN}} \sum_{x=0}^{M-1} \sum_{y=0}^{N-1} f(x, y)\, \emptyset_{j_0, m, n}(x, y) \tag{4.11.1}$$

$$W_{\varphi}^{H}(j, m, n) = \frac{1}{\sqrt{MN}} \sum_{x=0}^{M-1} \sum_{y=0}^{N-1} f(x, y)\, \varphi^{H}{}_{j, m, n}(x, y) \tag{4.11.2}$$

$$W_{\varphi}^{V}(j, m, n) = \frac{1}{\sqrt{MN}} \sum_{x=0}^{M-1} \sum_{y=0}^{N-1} f(x, y)\, \varphi^{V}{}_{j, m, n}(x, y) \tag{4.11.3}$$

$$W_{\varphi}^{D}(j, m, n) = \frac{1}{\sqrt{MN}} \sum_{x=0}^{M-1} \sum_{y=0}^{N-1} f(x, y)\, \varphi^{D}{}_{j, m, n}(x, y) \tag{4.11.4}$$

The IDWT is used for the reconstruction of an image. Mathematically it can be expressed as:

$$\begin{aligned} f(x, y) = {} & \frac{1}{\sqrt{MN}} \sum_{m} \sum_{n} W_{\emptyset}(j_0, m, n) \emptyset_{j_0, m, n}(x, y) \\ & + \frac{1}{\sqrt{MN}} \sum_{i=H,V,D} \sum_{j=j_0}^{\infty} \sum_{m} \sum_{n} W_{\varphi}^{i}(j, m, n) \varphi_{j, m, n}(x, y) \end{aligned} \tag{4.12}$$

A 2-D separable transform is equivalent to two 1-D transforms in series. The functionality of wavelets in 2-D is that the columns of the original image is passed through a high-pass and low-pass filter. Then the rows of the filtered image are passed through the high-pass and low-pass filter. If the image is transformed by another level, then the approximate coefficients will be used to transform the image. Each passes through the filter decrease both the row and column by a multiple of two. Figure 4.6 depicts a one level 2-D DWT of an image of size M X N pixels.

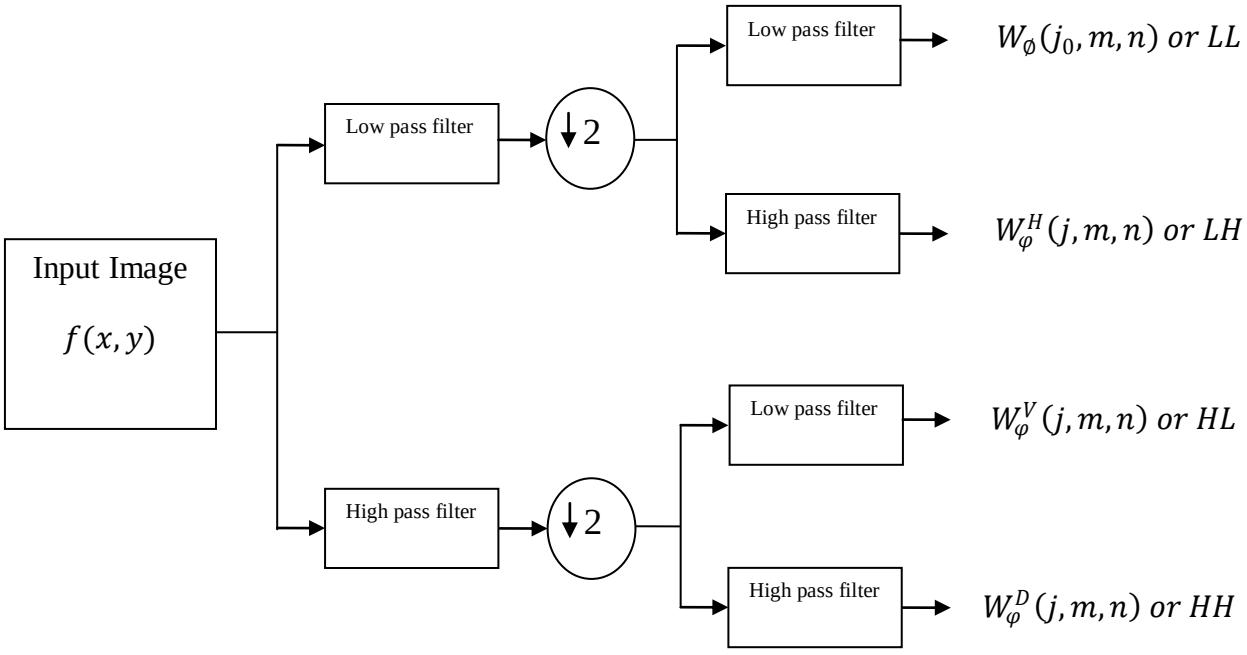

Figure 4.6 Block Diagram of one level 2-D DWT

After the wavelet decomposition has been completed, the image will be divided into four sub images which are the approximate, horizontal, vertical, and diagonal. In order to obtain the approximate coefficients, the rows and columns are passed through the low-pass filter which resembles the original image, but at a smaller resolution. Next the horizontal coefficients are obtained by passing the rows through the low-pass filter and the columns through the high-pass filter which will emphasize the horizontal edges. Also the vertical coefficients obtained by passing the columns through the low-pass filter and the rows through the high-pass filter that will stress the vertical edges. The diagonal coefficients are obtained by passing rows and columns through high pass filter. Figure 4.7 and 4.8 shows the procedure of getting multi-resolution of an image. In one level 2-D DWT, we get 1 set of approximation coefficient (LL) and 3 sets of detailed coefficients (LH, HL, and HH). In two level 2-D DWT, we get total 7 sets of coefficients. At first level, 3 detailed coefficients (LH, HL, and HH) and in the second level, 1 set of approximation coefficient (LL2) and 3 sets of detailed coefficients (LH2, HL2 and HH2).

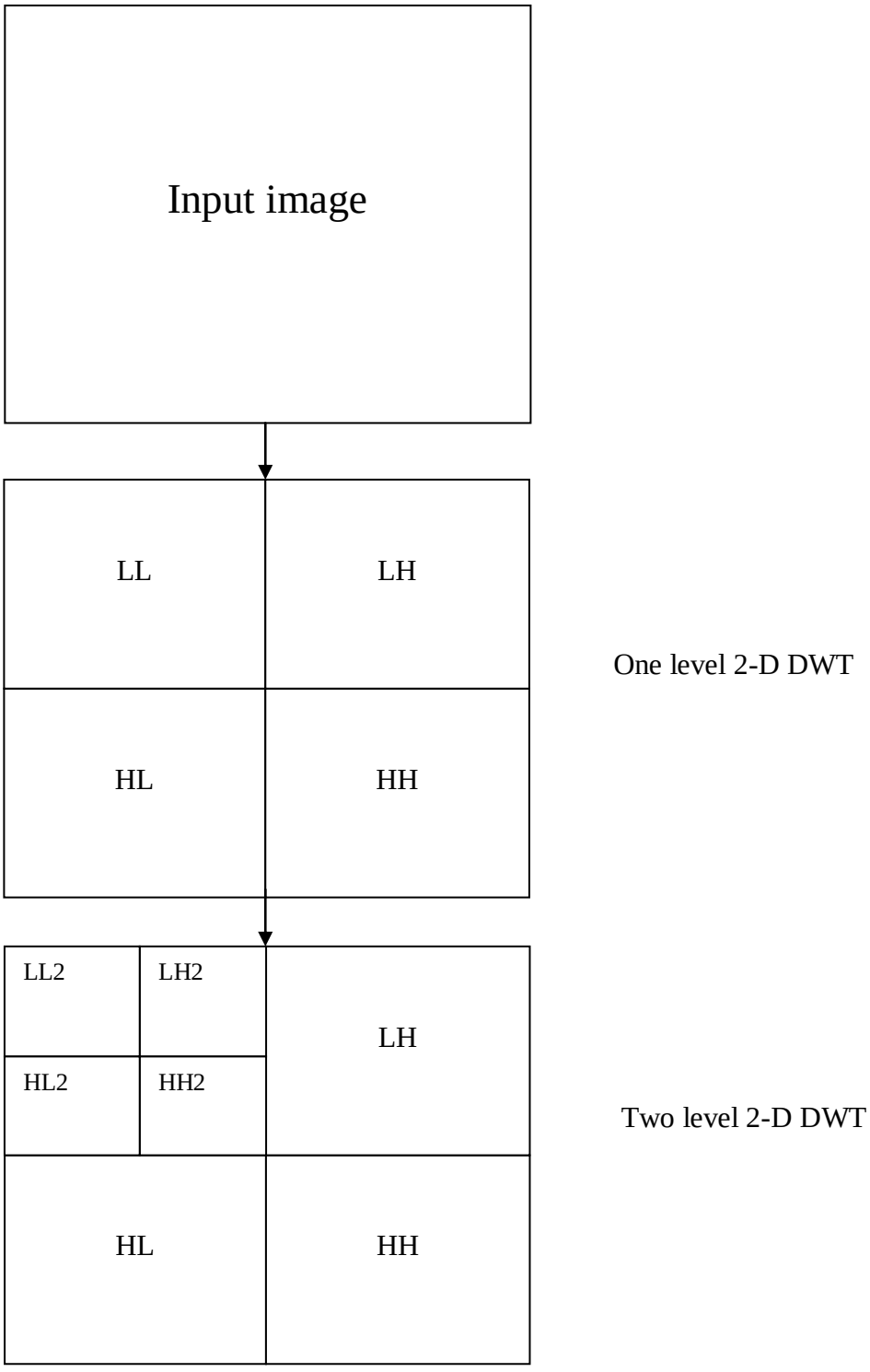

Figure 4.7 One level and two level subbands of 2-D DWT


50
100
150
200
250
300
350
400
450
500

(a)

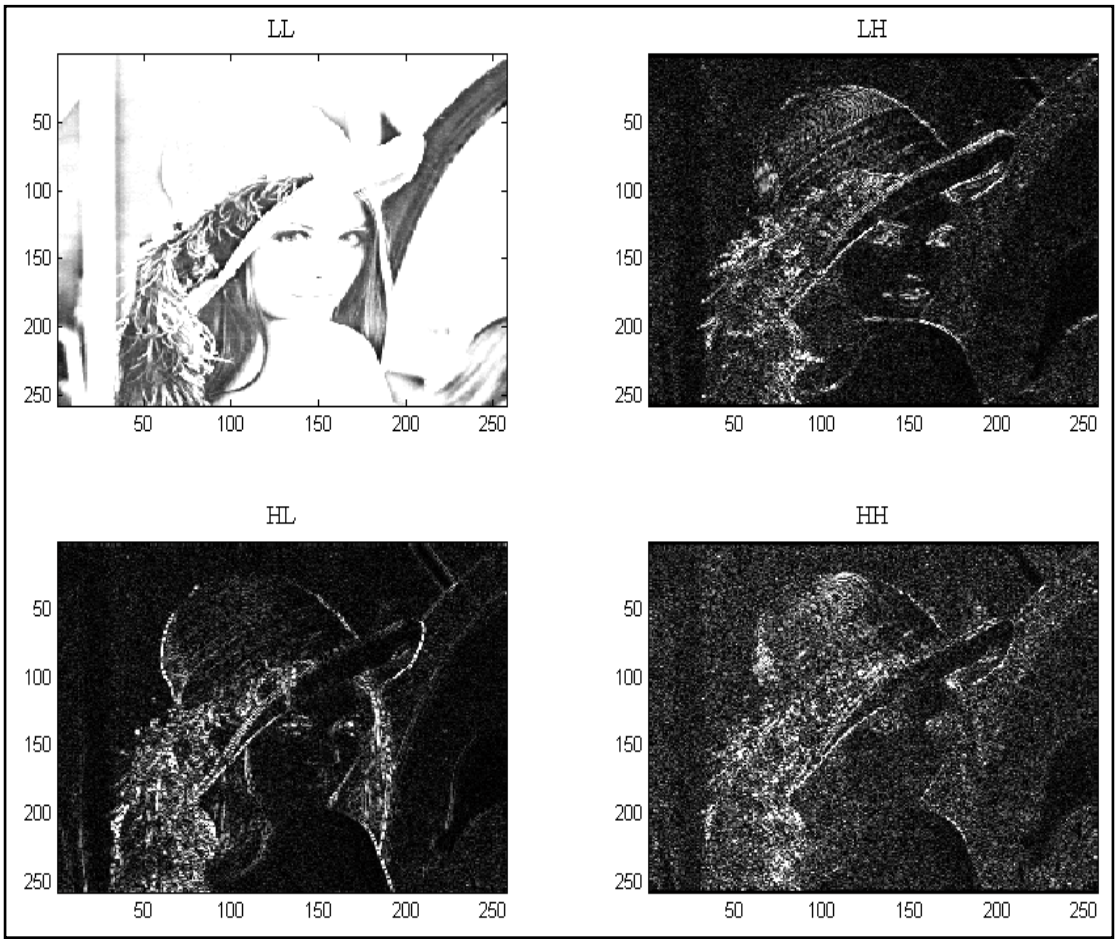
LL
LH
HL
HH
50
100
150
200
250

(b)

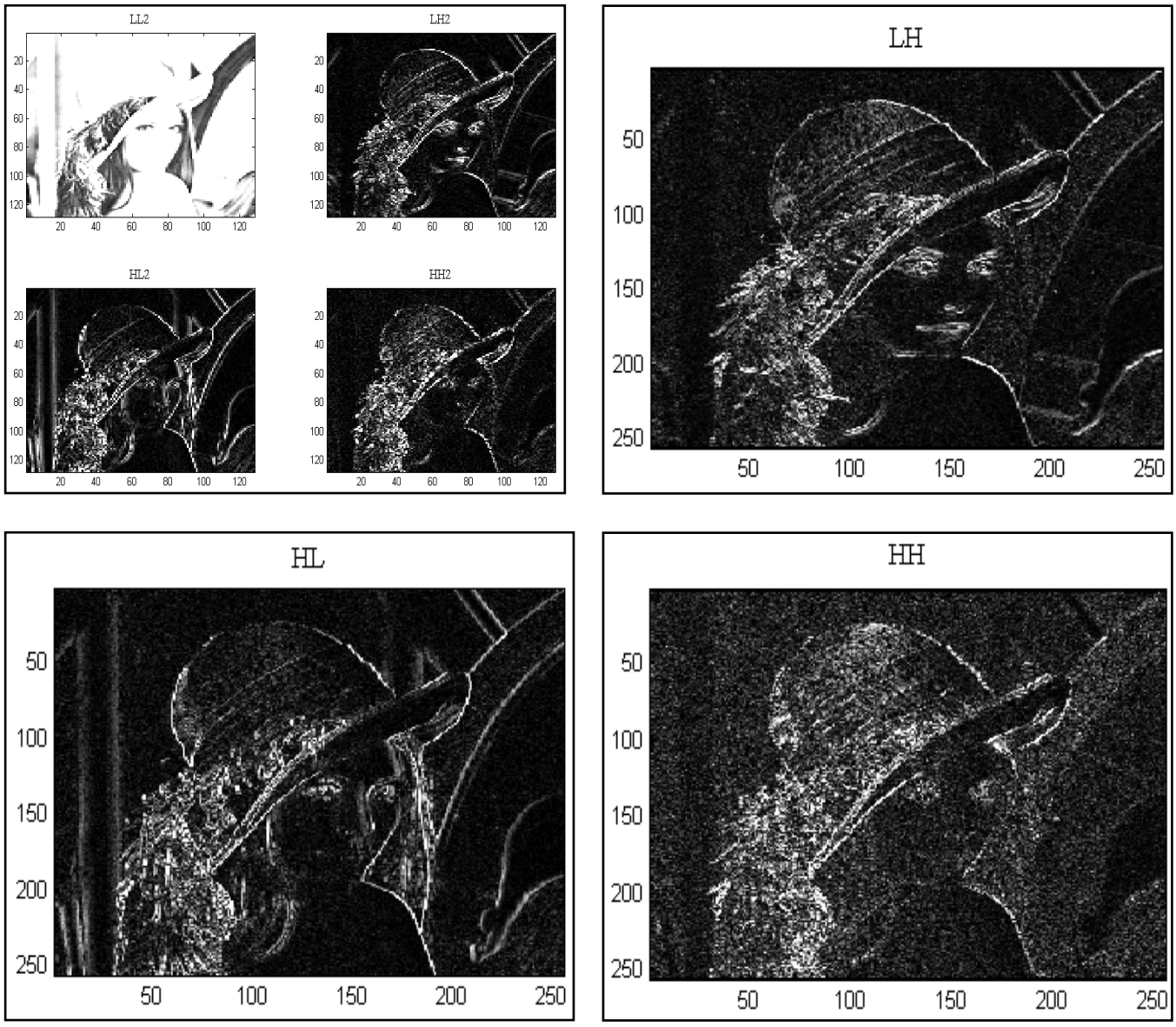

(c)

Figure 4.8 (a) Input image, (b) One level, and (c) Two level 2-D DWT of an image

4.7 STATIONARY WAVELET TRANSFORM

SWT is similar to the DWT in that the high-pass and low-pass filters are applied to the input signal at each level. However, in the SWT, the output signal is never sub sampled (not decimated). Instead, the filters are up sampled at each level [44]. Suppose we are given a signal $x[n]$ of length N where N = 2 j for some integer j. Let $h_1[n]$ and $g_1[n]$ be the low-pass filter and the high-pass filter defined by a orthogonal wavelet. At the first level of SWT, the input signal

$x[n]$ is convolved with $h_1[n]$ to obtain the approximation coefficients $a_1[n]$, and convolved with $g_1[n]$ to obtain the detail coefficients $d_1[n]$.

$$a_1[n] = h_1[n] * x[n] = \sum_k h_1[n-k]x[k] \quad (4.13)$$

$$d_1[n] = g_1[n] * x[n] = \sum_k g_1[n-k]x[k] \quad (4.14)$$

Because no sub sampling is performed, $a_1[n]$ and $d_1[n]$ are of length N instead of N=2 as in the DWT case. At the next level of the SWT, $a_1[n]$ is split into two parts using the same scheme, but with modified filters $h_2[n]$ and $g_2[n]$ obtained by dyadically upsampling $h_1[n]$ and $g_1[n]$. This process is continued recursively. For $j = 1, 2, \ldots, j_0 - 1$, where $j_0 \leq j$, we define

$$a_{j+1}[n] = h_{j+1}[n] * a_j[n] = \sum_k h_{j+1}[n-k]a_j[k] \quad (4.15)$$

$$d_{j+1}[n] = g_{j+1}[n] * a_j[n] = \sum_k g_{j+1}[n-k]a_j[k] \quad (4.16)$$

where, $h_{j+1}[n]$ = UpSample $h_j[n]$ and $g_{j+1}[n]$ = Up Sample $g_j[n]$. Here UpSample (x$[n]$) is the up sampling operator that inserts a zero between every adjacent pair of elements of x$[n]$.The output of the SWT is then the detail coefficients $d_1[n].d_2[n]\ldots\ldots, d_{jo}[n]$ and the approximation coefficients$a_j[n]$. The general idea of SWT denoising is to zero out small wavelet coefficients whose absolute values are below a certain threshold¸ in the detail coefficients $d_1[n], d_2[n], \ldots\ldots, d_{jo}[n]$, and then reconstruct the signal using the thresholded detail coefficients and the intact $a_{jo}[n]$.

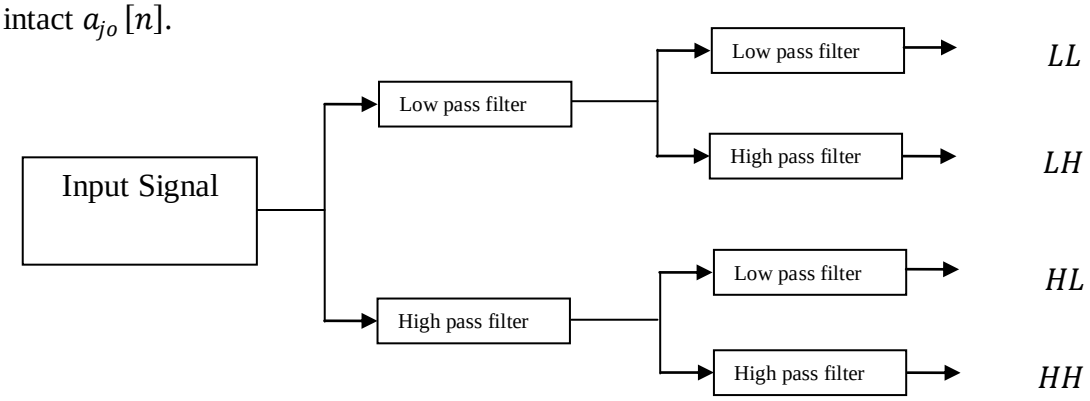

Figure 4.9 Block Diagram of one level 2-D SWT

In the DWT, a fundamental computational step is down sampling. Contrarily, the SWT is implemented without down sampling, keeping all the elements in the coefficients across all the decomposition levels is shown in Figure 4.9. In the DWT, down sampling at each decomposition level removes the redundancy. However, the cost of non redundancy is time variance. In fact, the DWT is not a time invariant transform. The DWT of a translated version of a signal *x* is not, in general, the translated version of the DWT of *x*. The translation invariance, a property lost in the DWT can be achieved in the SWT.

The time-variance resulted in the DWT and the time-invariance kept by the SWT is illustrated in figure 4.10. The input A in the figure is an impulse response pulse with B its shifted version in time. The corresponding output A and output B are the reconstructed signals using only the approximation coefficients on level 1 in both transforms. It is observed that the outputs of the DWT are not consistent for both the inputs in terms of the wave shape, but the outputs of the SWT are practically identical except the shift in time axis. The value of shift in time was found the same as that between the input pulses A and B. Thus, in terms of retaining wave shape, the SWT does better than the DWT as it keeps all the coefficients in the decomposition.

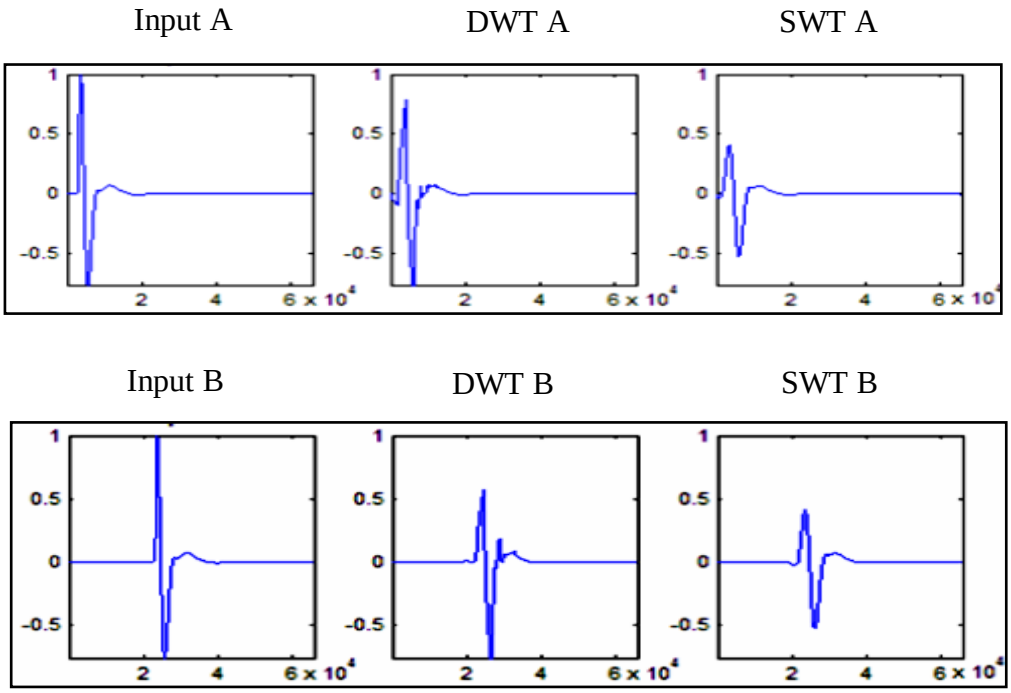

Figure 4.10 Impulse Response of Input, and its shifted version

4.7.1 Two Dimensional Stationary Wavelet Transform

SWT decomposes an image into different sub-band images, namely Low-Low (LL), High-Low (HL), Low-High (LH), and High-High (HH). Mathematically, these sub bands can be expressed as:

$$A_{LL,j+1}(x,y) = \sum_m \sum_n h[n]h[m]\, A_{LL,j}\left(2^{j+1}m - x, 2^{j+1}n - y\right) \tag{4.17}$$

$$D_{HL,j+1}(x,y) = \sum_m \sum_n h[n]g[m]\, A_{LL,j}\left(2^{j+1}m - x, 2^{j+1}n - y\right) \tag{4.18}$$

$$D_{LH,j+1}(x,y) = \sum_m \sum_n g[n]h[m]\, A_{LL,j}\left(2^{j+1}m - x, 2^{j+1}n - y\right) \tag{4.19}$$

$$D_{HH,j+1}(x,y) = \sum_m \sum_n g[n]g[m]\, A_{LL,j}\left(2^{j+1}m - x, 2^{j+1}n - y\right) \tag{4.20}$$

where h [·] and g [·] represent the low pass filter and high pass filter. j represents the wavelet level. And $A_{LL,\,0}\,(x, y) = f\,(x, y)$ [56]. The ISWT is used for the reconstruction of an image and can be defines as

$$\begin{aligned} A_{LL,j}(x,y) = {} & \frac{1}{4}\sum_m \sum_n h[n]h[m]\, A_{LL,j+1}\left(x - 2^{j+1}m, y - 2^{j+1}n\right) \\ & + \frac{1}{4}\sum_m \sum_n h[n]g[m]\, D_{HL,j+1}\left(x - 2^{j+1}m, y - 2^{j+1}n\right) \\ & + \frac{1}{4}\sum_m \sum_n g[n]h[m]\, D_{LH,j+1}\left(x - 2^{j+1}m, y - 2^{j+1}n\right) \\ & + \frac{1}{4}\sum_m \sum_n g[n]g[m]\, D_{HH,j+1}\left(x - 2^{j+1}m, y - 2^{j+1}n\right) \end{aligned} \tag{4.21}$$

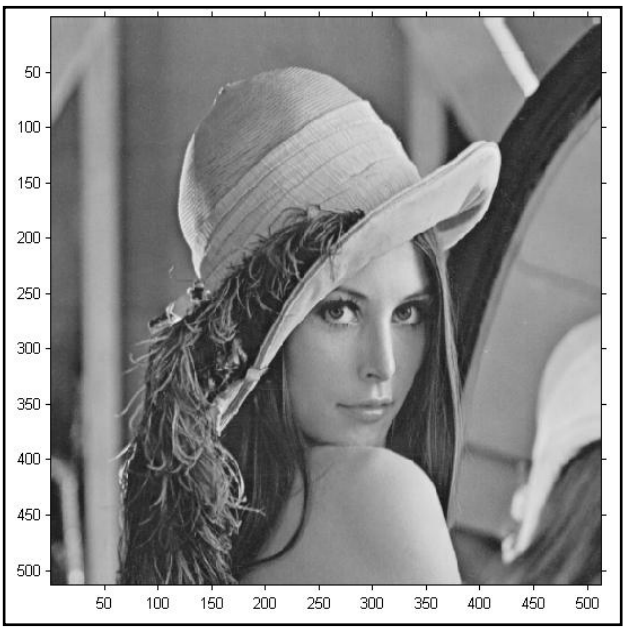

(a)

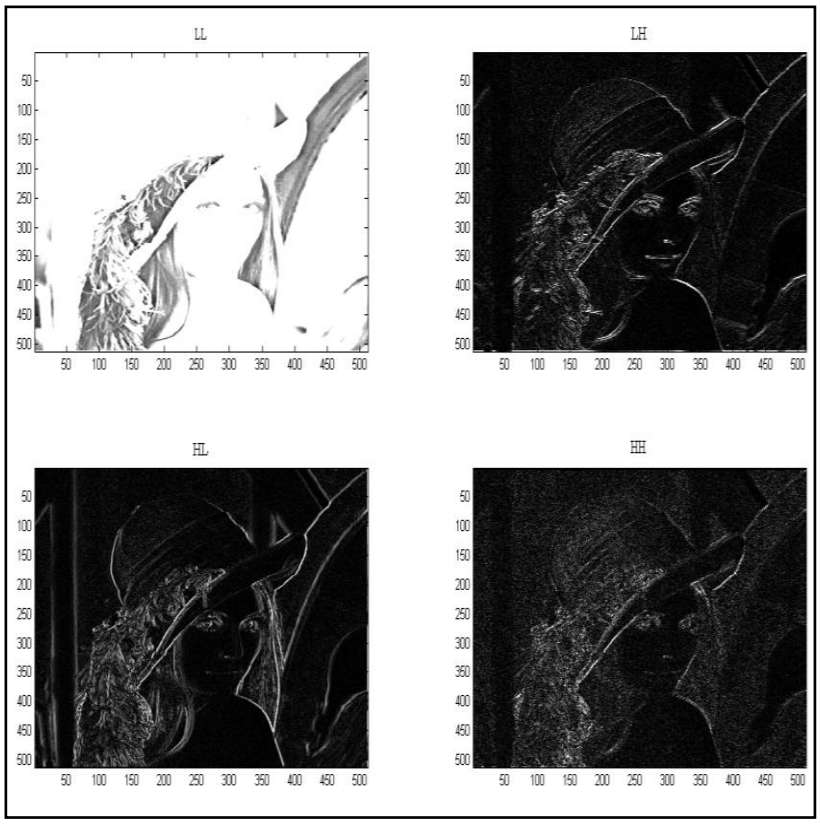

(b)

Figure 4.11 (a) Input image, and (b) One level 2-D SWT of an image

4.8 ADVANTAGES AND DISADVANTAGES OF DWT AND SWT

The main requirement for image resolution enhancement is that the algorithm should enhance the image details. DWT is not sensitive to noise and it does not smooth the sharp edges. DWT helps in preserving high frequency components. But the downsampling at each level of decomposition cause loss of information in respective subbands. There are three main disadvantages of DWT: shift sensitivity, poor directionality and lack of phase information.

Compare with the DWT, the SWT has such advantage as follows: First each sub band has the same size, so it is easier to gain the relationship among the subbands. Second the resolution can be kept since the original data is not decimated, at the same time the wavelet coefficients has more redundant information which helps to distinguish the noise from feature [44]. SWT is used to fill the gap caused by DWT during decimation. But this will lead to over determined and redundant representation of data.

CHAPTER 5

IMAGE RESOLUTION ENHANCEMENT TECHNIQUES

5.1 FUNDAMENTALS

Whenever an image is converted from one form to another, for example, scanned, copied, transmitted, or displayed, the "quality" of the output image is lower than that of the input. In the absence of knowledge about how the given image was actually degraded, it is difficult to predict in advance how effective a particular enhancement method will be. Image resolution enhancement aims to improve human perception and interpretability of information in images or to provide more useful input for other automated image processing techniques [4]. Conventional image resolution enhancement methods such as nearest neighbor and bilinear interpolation may generate false information and blurred images because they do not utilize any information relevant to edges in the original image. In general, image resolution enhancement techniques can be divided into three categories:

1. Spatial-domain methods that directly manipulate pixels in an image.
2. Frequency-domain methods that operate on the Fourier transform or other frequency domains of an image.
3. Combinational methods that process an image in both spatial and frequency domains.

Image enhancement methods are application specific and often developed empirically. When image enhancement techniques are used as preprocessing tools for other image processing techniques, some quantitative measures can be used to determine which techniques are most appropriate. Image enhancement involves three types of processes: point process, mask process, and global process. In a point process, each pixel is modified according to a particular equation depending on the input only at the same pixel, which is independent of other pixel values. The input may be one or more images. For example, the difference or product of two images can be taken point by point. In a mask process, each pixel is modified according to the values of the pixel's neighbors using convolution masks. For example, an average of the pixels can be taken in the neighborhood as a low-pass filter. In a global process, all the pixel values in the image are taken into consideration. For example, histogram equalization remaps the histogram of the entire

input pixels to a uniformly distributed histogram. Spatial-domain processing methods include all three types, but frequency domain methods, by the nature of frequency transforms, are global processes.

5.2 GRAY SCALE TRANSFORMATIONS

The aim of Grayscale transformations is to change the gray levels of an entire image in a uniform way or intends to modify the gray levels within a defined window by a mapping function. This transformation is usually expected to enhance the image contrast, so the details of an image can be more visible. The value of a pixel with coordinates (x, y) in the enhanced image f is the result of performing some operation on the value of f at (x, y). Thresholding is the simplest case to replace the intensity profile by a step function, jumping at a chosen threshold value. In this case, any pixel with a gray level below the threshold in the input image receives 0 in the output image, and above or equal to the threshold receives 255.

Another simple operation is image negative; it reverses the order of pixel intensities from black to white, so the intensity of output decreases as the intensity of input increases [46]. It is a reversed image where the image that is usually black on a white background is reversed to be white on a black background. Let the input gray level r and the output gray level s be in the range [0,$L-1$] The relationship between the input and output gray levels is given by $s = L-1-r$. Figure 5.1 shows the Lena image and its image negative. This image negative operation is equivalent to a photographic negative. It is quite useful to show the details of small white or gray regions when they appear in a large dark background.

Some examples of mapping from the input gray level r to the output gray level s are illustrated in Figure 5.2, including identity, negative, and thresholding. The mapping function can use mathematical operations (e.g., logarithm, exponential, root, power, etc.) and any degree of polynomial functions. For example, the log mapping is given by $s = c\ log\ (1+r)$, where c is a constant. A useful application of log mapping is to compress the large dynamic range of gray-level values, so the brightest pixels will not dominate the display and the darker pixels will still be visible.

(a) **(b)**

Figure 5.1 (a) The Lena image, and (b) Its negative image.

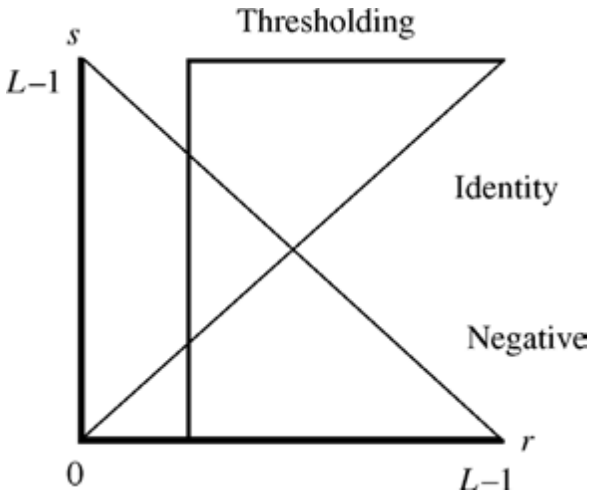

Figure 5.2 Mapping from an input image to an output image [46]

5.3 PIECEWISE LINEAR TRANSFORMATIONS

The piecewise linear transformations uses different linear functions to map different input gray-level intervals. A low-contrast image could occur due to poor illumination, lack of dynamic range in the sensor, or a wrong setting in a lens. Contrast stretching aims to improve the contrast

in an image by stretching the narrow range of input intensity values to span a desired range of intensity values (usually the full range of gray values). It only applies a linear scaling function to the input. A general function for contrast stretching is illustrated in Figure 5.3 and its example is shown in figure 5.4. The locations of (r_1, s_1) and (r_2, s_2) control the shape of the transformation function. The constraints for this function are $r_1 \leq r_2$ and $s_1 \leq s_2$. The function is single valued and monotonically increasing, so the order of gray levels in the output is preserved.

If $r_1 = s_1$ and $r_2 = s_2$, it is a linear function indicating no changes in the output gray levels. If $r_1 = r_2$, $s_1 = 0$, and $s_2 = L$-1, it is a thresholding function and the output is a binary image. If $r_1 <$ $r2$, $s_1 = 0$; and $s_2 = L$-1, it is a linear scaling. Let the input gray level r be mapped to the output gray level s in the full range of [0, L-1].

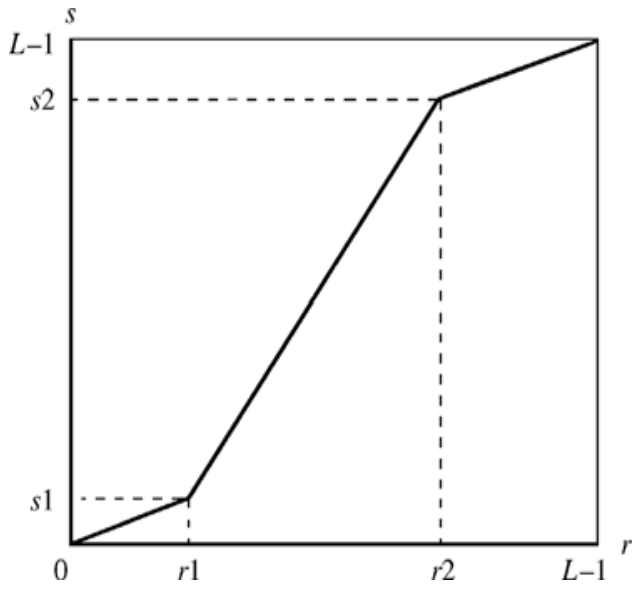

Figure 5.3 Mapping function of contrast stretching [46]

Let the minimum and maximum values of the input image be denoted as “min” and “max,” respectively. The following equation is used to perform the linear scaling and round the floating point value to the closest integer for the output image to display as

$$s = \frac{L-1}{max - min}(r - min) \tag{5.1}$$

(a) **(b)**

Figure 5.4 (a) A low-contrast image and (b) The image after contrast stretching

5.4 HISTOGRAM PROCESSING

The histogram of a digital image with gray levels in the range [0, L-1] is a discrete function $h(r_k)=n_k / M\ X\ N$, where r_k is the k^{th} gray level, n_k is the number of pixels in the image with that gray level r_k,, $M\ X\ N$ is the total number of pixels in the image, and k=0,1..L-1**.** h (r_k) gives an estimate of the probability of occurrence of gray level r_k. Histogram manipulation can be used for image enhancement [47]. Figure 5.5 shows the four basic intensity characteristics: (a) light, (b) dark, (c) low contrast, (d) and high contrast.

The shape of the histogram of an image gives us useful information about the possibility for contrast enhancement. Note that in the dark image, the components of histograms are concentrated on the low side of the intensity scale. Similarly, the components of the histogram on the light image are biased towards the high side of the scale. A histogram of a narrow shape indicates little dynamic range and thus corresponds to an image having low contrast.

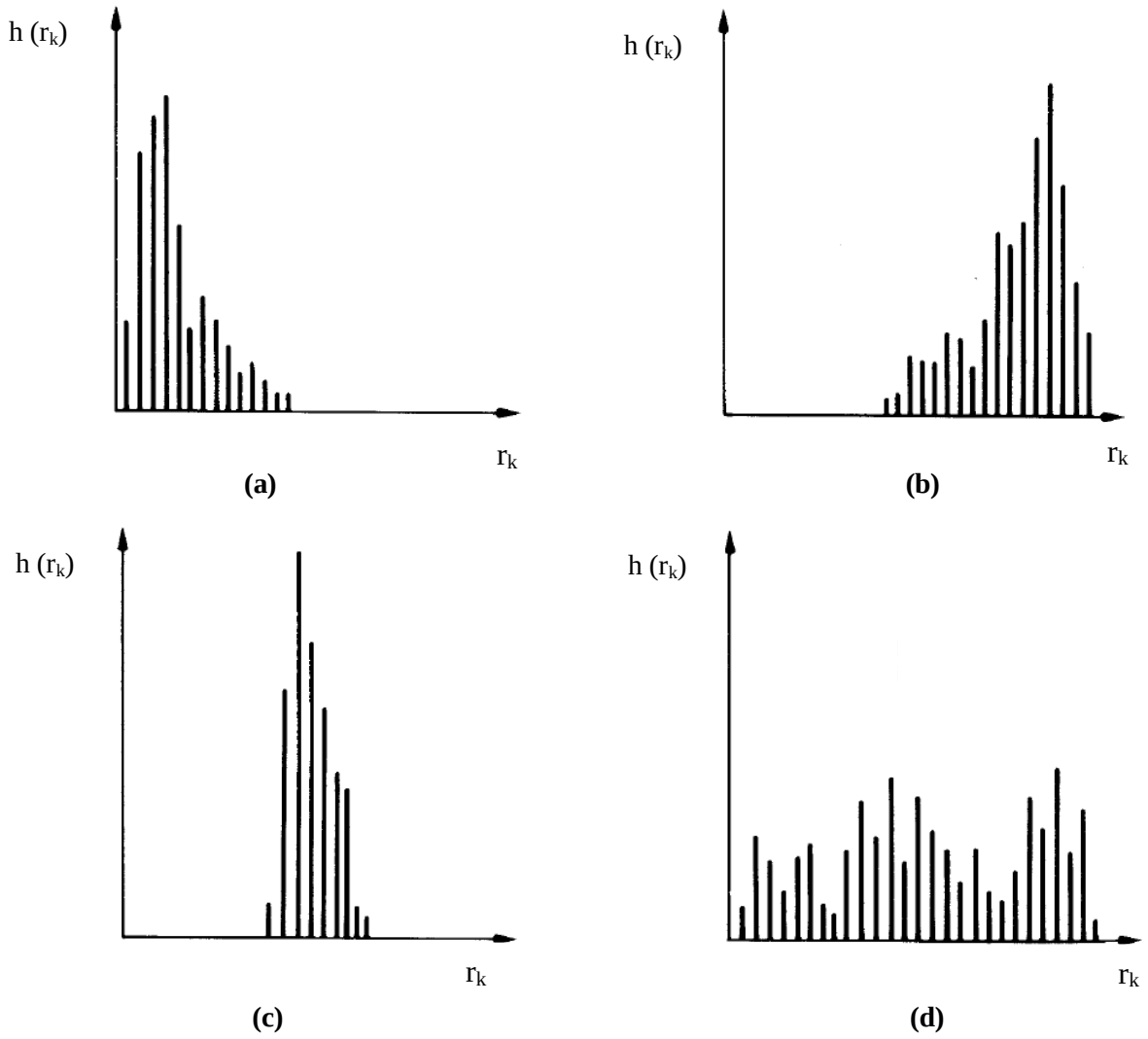

Figure 5.5 Histogram Processing [47]

5.4.1 Histogram Equalization

Histogram equalization employs a monotonic nonlinear mapping that reassigns the intensity values of pixels in an input image, such that the output image contains a uniform distribution of intensities (i.e. a histogram that is constant for all brightness values). This corresponds to a brightness distribution where all values are equally probable. Unfortunately, this technique can only achieve the approximation of this uniform distribution for a digital image. This technique is often used in image comparison because it is effective in detail enhancement and in the correction of nonlinear effects introduced by a digitizer or a display system [48]. In general, the histogram equalization causes the dynamic range of an image to be stretched; the density

distribution of the resultant image is made flat, so that the contrast of the image is enhanced. However, the histogram equalization method causes several problems. Since the contrast is enhanced by stretching the dynamic range, background noise is simultaneously increased by the equalization, and the image quality in a near-constant region may be degraded. Figure 5.6 (a) shows a low-contrast input image, and (b) its resulting image after histogram equalization.

Consider an image pixel value $r \geq 0$ to be an element of random variable R with a continuous probability density function $p_r(r)$ and cumulative probability distribution $F_R(r) = P(R \leq r)$. Let the mapping function be $s = f(r)$ between the input and output images. To equalize the histogram of the output image, let the function $p_S(s)$ is constant. In particular, if the gray levels are assumed to be in the range between 0 and 1, then $p_s(s) = 1$ forms a uniform random variable S. The mapping function for histogram equalization

$$s = F_R(r) = \int_0^r p_r(r)dr \tag{5.2}$$

will be uniformly distributed over (0, 1) To implement this transformation on digital images, let n denote the total number of pixels, n_G the total number of gray levels, and n_{rj} the number of pixels in the input image with intensity value r_j. Let the input and output gray values are in the range of [0, 1, …., n_G-1]. Then, the histogram equalization transformation maps the input value r_k (where $k = 0, 1, \ldots, n_G-1$) to the output value s_k as

$$s_k = T(r_k) = n_G - 1 \sum_{j=0}^{k} \frac{n_{rj}}{n} = \frac{n_G - 1}{n} \sum_{j=0}^{k} n_{rj} \tag{5.3}$$

Note that the resulting floating point value will be rounded to its closest integer as the output value.

5.4.2 Histogram Specification

Histogram equalization intends to map any input image into an output image with the uniformly distributed histogram. Sometimes, a particularly distributed histogram of output images is desired in specific applications. Therefore, histogram specification is used to convert an image, so that it has a particular histogram of output images as specified [50].

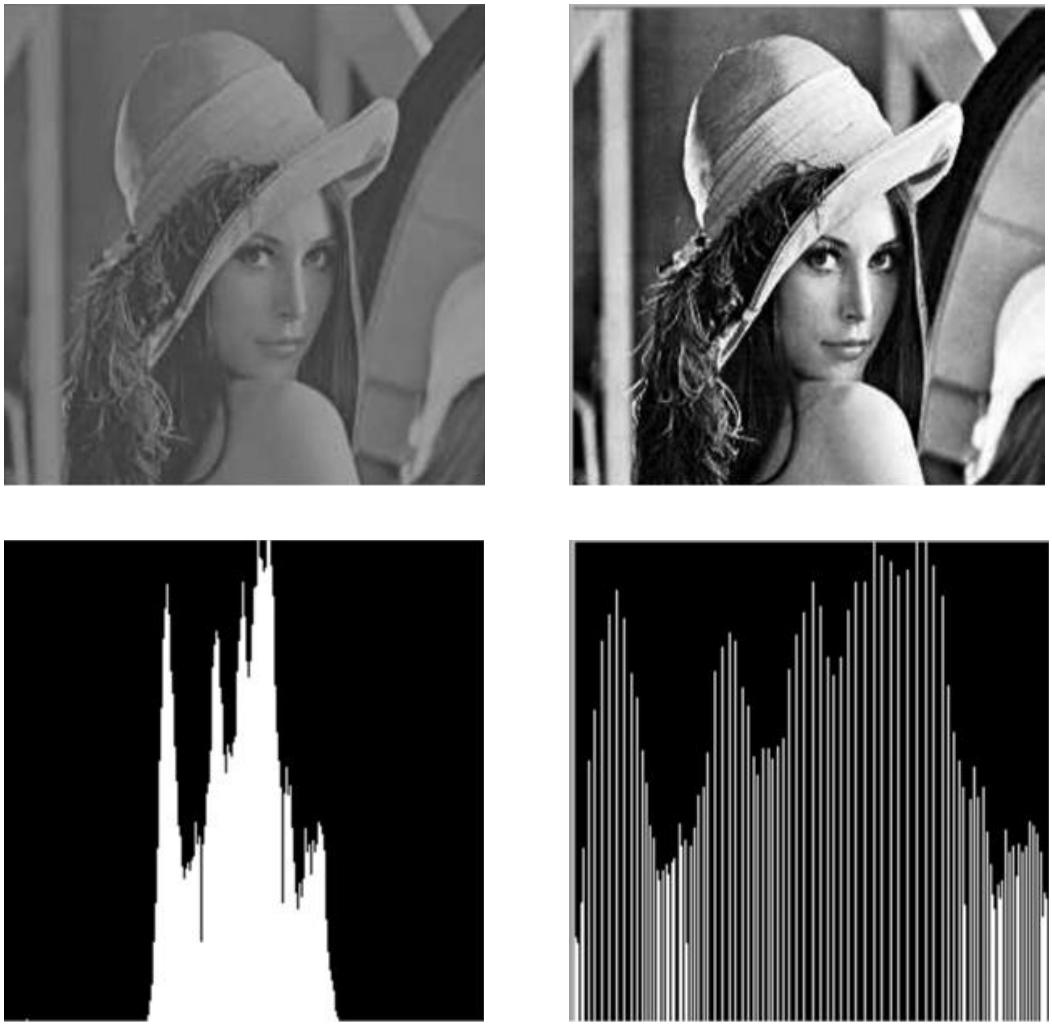

(a) **(b)**

Figure 5.6 Histogram Equalization

Let x and y denote the gray levels of the input and output images respectively. The probability $p_x(x)$ from the input image can be computed, and the specified probability $p_z(z)$, which the output image is desired to have, is designed for a particular application. In this method, the histogram equalization is first conducted as

$$y = f(x) = \int_0^x p_x(u)du \tag{5.4}$$

When the gray levels of the desired image z are available, it can also be equalized as

$$y' = g(z) = \int_0^x p_z(u)du \tag{5.5}$$

The inverse of the above transform is $z = g^{-1}(y')$. Since the images y and y' have the same equalized histogram, they are the same image and the overall transform from the given image x to the desired image z can be obtained by $z = g^{-1}(y) = g^{-1}(f(x)) = h(x)$, where $h(x) = g^{-1}(f(x))$ is the overall transform, and both f and g can be found from the corresponding histograms of the given image x and the desired image z, respectively [46]. The working of histogram specification can be explained with the example given below. Let the input image be

1	1	0	0	0	0	0	1
1	1	1	1	0	1	0	1
1	3	4	4	5	5	0	0
0	3	4	4	5	5	5	5
2	4	4	4	3	5	7	0
1	1	4	5	6	5	6	1
1	0	4	4	1	5	6	1
1	0	1	0	0	0	5	0

and input and output gray levels be in the range of [0, 7]. The expected gray level specifications is (0 : 5% ,1 : 5% , 2 : 10% ,3 : 10% ,4 : 25%, 5 : 5% ,6 : 25% , 7 : 15%).

From the input image

x	p_x	$\int_0^x p_x(u)du$
0	17/64	17/64=0.2656
1	18/64	35/64=0.5469
2	1/64	36/64=0.5625
3	3/64	39/64=0.6094
4	10/64	49/64=0.7656
5	11/64	60/64=0.9375
6	3/64	63/64=0.9844
7	1/64	64/64=1.0000

From the expected specification

x	P_z	$\int_0^x p_z(u)du$
0	0.05	0.05
1	0.05	0.10
2	0.10	0.20
3	0.10	0.30
4	0.25	0.55
5	0.05	0.60
6	0.25	0.85
7	0.15	1.00

Mapping from the input gray level to the output gray level of the expected specification yields

x	**Mapping**	Z
0	0.2656≈0.30	3
1	0.5469≈0.55	4
2	0.5625≈0.55	4
3	0.6094≈0.60	5
4	0.7656≈0.85	6
5	0.9375≈1.00	7
6	0.9844≈1.00	7
7	1.0000≈1.00	7

Therefore, the output image after histogram specification is

4	4	3	3	3	3	3	4
4	4	4	4	3	4	3	4
4	5	6	6	7	7	3	3
3	5	6	6	7	7	7	7
4	6	6	6	5	7	7	3
4	4	6	7	7	7	7	4
4	3	6	6	4	7	7	4
4	3	4	3	3	3	7	3

5.5 SPATIAL FILTERING

Spatial filters are designed to highlight or suppress features in an image based on their spatial frequency. The spatial frequency is related to the textural characteristics of an image. Rapid variations in brightness levels ('roughness') reflect a high spatial frequency; smooth areas with little variation in brightness level or tone are characterized by a low spatial frequency. Spatial filters are used to suppress noise in an image, or to highlight specific image characteristics.

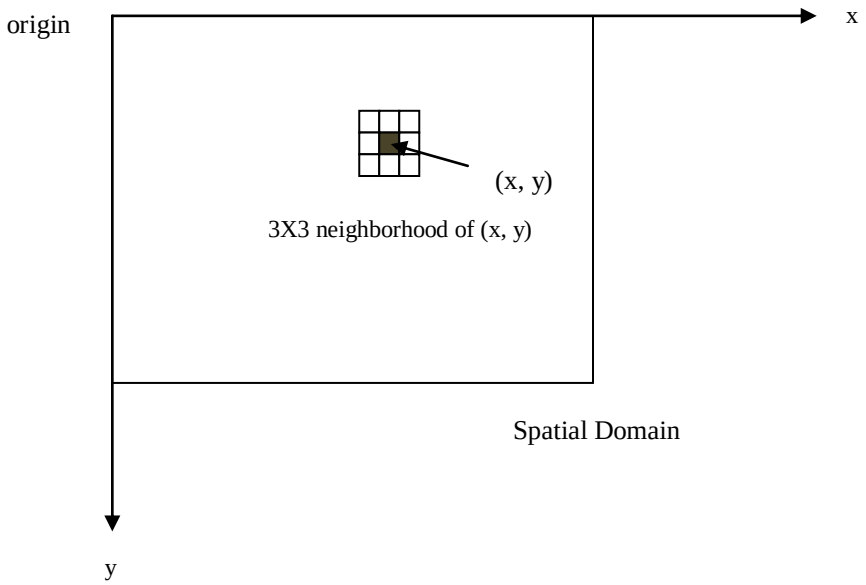

Figure 5.7 Spatial Filtering [51]

A spatial filter consists of neighborhood, and predefined operation that is performed on the image pixels encompassed by the neighborhood. Filtering creates a new pixel with coordinates equal to the coordinates of the centre of the neighborhood, and whose value is the result of filtering operation [51]. A filtered image is generated as the centre of the filter visits each pixel in the input image. The mechanism of linear spatial filtering using 3X3 neighborhood is explained in equation 5.6. At any point (*x*, *y*) in the image, the response, $g(x,y)$ of the filter is sum of products of the filter coefficients and the image pixels encompassed by the filter:

$$g(x,y) = w(-1,-1)f(x-1,y-1) + w(-1,0)f(x-1,y) + \cdots + w(0,0)f(x,y) + w(1,1)f(x+1,y+1) \quad (5.6)$$

Note that the centre coefficients of the filter $w\ (0\ ,0\ )$ aligns with the pixel at location (*x*, *y*). In general linear spatial filtering of an image is given by the expression

$$g(x,y) = \sum_{s=-a}^{a} \sum_{t=-b}^{b} w(s,t)\, f(x+s,y+t) \quad (5.7)$$

where, *x* and *y* are varied so that each pixel in w visits every pixel in *f*.

5.5.1 Smoothing Spatial filters

Smoothing filters are used for blurring and for noise reduction. Blurring is used in preprocessing steps, such as removal of small details from an image prior to object extraction, and bridging of small gaps in lines or curves. Noise reduction can be accomplishing by blurring with a linear filter and also by nonlinear filtering [51].

A simple mean smoothing filter or operation intends to replace each pixel value in an input image by the mean (or average) value of its neighbors, including itself. Figure 5.8 shows an example of applying the 3 X 3 averaging kernel. This has an effect of eliminating pixel values that are unrepresentative of their surroundings. Like other convolution filters, it is based around a kernel, which represents the shape and size of the neighborhood to be sampled in calculation.

Often a3 X 3square kernel is used, as shown below

$$\frac{1}{9}\begin{bmatrix}1 & 1 & 1\\ 1 & 1 & 1\\ 1 & 1 & 1\end{bmatrix}$$

(a) **(b)**

Figure 5.8 (a) The Lena image and (b) The resulting image after a 3X3 averaging filter.

Smoothing filters replacing the value of every pixel in an image by the average of the intensity levels in the neighborhood defined by filter coefficients, this process results in an image with reduced sharp transitions in intensities. Because random noise typically consists of sharp transitions in intensity levels. However, edges are also characterized by sharp intensity transitions, so averaging filters have undesirable effects that they blur edges.

Another method of image smoothing convolves an input image by the Gaussian filter. The Gaussian filter will screen noise with the high spatial frequencies and produce a smoothing effect [46]. The 1-D Gaussian filter function is

$$G(x) = \frac{1}{\sqrt{2\pi}\sigma} e^{\frac{-x^2}{2\sigma^2}} \qquad (5.8)$$

where, σ is the standard deviation of the distribution. The distribution of mean zero and $\sigma = 1$ is shown in Figure 5.9 and 5.10. In two dimensions, an isotropic (i.e., circularly symmetric) Gaussian filter function is

$$G(x,y) = \frac{1}{\sqrt{2\pi\sigma^2}} e^{\frac{-(x^2+y^2)}{2\sigma^2}} \tag{5.9}$$

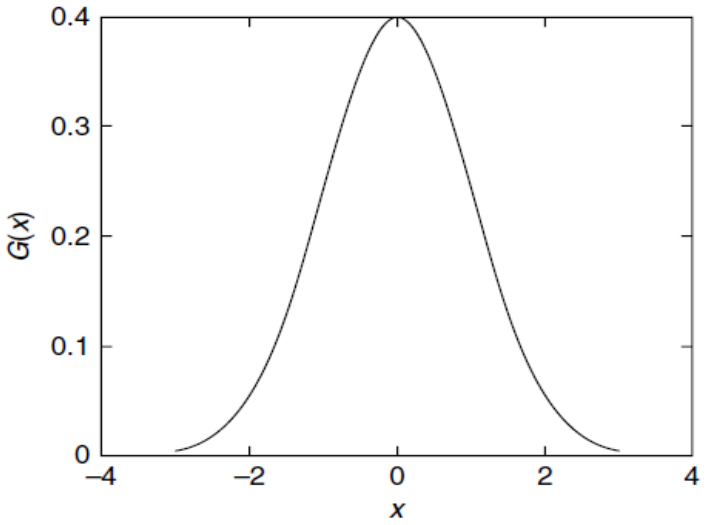

Figure 5.9 One dimensional Gaussian filter function with mean zero and σ =1

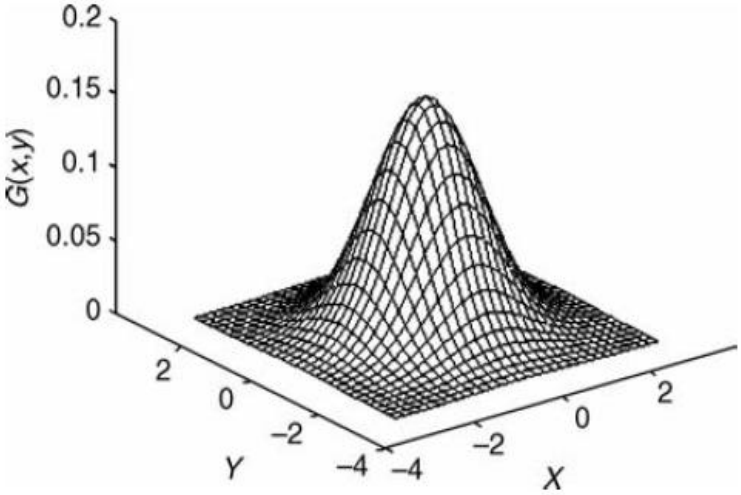

Figure 5.10 Two dimensional Gaussian filter function with mean zero and σ =1

Another smoothing filter used for image enhancement is non-linear spatial filter, whose response is based on ranking the pixels contained in the image area encompassed by the filter, and then replacing the value of the centre pixel with the value determined by the ranking result. The best known filter in this category is the median filter. These filters can provide excellent noise reduction capabilities, with considerably less blurring than linear smoothing filters of similar size. It is especially effective for removing impulse noise, which is characterized by bright and/or dark high-frequency features appearing randomly over the image [22]. Statistically, impulse noise falls well outside the peak of the distribution of any given pixel neighborhood, so the median is well suited to learn where impulse noise is not present, and hence to remove it by exclusion. The median of a distribution is the value for which larger and smaller values are equally probable.

(a) **(b)**

Figure 5.11 (a) A noisy image and (b) The resulting image after median filtering

5.5.2 Sharpening Spatial Filters

Sharpening filter is used to enhance the edges of objects and adjust the contrast of object and background transitions. They are sometimes used as edge detectors by combining with thresholding. Sharpening or high-pass filter allows high-frequency components to pass and

delete the low frequency components. For a kernel to be a high-pass filter, the coefficients near the center must be set positive and in the outer periphery must be set negative. Sharpening filter can be categorized into four types: high-pass filter, Laplacian of Gaussian (LoG) filter, derivative filter, and high-boost amplifier.

A high-pass filter, opposite of a low-pass filter, is a filter that passes high frequency components, but attenuates (or delete) the components whose frequency is lower than the cutoff frequency. A simple 3 X 3 high-pass filter is given as

$$\frac{1}{9}\begin{bmatrix} -1 & -1 & -1 \\ -1 & 8 & -1 \\ -1 & -1 & -1 \end{bmatrix}$$

An example of applying the high-pass filter on the Lena image is shown in Figure 5.12.

(a) **(b)**

Figure 5.12 (a) An input image and (b) The resulting image after high pass filtering

Another sharpening filter is the derivative (or gradient) operator. Edge Detection is most commonly used approach for detecting meaningful discontinuities in intensity level [6]. Such discontinuities are detected by using first and second order derivatives. An image is a 2-D

function, so operators describing edges are expressed using partial derivatives [6]. The gradient of a 2-D function $f\ (x, y)$, is defined as the vector

$$\nabla f\ =\ \begin{bmatrix} Gx \\ Gy \end{bmatrix}\ =\ \begin{bmatrix} \frac{\partial f}{\partial x} \\ \frac{\partial f}{\partial y} \end{bmatrix} \tag{5.10}$$

The magnitude of this vector is

$$\nabla f = mag(\nabla f) = [Gx^2 + Gy^2]^{1/2}$$

$$\nabla f = \left[\left(\frac{\partial f}{\partial x}\right)^2 + \left(\frac{\partial f}{\partial y}\right)^2\right]^{1/2} \tag{5.11}$$

To simplify computation, omit the square-root term

$$\nabla f \approx\ Gx^2 + Gy^2 \qquad or$$

$$\nabla f \approx\ |Gx| + |Gy| \tag{5.12}$$

A fundamental property of the gradient vector is that it points in the direction of the maximum rate of change of f at coordinates (x, y). The angle at which the maximum rate of change occurs is

$$\alpha(x, y) =\ tan^{-1}\left(\frac{Gy}{Gx}\right) \tag{5.13}$$

Second-order derivatives in image processing are generally computed using the Laplacian function.

$$\nabla^2 f\ (x, y) =\ \frac{\partial^2 f\ (x, y)}{\partial x^2} + \frac{\partial^2 f\ (x, y)}{\partial y^2} \tag{5.14}$$

An edge is judged present if the gradient exceeds the threshold [6]. When second-order differentiation is performed, an edge is judged present if there is a significant spatial change in the polarity of the second derivative.

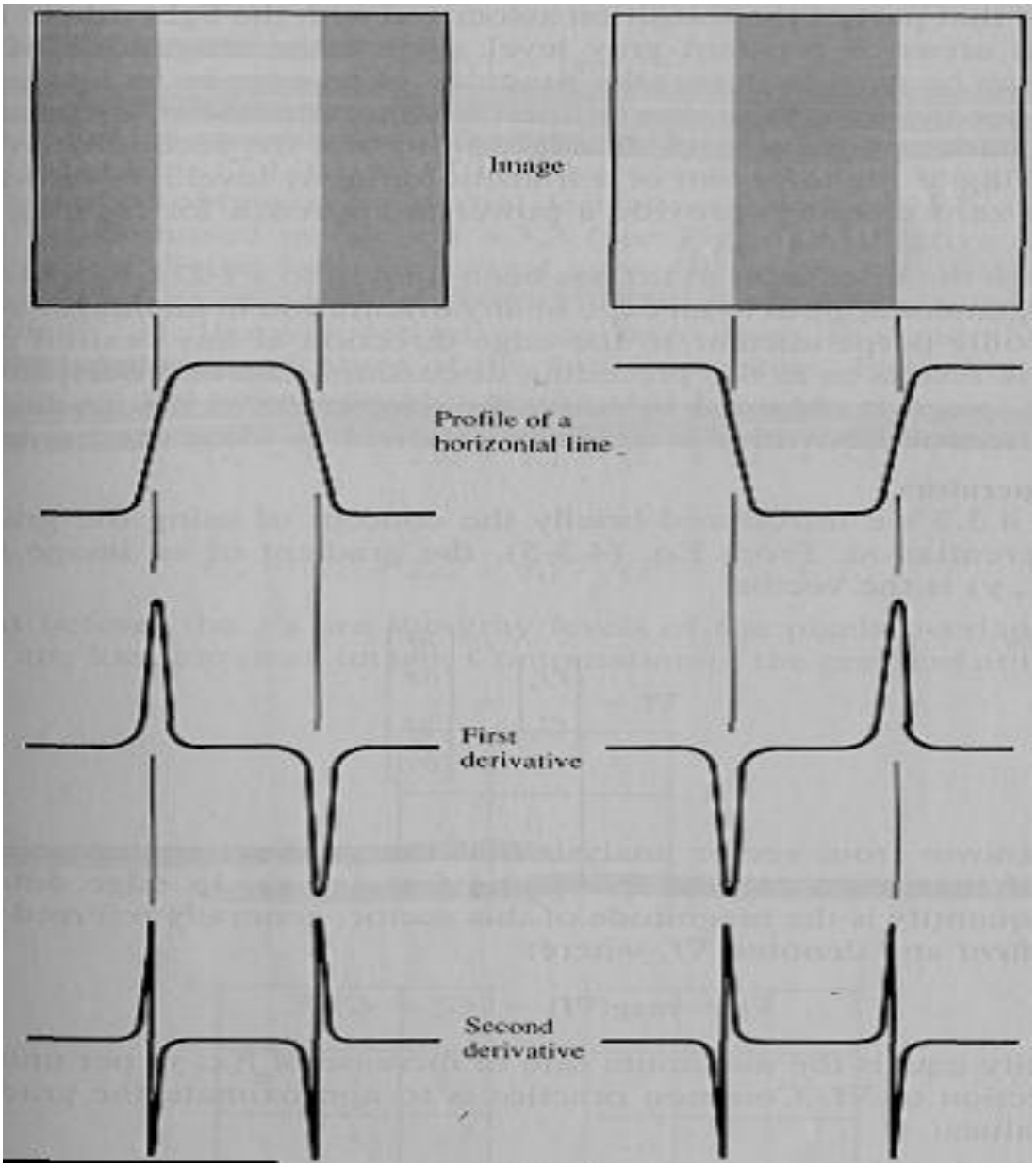

Figure 5.13 Edge Detection using first and second derivative [6]

For digital images, the derivatives of the gradient operator are the two differences: $f_x = f(x+1, y) - f(x, y)$ and $f_y = f(x, y+1) - f(x, y)$. Its magnitude can be approximated in a number of ways, which result in a number of operators such as Roberts, Prewitt and Sobel operators for computing its value.

1	0
0	-1

0	1
-1	0

(a)

-1	-1	-1
0	0	0
1	1	1

-1	0	1
-1	0	1
-1	0	1

(b)

-1	-2	-1
0	0	0
1	2	1

-1	0	1
-2	0	2
-1	0	1

(c)

Figure 5.14 (a) Roberts, (b) Prewitt, and (c) Sobel Operators

The Laplacian of Gaussian filter (LoG) is the combination of the Laplacian and Gaussian filters where its characteristic is determined by the σ parameter and the kernel size, as shown in the mathematical expression of the kernel:

$$LOG(i,j) = -\frac{1}{\pi\sigma^4}\left(1 - \frac{i^2+j^2}{2\sigma^2}\right)e^{-\frac{i^2+j^2}{2\sigma^2}} \quad (5.15)$$

A discrete 9X9 kernel that approximates this function (for a Gaussian $\sigma = 1.4$) is shown in Figure 5.15. An example of applying this kernel on the Lena image is shown in Figure 5.16.

0	1	1	2	2	2	1	1	0
1	2	4	5	5	5	4	2	1
1	4	5	3	0	3	5	4	1
2	5	3	-12	-12	-12	3	5	1
2	5	0	-24	-24	-24	0	5	2
2	5	3	-12	-12	-12	3	5	2
1	4	5	3	3	3	5	4	1
1	2	4	5	5	5	4	2	1
0	1	1	2	2	2	1	1	0

Figure 5.15 The discrete approximation to LoG function with Gaussian $\sigma = 1.4$

(a) **(b)**

Figure 5.16 (a) The Lena image and (b) The result after applying 9 X 9 LoG filter.

The high-boost filter is used to emphasize high-frequency components representing the image details without eliminating low-frequency components. It multiplies the original image by an amplification factor A as

$$\text{High boost} \begin{cases} = \text{A X original image -low pass filtered image} \\ = \text{(A-1) X original image + (original image -low pass filtered image)} \\ = \text{(A-1) X original image +high pass filtered image} \end{cases}$$

An example of applying the high-boost filter with A=1.5 on the Lena image is shown in Figure 5.17.

(a) **(b)**

Figure 5.17 (a) Original image, (b) High-boost filtered image with A=1.5

5.6 IMAGE SUPER RESOLUTION USING DWT AND BICUBIC INTERPOLATION

Since the demand for high-quality imaging has increased recently, SR techniques that restore high resolution images from low resolution images are of interest. Image enhancement algorithms assume that low resolution images are degraded versions of an original high

resolution images that is formed by low pass filtering followed by downsampling. Therefore, SR is an inverse problem of estimating a high resolution image from a low resolution image along with given low pass filter coefficients and a known downsampling ratio.

DWT is one of the recent wavelet transforms used in image enhancement. The main loss of an image after being super resolved by applying interpolation is on its high frequency components, that is, the edges. This loss is due to the smoothing caused by interpolation. Hence, in order to increase the quality of the super resolved image, preserving the edges is essential. In this method, DWT [43] has been employed in order to preserve the high frequency components of the image. DWT decomposes an image into different subband images; namely, low-low (LL), low-high (LH), high-low (HL), and high-high (HH). Out of these sub bands LH, HL, and HH contain the high frequency components of the input image. Bicubic interpolation is applied to high frequency subband images.

In the wavelet domain, the low resolution image, LL, is obtained by low pass filtering of the high resolution image. In other words, the LL subband image is the low resolution of the original image. Therefore, instead of using LL, which contains less information, we are using the low resolution input image for interpolation. Hence, using low resolution image instead of the LL subband image increases the quality of the super-resolved image. Note that low resolution image is interpolated with half of the interpolation factor α, used to interpolate the high frequency subbands, as illustrated in Figure 5.18. By interpolating low resolution image by $\alpha/2$, and interpolating HH, HL, and LH by α, and then applying IDWT, the output image will contain sharper edges than the interpolated image obtained by interpolation of the input image directly. This is because the interpolation of isolated high frequency components in HH, HL, and LH will preserve more high frequency components after the interpolation of the respective subbands separately than interpolating input image directly.

The original high resolution images have been used as the ground truth to calculate the PSNR values. Low resolution images (128 X 128) have been generated by two consecutive downsampling of the original high-resolution images (512 X 512) using DWT as shown in Figure 5.19.

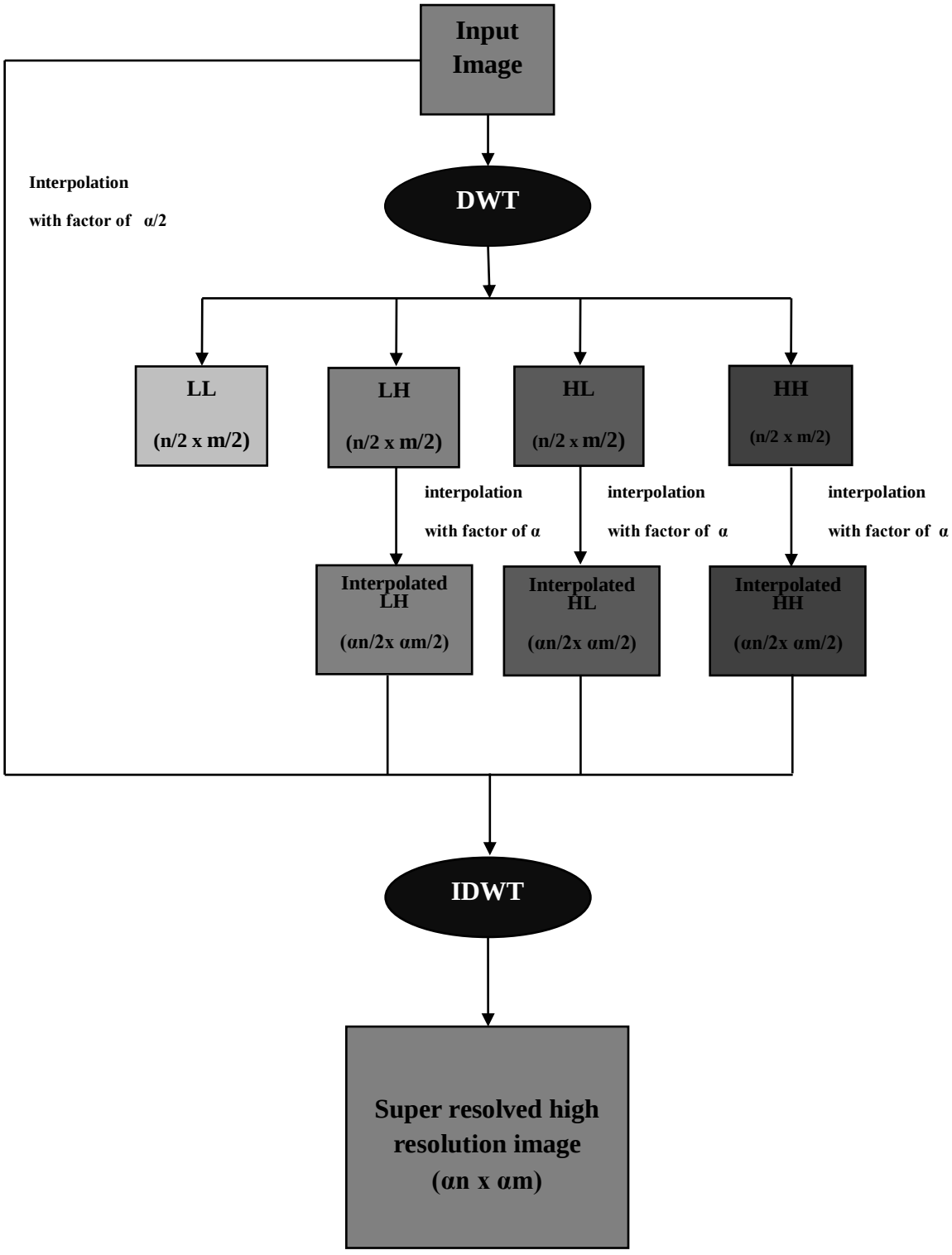

Figure 5.18 Block diagram of Image Super Resolution using DWT and bicubic interpolation

(a) **(b)**

(c)

Figure 5.19 Low Resolution Image obtained from High Resolution image (a) 512 X 512, (b) 256 X 256, and (c) 128 X 128

5.7 EXPERIMENTAL RESULTS

The quality of super resolved image can be measured by two most important parameters namely MSE and PSNR. The average of the square of the difference between the desired response and the actual system output or the MSE is a measure of the differences between values predicted and the values actually observed. MSE can be obtained by

$$MSE = \frac{\sum_{x,y}\left(f_p(x,y) - f_o(x,y)\right)^2}{M \times N}$$

where, M X N is the size of an image. $f_p(x,y)$ is the processed image and $f_o(x,y)$ is the original image. PSNR has been implemented in order to obtain some quantitative results for comparison. PSNR can be defined as difference between the processed image and original image. The larger the PSNR value, the better will be the image quality. PSNR can be obtained by using the following formula:

$$PSNR = 10log_{10}\left(\frac{R^2}{MSE}\right)$$

where, R is the maximum fluctuation in the input image (255 in here as the images are represented by 8 bit, i.e. 8- bit grayscale representation has been used).

In this experiment, eight well known images Lena, Baboon, Peppers, Living room, House, Cameraman, Elaine, and woman blonde have been used for image resolution enhancement using DWT and bicubic interpolation. All these images are gray scale images of size 512 X 512 and are used as ground truth. The zooming results of Lena and Baboon image has been presented in this section to show the aliasing effect.

5.7.1 Lena image

Figure 5.20 (a) shows the low resolution Lena image of size 128X128. Figure 5.20 (b) shows image obtained from bicubic interpolation. Figure 5.20 (c) shows the resultant image obtained by using DWT and bicubic interpolation, whereas Figure 5.20 (d) shows an original high resolution image of size 256 X 256 respectively.

(a) **(b)**

(c) **(d)**

Figure 5.20 Experimental results for Lena image

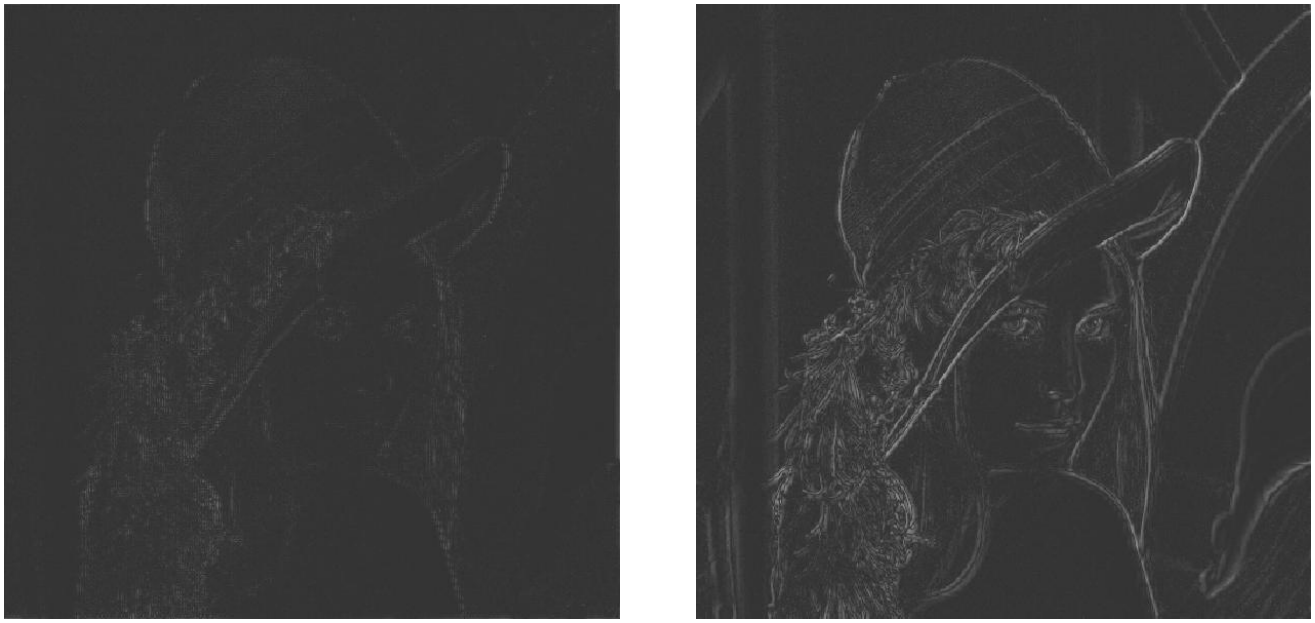

(a) **(b)**

Figure 5.21 (a) Difference images

If we compare the difference images, which are obtained from subtracting the reconstructed image from the original one. Figure 5.21 (a), and (b) shows the difference image between the original high resolution Lena image with the resultant image obtained by using DWT and bicubic interpolation, and the difference image obtained by using bicubic interpolation. DWT and bicubic interpolation preserves the high frequency details more than bicubic interpolation alone. Figure 5.21 (a) reflects this by including less high frequency details in the error image.

Figure 5.22 (a) show the low resolution Lena image of size 128X128. Figure 5.22(b) shows image obtained from bicubic interpolation, Figure 5.22 (c) shows the resultant image of size 512 X 512 obtained by using DWT and bicubic interpolation, whereas Figure 5.22 (d) shows an original high resolution image of size 512 x512.

(a)

(b)

(c)

(d)

Figure 5.22 Experimental results for Lena image of size 128X128 pixels

5.7.2 Baboon image

Figure 5.23 (a) show the low resolution Baboon image of size 128X128. Figure 5.23 (b) shows the resultant image of size 512 X 512 obtained by using DWT and bicubic interpolation, whereas Figure 5.23 (c) shows an original high resolution image of size 512 x512.

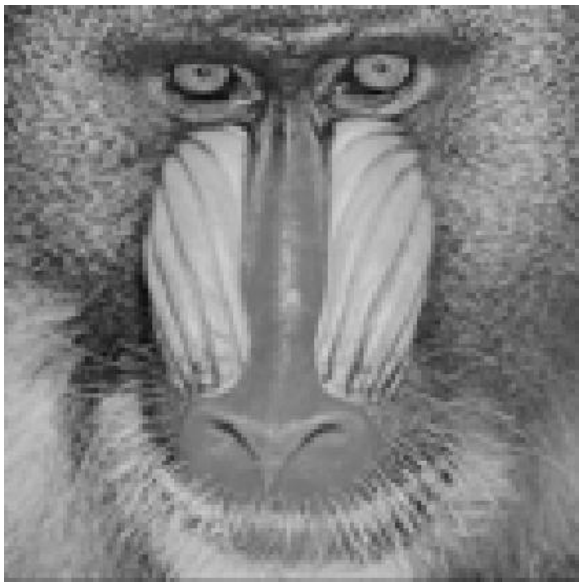

(a)

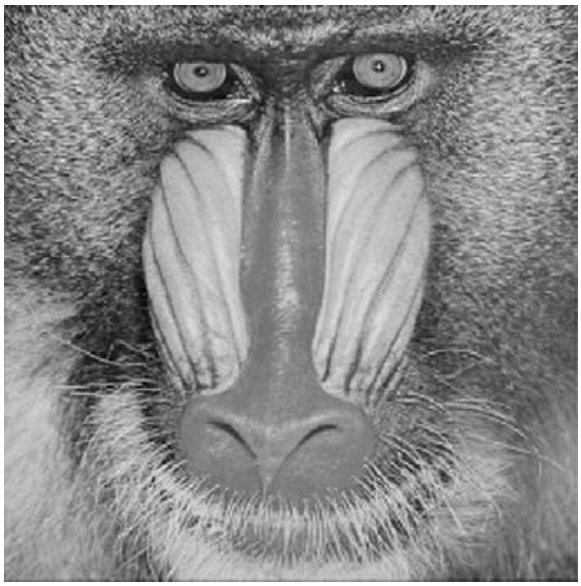

(b)

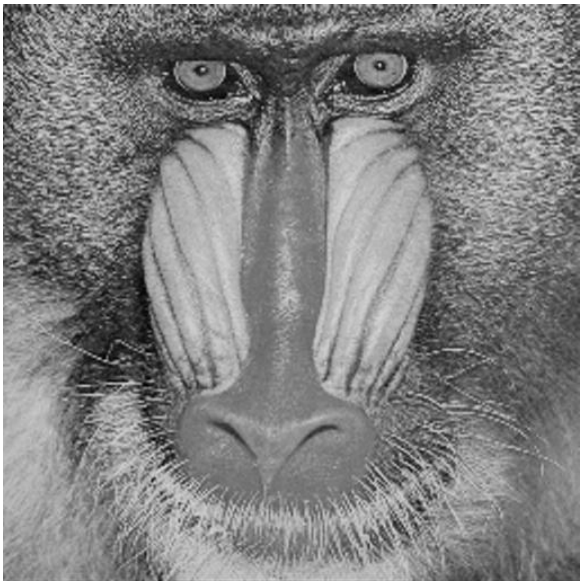

(c)

Figure 5.23 Experimental results for Baboon image

5.7.3 Lena image with zooming of left eye region

Figure 5.24 (a) shows the original high resolution image of Lena with 400% zooming. Figure 5.24 (b) shows the results obtained by using bicubic interpolation, whereas Figure 5.24 (c) shows the resultant image obtained by using DWT and bicubic interpolation.

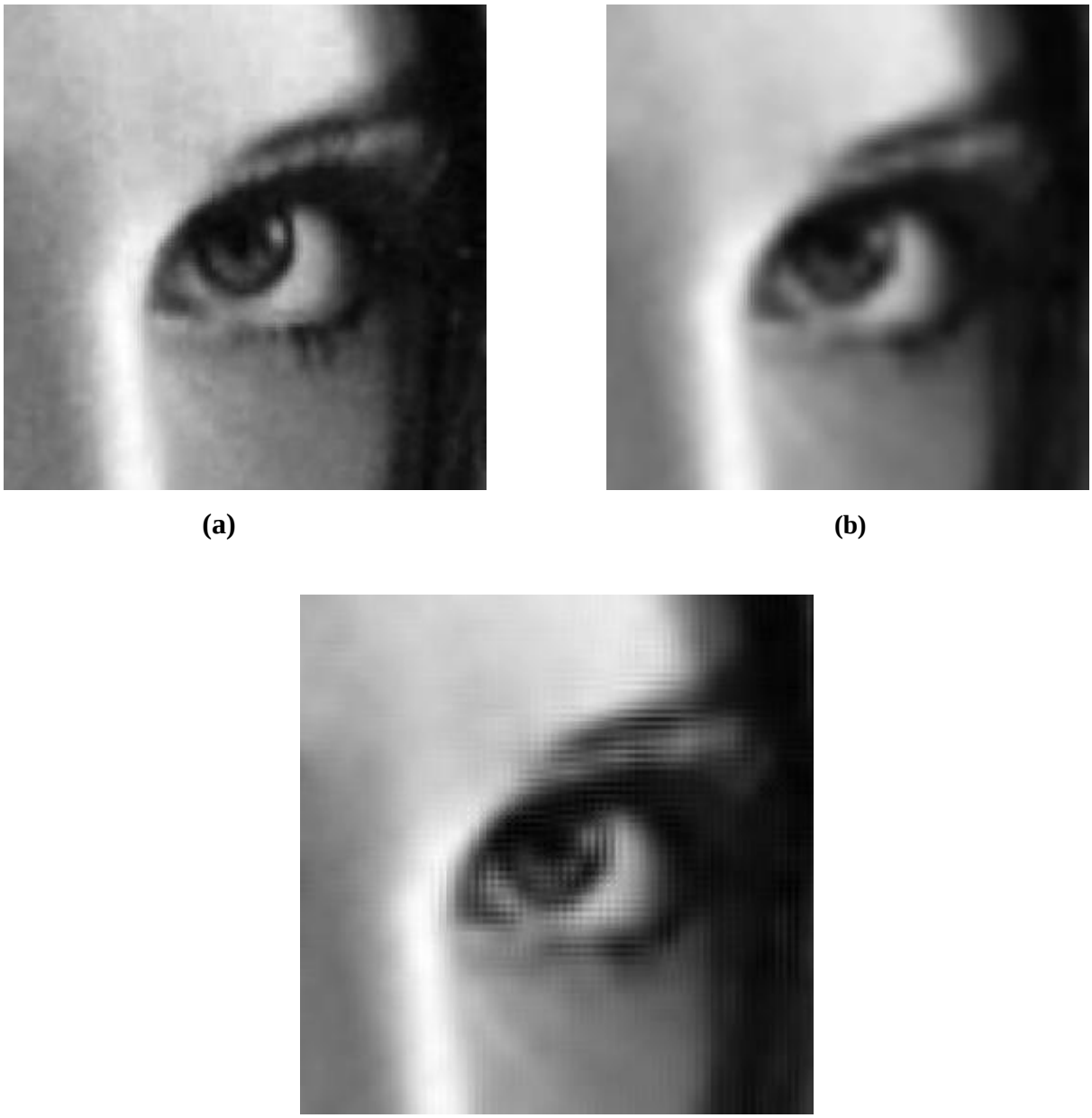

(a) **(b)**

(c)

Figure 5.24 Lena image with 400% zooming of left eye region

Due to the fact that the high-frequency subbands contain directional frequencies, embedding the interpolated high frequency components, that is, edges, into the reconstruction process by using IDWT introduces aliasing effects on the super resolved image as shown in Figure 5.24 (c). However, the achieved gain on the quality of the image is much higher than the loss caused by distortion, and the super resolved image is sharper and less blurred.

5.7.4 Baboon image with zooming of right eye region

Figure 5.25 (a) shows the original high resolution image of Baboon with 200% zoom, and Figure 5.25 (b) shows the resultant image obtained by using DWT and bicubic interpolation.

(a)

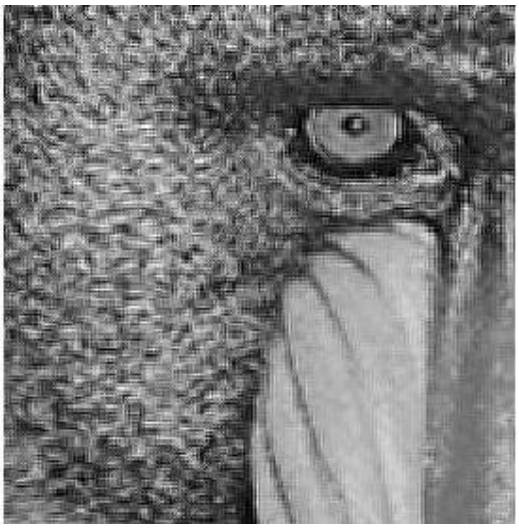

(b)

Figure 5.25 Baboon image with 200% zooming of Left eye region

5.7.5 Peppers image

Figure 5.26 (a) show the low resolution Peppers image of size 128X128. Figure 5.26 (b) shows the resultant image of size 512 X 512 obtained by using DWT and bicubic interpolation, whereas Figure 5.23 (c) shows an original high resolution image of size 512 x512.

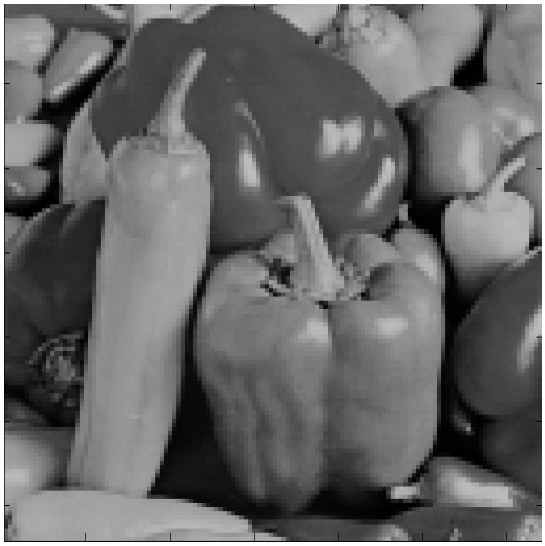

(a)

(b)

(c)

Figure 5.26 Experimental results for Peppers image

5.7.6 Living room image

Figure 5.27 (a) show the low resolution Living room image of size 128X128. Figure 5.27 (b) shows the resultant image of size 512 X 512 obtained by using DWT and bicubic interpolation, whereas Figure 5.27 (c) shows an original high resolution image of size 512 x512.

(a)

(b)

(c)

Figure 5.27 Experimental results for living room

5.7.7 House image

Figure 5.28 (a) show the low resolution House image of size 128X128. Figure 5.28 (b) shows the resultant image of size 512 X 512 obtained by using DWT and bicubic interpolation, whereas Figure 5.28 (c) shows an original high resolution image of size 512 x512.

(a)

(b)

(c)

Figure 5.28 Experimental results for House image

5.7.8 Cameraman image

Figure 5.29 (a) show the low resolution Cameraman image of size 128X128. Figure 5.29 (b) shows the resultant image of size 512 X 512 obtained by using DWT and bicubic interpolation, whereas Figure 5.29 (c) shows an original high resolution image of size 512 x512.

(a)

(b)

(c)

Figure 5.29 Experimental results for Cameraman image

5.7.9 Elaine image

Figure 5.30 (a) show the low resolution Elaine image of size 128X128. Figure 5.30 (b) shows the resultant image of size 512 X 512 obtained by using DWT and bicubic interpolation, whereas Figure 5.30 (c) show an original high resolution image of size 512 x512.

(a)

(b)

(c)

Figure 5.30 Experimental results for Elaine image

5.7.10 Woman blonde image

Figure 5.31 (a) show the low resolution Woman blonde image of size 128X128. Figure 5.31 (b) shows the resultant image of size 512 X 512 obtained by using DWT and bicubic interpolation, whereas Figure 5.31 (c) shows an original high resolution image of size 512 x512.

(a)

(b)

(c)

Figure 5.31 Experimental results for Woman blonde image

Table 1: MSE and PSNR results for image super resolution using DWT and bicubic interpolation from 128 X 128 to 512 X 512

Images	MSE	PSNR (dB)
Lena	21.72	34.76
Baboon	304.78	23.29
Peppers	39.53	32.16
Living room	266.68	23.87
House	48.97	31.23
Cameraman	71.94	29.56
Elaine	34.67	32.73
Woman blonde	519.99	20.97

5.8 IMAGE RESOLUTION ENHANCEMENT USING HYBRID WAVELETS AND INTERPOLATION

The main requirement for image resolution enhancement is that the algorithm should only enhance the image details; the filter is not sensitive to noise and does not smooth sharp edges. DWT has been employed in order to preserve the high frequency components of the image. One level DWT is used to decompose an input image into different subband images. Three high frequency subbands (LH, HL, HH) contains the high frequency components of the input image. Downsampling in each of the DWT subband cause loss of information in the respective subbands. SWT has been employed to minimize these losses. Bicubic interpolation with enlargement factor of 2 is applied to high frequency subband images. The interpolated high frequency subbands and the SWT high frequency subbands have the same size which means they can be added with each other. The new corrected high frequency subbands can be interpolated further for higher enlargement. Figure 5.32 illustrates the block diagram of the image resolution enhancement technique using hybrid wavelets and bicubic interpolation. By interpolating input image by $\alpha/2$, high frequency subbands by 2, and α in the intermediate and final interpolation stages respectively, and then by applying IDWT, the output image will contain sharper edges than the interpolated image obtained by interpolation of the input image directly. This is due to the fact that, the interpolation of isolated high frequency components in high frequency subbands and using the corrections obtained by adding high frequency subbands of SWT of the input image, will preserve more high frequency components.

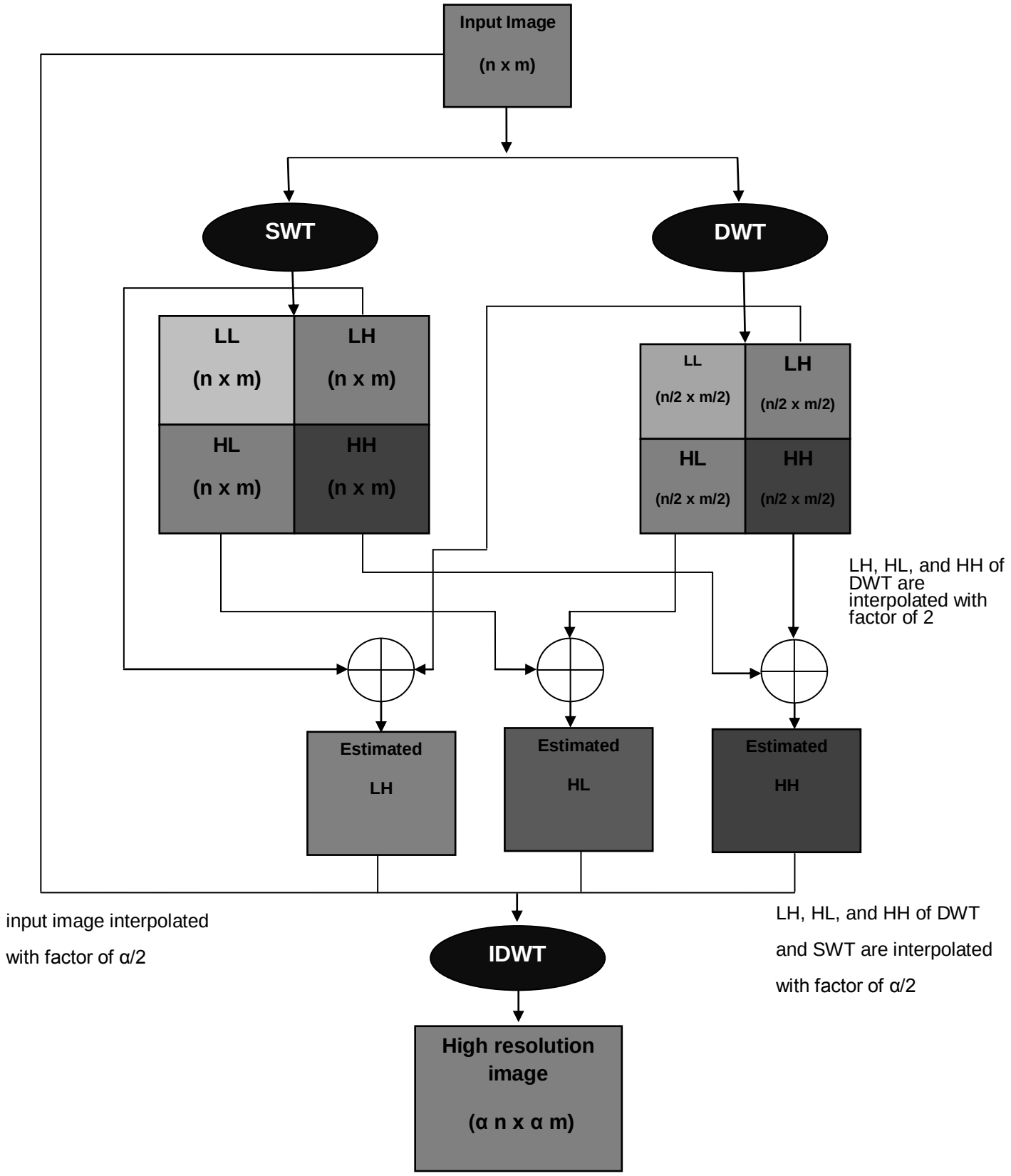

Figure 5.32 Block diagram of image resolution enhancement using hybrid wavelets and interpolation

5.9 EXPERIMENTAL RESULTS

The results of image resolution enhancement using hybrid wavelets and bicubic interpolation have been presented in this section.

5.9.1 Lena image

Figure 5.33 (a) shows the low resolution Lena image of size 128X128. Figure 5.33 (b) shows an image obtained by using hybrid wavelets and bicubic interpolation, whereas Figure 5.33 (c) shows an original high resolution image of size 512 x512.

(a)

(b)

(c)

Figure 5.33 Experimental results for Lena image

5.9.2 Baboon image

Figure 5.34 (a) shows the low resolution Baboon image of size 128X128. Figure 5.34 (b) shows an image obtained by using hybrid wavelets and bicubic interpolation, whereas Figure 5.34 (c) shows an original high resolution image of size 512 x512.

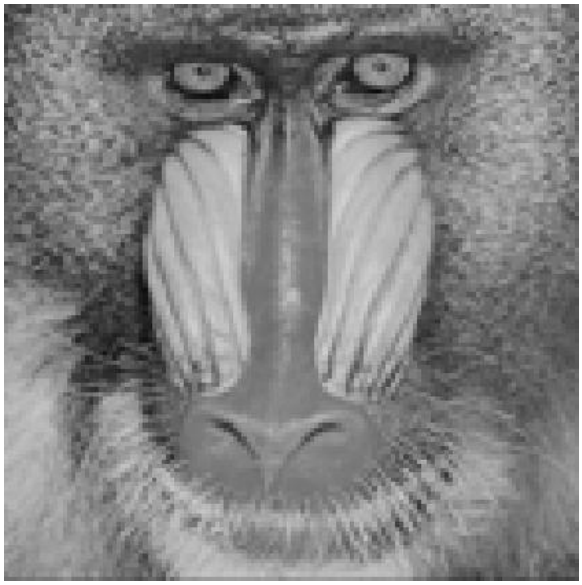

(a)

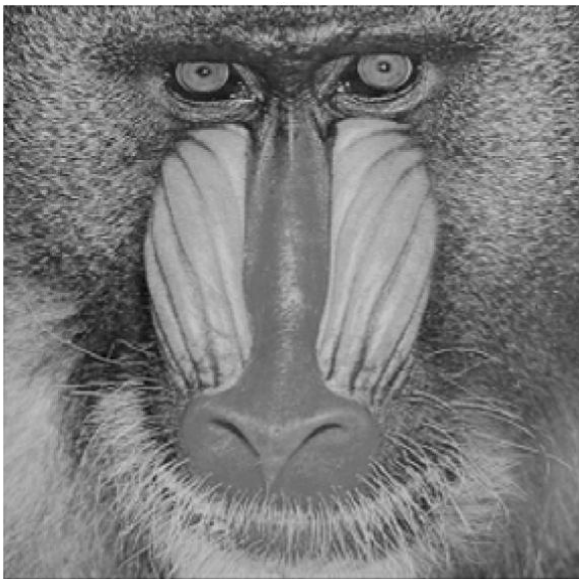

(b)

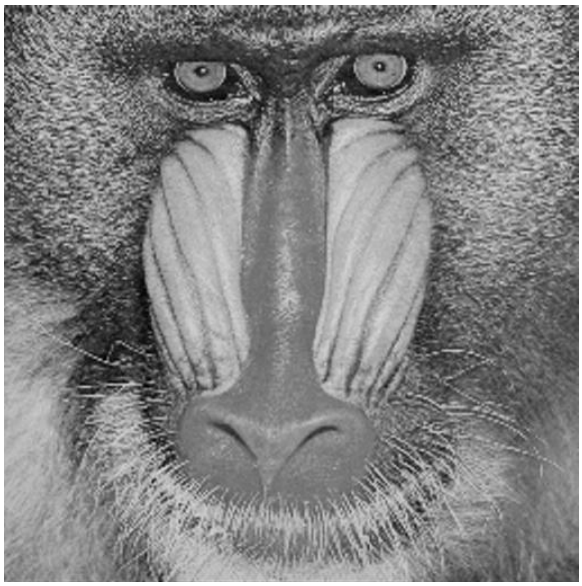

(c)

Figure 5.34 Experimental results for Baboon image

5.9.3 Lena image with zooming of left eye region

Figure 5.35 (a) shows low resolution Lena image of size 128X128 with 400 % zooming. Figure 5.35 (b) shows an image obtained by using hybrid wavelets and bicubic interpolation. Due to the fact that the high-frequency subbands of DWT and SWT contain directional frequencies, embedding the interpolated high frequency components, that is, edges, into the reconstruction process by using IDWT introduces less aliasing effects than DWT and bicubic interpolation as shown in Figure 5.35 (b).

(a)

(b)

Figure 5.35 Lena image with 400% zooming

5.9.4 Baboon image with zooming of right eye region

Figure 5.36 (a) shows the original high resolution image of Baboon with 200% zooming, and Figure 5.36 (b) shows the resultant image obtained by using hybrid wavelets and bicubic interpolation..

(a)

(b)

Figure 5.36 Baboon image with 200% zooming of left eye region

5.9.5 Peppers image

Figure 5.37 (a) shows the low resolution Peppers image of size 128X128. Figure 5.37 (b) shows the resultant image of size 512 X 512 obtained by using hybrid wavelets and bicubic interpolation, whereas Figure 5.37 (c) shows an original high resolution image of size 512 x512.

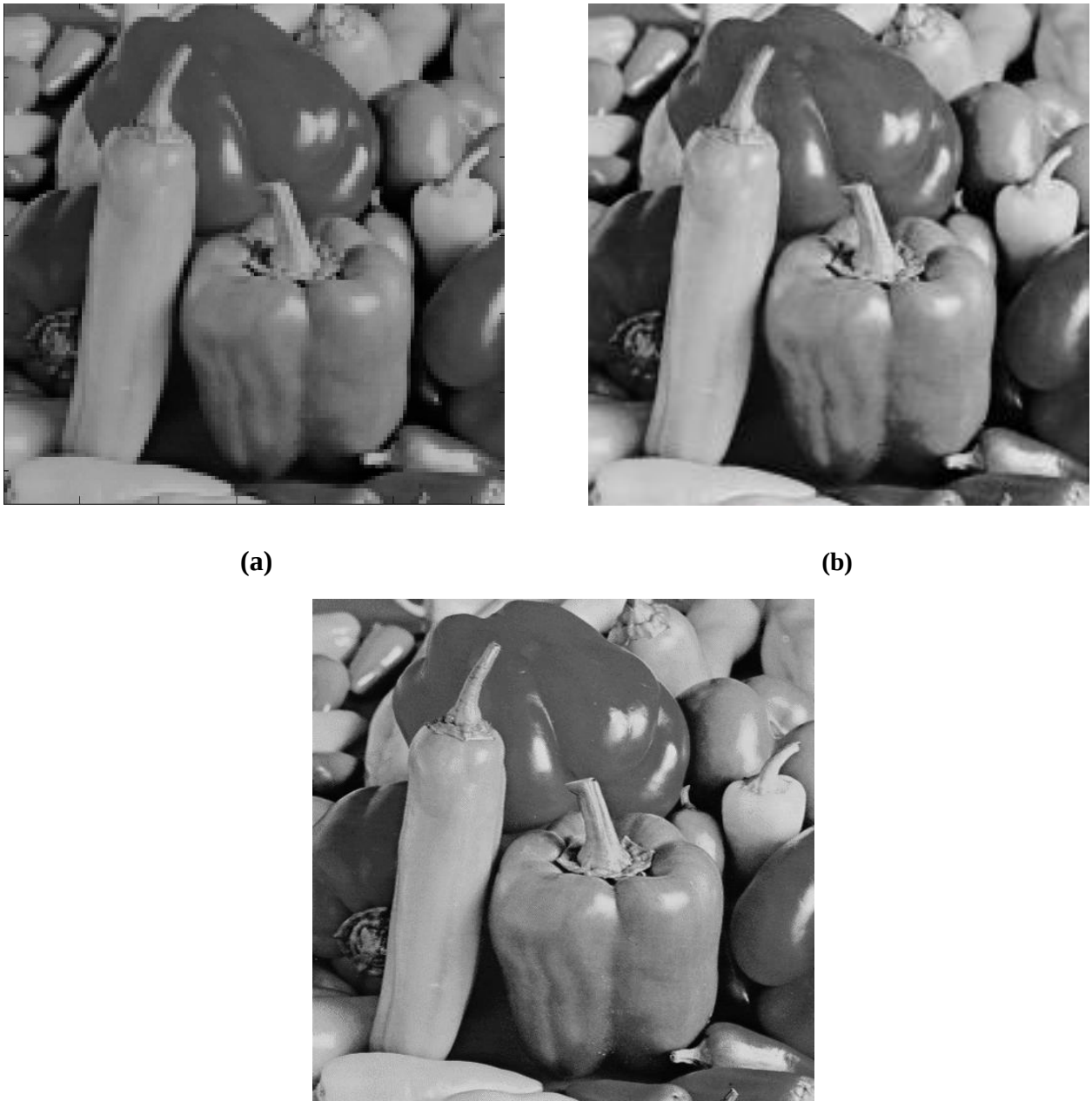

(a) **(b)**

(c)

Figure 5.37 Experimental results for Peppers image

5.9.6 Living room image

Figure 5.38(a) shows the low resolution Living image of size 128X128. Figure 5.38 (b) shows the resultant image of size 512 X 512 obtained by using hybrid wavelets and bicubic interpolation, whereas Figure 5.38 (c) shows an original high resolution image of size 512 x512.

(a)

(b)

(c)

Figure 5.38 Experimental results for Living room image

5.9.7 House image

Figure 5.39 (a) shows the low resolution House image of size 128X128. Figure 5.39 (b) shows the resultant image of size 512 X 512 obtained by using hybrid wavelets and bicubic interpolation, whereas Figure 5.39 (c) shows an original high resolution image of size 512 x512.

(a)

(b)

(c)

Figure 5.39 Experimental results for House image

5.9.8 Cameraman image

Figure 5.40 (a) shows the low resolution Cameraman image of size 128X128. Figure 5.40 (b) shows the resultant image of size 512 X 512 obtained by using hybrid wavelets and bicubic interpolation, whereas Figure 5.40 (c) shows an original high resolution image of size 512 x512.

(a)

(b)

(c)

Figure 5.40 Experimental results for Cameraman image

5.9.9 Elaine image

Figure 5.41 (a) shows the low resolution Elaine image of size 128X128. Figure 5.41 (b) shows the resultant image of size 512 X 512 obtained by using hybrid wavelets and bicubic interpolation, whereas Figure 5.41 (c) shows an original high resolution image of size 512 x512.

(a) **(b)**

(c)

Figure 5.41 Experimental results for Elaine image

5.9.10 Woman blonde image

Figure 5.42 (a) shows the low resolution Woman blonde image of size 128X128. Figure 5.42 (b) shows the resultant image of size 512 X 512 obtained by using hybrid wavelets and bicubic interpolation, whereas Figure 5.42 (c) shows an original high resolution image of size 512 x512.

(a)

(b)

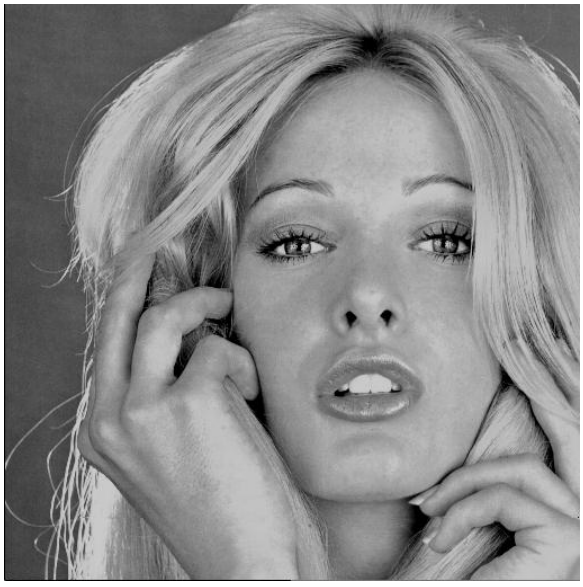

(c)

Figure 5.42 Experimental results for Woman blonde image

Table 2: MSE and PSNR results for image resolution enhancement using hybrid wavelets and bicubic interpolation from 128 X 128 to 512 X 512

Images	MSE	PSNR (dB)
Lena	21.42	34.82
Baboon	266.68	23.87
Peppers	32.13	33.06
Living room	271.64	23.79
House	49.77	31.16
Cameraman	70.46	29.65
Elaine	20.51	35.01
Woman blonde	534.56	20.85

5.10 COMPARATIVE ANALYSIS

A comparison of two image resolution enhancement methods has been done in this section.

On comparing Table 1 and Table 2, it has been observed that PSNR of images Lena, Baboon, Pepper, Cameraman, and Elaine is better in hybrid wavelets and bicubic interpolation as compared to DWT and bicubic interpolation. This is due to the fact that the detailed information of high frequency subbands i.e. edges has been lost in DWT; while SWT has the ability to preserve this information. Hybrid wavelet and bicubic interpolation provides considerable improvement in texture based images such as Baboon and Pepper, because the texture regions of an image have been efficiently segmented by using hybrid wavelets. In addition, segmented regions can be directly used for the purpose of image reconstruction by applying IDWT.

By zooming the images Lena and Baboon, it has been observed that hybrid wavelets and bicubic interpolation gives less aliasing effect as compared to DWT and bicubic interpolation. This is due to the fact that high frequency subbands of hybrid wavelets containing improved directional frequencies, along with the interpolated high frequency components into the reconstruction process by using IDWT, which helps us to reduce the aliasing.

However Living room, House, and Woman blonde are low contrast images and most of pixels are at same intensity level. When these images are decomposed by using SWT, smoothness increases due to over determination and redundant representation of pixels. Hence, PSNR of these images is less in hybrid wavelets and bicubic interpolation than that of DWT and bicubic interpolation. So, we can say that texture and contrast of an image plays an important role to select the method for improving the PSNR.

.

CHAPTER 6

CONCLUSION AND FUTURE SCOPE

6.1 CONCLUSION

This thesis describes two methods of the image resolution enhancement. In the first method, super resolved image is obtained by interpolating the high-frequency subband images obtained by DWT and the input image. This technique uses DWT to decompose an image into different subband images. The high-frequency subband images are interpolated. An original image is interpolated with half of the interpolation factor used for interpolating the high-frequency sub band images. Afterwards all these images are combined using IDWT to generate a super-resolved image.

In the second method, an enhanced image is obtained by interpolating high frequency subbands obtained by DWT, correcting the high frequency subband estimation by using SWT high frequency subbands, and the input image. This technique uses DWT to decompose an image into different subbands, and then the high frequency subband images have been interpolated. The interpolated high frequency subband coefficients have been corrected by using the high frequency subbands achieved by SWT of the input image. An original image is interpolated with half of the interpolation factor used for interpolation the high frequency subbands. Then all these images are combined using IDWT to generate a more enhanced image.

The performance of these two methods has been compared on the basis of PSNR and visual quality. Experimental results shows that hybrid wavelets and bicubic interpolation provide significant improvement in texture based images by efficiently segmenting the texture regions. This method also helps in preserving the detailed information and improves the PSNR. Hybrid wavelets and bicubic interpolation produces less aliasing as compared to DWT and bicubic interpolation. Due to over determination and redundant representation of pixels caused by SWT in low contrast images, PSNR is less in hybrid and bicubic interpolation.

6.2 FUTURE SCOPE

In this thesis, different parameters and methods have been discussed for image resolution enhancement. Although improved resolution enhancement has been achieved, but still there is a scope for further improvement. The following points may be used to improve the system:

1. This work can be extended by using different types of wavelets, by implementing on different type and formats of images, for example color images, and DICOM images.
2. Real-valued filtering has been used in DWT, which removes the phase information. CWT can be used as alternative to DWT. One level CWT uses complex-valued filtering that decompose an image into two complex-valued low frequency subband images and six complex-valued high frequency subbands images to preserve the phase information. Other multi resolution analyzer such as contourlet transform, curvelet transform, and ridgelet transforms may be used in future.
3. Use of non-linear interpolation increases the computational complexity, but Wavelet transforms along with non-linear interpolation can be used for further improvements.

REFERENCES

[1] C. Solomon and T. Breckon, *"Fundamentals of Digital Image Processing*, 1st edition, West Sussex, UK-Wiley, 2011.

[2] A. McAndrew, "*An Introduction to Digital Image Processing with MATLAB"*, School of Computer Science and Mathematics, Victoria University of Technology, 2004.

[3] C. S. Burrus, R A Gopinath and H Guo, *"Introduction to Wavelets and Wavelet Transforms"*, NJ -Prentice Hall, 1998.

[4] W. Burger and M. J. Burge, *"Principles of Digital Image Processing: fundamental techniques"*, 1st edition, New York- Springer, 2009.

[5] J. L. Moigne, W. Campbell and R. Cromp, *"An Automated Parallel Image Registration technique based on the Correlation of Wavelet Features"*, IEEE Transactions on Geoscience and Remote Sensing, vol.40, no.8, pp. 1849–1864, 2002.

[6] Edge Detection, "www.cse.unr.edu/~bebis/CS791E/Notes/EdgeDetection.pdf".

[7] S.C. Park, M. K. Park and M. G. Kang, *"Super Resolution Image Reconstruction: A Technical Review"*, IEEE Signal Processing Magazine, vol.20, pp.21-36, 2003.

[8] K. R. Castleman, *"Digital Image Processing*", 1st edition, NJ- Prentice Hall, 1996.

[9] R.G. Keys, *"Cubic Convolution Interpolation for Digital Image Processing"*, IEEE Transactions on Acoustics, Speech, and Signal processing, vol. 29, no. 6, pp. 1153-1160, 1981.

[10] J. Pan, "*Image Interpolation using Spline Curves"*, Department of Mechanical Engineering, The University of Western Australia, pp. 1-10, 2003.

[11] T. Wittman, "*Mathematical Techniques for Image Interpolation"*, Department of Mathematics, University of Minnesota, USA, 2005.

[12] J. A. Parker, R. V. Kenyon and D. E. Troxel, *"Comparison of Interpolating Methods for Image Resampling"*, IEEE Transactions on Medical Imaging, vol.2, no.1, pp. 31-39, 1983.

[13] C. L. Liu, "*A Tutorial of the Wavelet Transform"*, 2010.

[14] G. Strang and T. Nguyen, *"Wavelets and Filter Banks"*, Wellesley-Cambridge Press, Wellesley, MA, 1997.

[15] J. C. Pesquet, H. Krim, and H. Carfantan, *"Time Invariant Orthonormal Wavelet Representation"*, IEEE Transactions on Signal Processing, vol. 44, no 8, 1996

[16] P. Miklos, *"Comparison of Convolution Based Interpolation Techniques in Digital Image Processing"*, 5th International Symposium on Intelligent Systems and Informatics, pp. 87-90, 2007.

[17] M. Weeks, *"Digital signal Processing using MATLAB and Wavelets"*, Hingham, Massachusetts- Infinity Science Press, 2006.

[18] P. Miklos, *"Image Interpolation Techniques"*, 2007.

[19] H. Ibrahim and N.S. Kong, *"Image Sharpening using Sub Regions Histogram Equalization"*, IEEE Transactions on consumer Electronics, vol.55, no.2, pp.891-895, 2009.

[20] Z. J. Xiang and P. J. Ramadge, *"Edge–Preserving Image Regularization Based on Morphological Wavelets and Dyadic Trees"*, IEEE Transactions on Image Processing, vol.21, no.4, pp.1548-1560, 2012.

[21] Y. Niu, W. Xiaolin , G. Shi and X. Wang, *"Edge-Based Perceptual Image Coding"*, IEEE Transaction on Image Processing, vol.21, no.4, pp.1899-1910, 2012.

[22] D. Humphrey and D. Taubman, *"A Filtering Approach to Edge Preserving MAP Estimation of Images"*, IEEE Transactions on Image Processing, vol.20, no.5, pp.1234-1248, 2012.

[23] S. Rahmani, M. Strait, D. Merkurjev, M. Moeller , and T. Wittman , *"An Adaptive IHS Pan-Sharpening Method"*, IEEE Geoscience and Remote Sensing letters, vol. 7, no. 4, pp.746-750, 2010.

[24] F.Russo, *"An Image Enhancement Combining Sharpening and Noise Reduction"*, IEEE Transactions on Instrumentation and Measurement Technology, vol.51, no.4, pp.824-828, 2002.

[25] H.S.Kam, M. Hanmandlu and W. H. Tan, *"An Improved Image Enhancement Combining smoothing and Sharpening"*, IEEE TENCON, vol.1, pp.36 -42, 2003.

[26] L. Meylan and S. Susstrunk, *"High Dynamic Range Image Rendering Using a Retinex-based Adaptive Filter"*, IEEE Transactions on Image Processing, vol. 15, no. 9, pp. 2820–2830, Sep. 2006.

[27] G. Deng, *"A Generalized Unsharp Masking Algorithm"*, IEEE Transactions on Image Processing, vol.20.no5, pp.1249-1261, 2011.

[28] G. Ramponi, *"A Cubic Unsharp Masking Technique for Contrast Enhancement"*, IEEE Transaction on Signal Processing, vol.67, no. 2, pp. 211–222, 1998.

[29] X. Li and M. T. Orchard, *"New edge-directed interpolation"*, IEEE Transactions on Image Processing, vol. 10, no. 10, pp. 1521–1527, 2001.

[30] H. Aftab, A. B. Mansoor and M. Asim, *"A New Single Image Interpolation Technique for Super Resolution"*, Proceedings of the 12th IEEE International Multi topic Conference, pp. 592-596, 2008.

[31] T. Blu, P. Thévenaz, and M. Unser, *"Linear Interpolation Revitalized"*, IEEE Transaction on Image Processing, vol. 13, no. 5, pp. 710-719, 2004.

[32] Y. Tamura and K. Tanaka, *"Image Enlargement using Bi-directional Shifted Linear Interpolation"*, International Symposium on Intelligent Signal Processing and Communication Systems, pp.1-4, 2008

[33] M. F. Al-Samaraie and N. A. M. Al Saiyd, *"Medical Colored Image Enhancement using Wavelet Transform followed by Image Sharpening"*, Ubiquitous Computing and Communication Journal, vol.6, no.5, pp.1-5, 2010.

[34] L. Ying, N. T. Ming and L. B. Keat , *"Wavelet Based Image Sharpening Algorithm"*, International Conference on Computer Science and Software Engineering, pp.1053-1056, 2008.

[35] H. Demirel and G. Anbarjafari, *"Discrete Wavelet Transform-based Satellite Image Resolution Enhancement"*, IEEE Transactions on Geoscience and Remote Sensing, vol.49, no.6, pp.1997-2004, 2011.

[36] N. Haq, K. Hayat, N. Nooren, and W. puech *,"Image Sharpening by DWT-Based Hysteresis*", Proceedings of the 13th international conference on Advanced concepts for intelligent vision systems, vol. 69, no. 15, pp.429-436, 2011.

[37] Y. Piao, I. Shin, and H. W. Park, *"Image Resolution Enhancement Using Inter-subband Correlation in Wavelet Domain"*, IEEE International Conference on Image Processing, 2007, vol. 1, pp.445–448.

[38] W. K. Carey, D. B. Chuang, and S. S. Hemami, *"Regularity-Preserving Image Interpolation"*, IEEE Transactions on Image Processing, vol. 8, no. 9, pp. 1295–1297, Sep. 1999.

[39] F. C. A. Fernandes, R. L. C. Spaendonck, and C. S. Burrus, *"A New Framework for Complex Wavelet Transforms"*, IEEE Transactions on Signal Processing, vol.51, no.7, pp. 1825-1837, 2003.

[40] G.P. Nason and B.W. Silverman, *"The Stationary Wavelet Transform and some Statistical Applications"*, vol. 103, pp. 281-299, 1995.

[41] H. Demirel and G. Anbarjafari, *"Satellite Image Resolution Enhancement Using Complex Wavelet Transform"*, IEEE Geoscience and Remote Sensing Letter, vol. 7, no. 1, pp. 123–126,2010.

[42] G. N. S. Prasad, H. Khan, B.K. Muralidhar and T.S. Kiran, *"Image Enhancement Using Wavelet Transforms and SVD"*, International Journal of Engineering Science and Technology (IJEST), vol. 4, no.03, pp. 1080-1087, 2012.

[43] A. Temizel, *"Image Resolution Enhancement using Wavelet Domain Hidden Markov Tree and Coefficient Sign Estimation"*, IEEE International Conference on Image Processing, vol. 5, pp. 381–384, 2007.

[44] Y. Wang and S. Wang, *"A Novel Stationary Wavelet Denoising Algorithm for Array-based DNA Copy Number data"*, International Journal of Bio informatics Research and Applications, vol. 3, no.2, pp. 206 - 222, 2007.

[45] H. Demirel and G. Anbarjafari, *"Image resolution Enhancement by Using Discrete and Stationary Wavelet Decomposition"*, IEEE Transaction on Image Processing, vol.20, no.5, pp.1458-1460, 2011.

[46] F. Y. Shih, *"Image Processing and Pattern Recognition Fundamentals and Techniques"*, 1st Edition, New Jersey, John Wiley, 2011.

[47] S.S. Agaian, B. Silver, K. A. Panetta, *"Transform Coefficient Histogram-Based Image Enhancement Algorithms Using Contrast Entropy"*, IEEE Transactions on Image Processing, vol. 16, no. 3, March 2007.

[48] J. A. Stark, *"Adaptive Image Contrast Enhancement Using Generalizations of Histogram Equalization"*, IEEE Transactions on Image Processing, vol.9, no.5, pp.889-896, 2000.

[49] D. L. Fugal, *"Conceptual Wavelets"*, Space & Signals Technical Publishing, edition 2009.

[50] C. C. Sun, S. J. Ruan, C. Shie and T. W. Pai, *"Dynamic Contrast Enhancement based on Histogram Specification"*, IEEE Transactions on Consumer Electronics, vol.51, no. 4, pp.1300-1305, 2005.

[51] R. C. Gonzalez, R. E. Woods, *"Digital Image Processing"*, 3rd Edition, Prentice Hall, 2008.

[52] http://en.wikipedia.org/wiki/Bilinear_interpolation.

[53] Math Works, "MATLAB help files, Wavelet Toolbox", version 7.5., 2007.

[54] O Rioul, and M Vetterli, "*Wavelets and Signal Processing"*, IEEE Signal Processing Magazine, 14-38, 1991.

[55] M. Shnaider and A. P. Paplinski, *"Wavelet Transform in Image Coding"*, Department of Robotics and Technology, Monash University, 1994.

[56] J. Yeng, R. Feng and W. Deng, *"A New Algorithm of Image Denoising Based on Stationary Wavelet Multi-scale Adaptive Threshold"*, International Conference on Electronic & Mechanical Engineering and Information Technology, pp. 4550-4553, 2011.

LIST OD PUBLICATIONS

[1] Gaurav Kumar, and Kulbir Singh, ***"****Image Super Resolution on the basis of DWT and bicubic interpolation"*, International Journal of Computer Applications, vol. 65, no. 15, pp.12-17, 2013.